INVESTIGATING THE INTEGRATIVE ROLE OF SUBSTRATE STIFFNESS, STRAIN, AND TONE ON THE FUNCTIONAL AND PHENOTYPIC REPONSE OF AIRWAY SMOOTH MUSCLE IN ASTHMATIC AIRWAYS

by

Rachel Wise

Submitted in partial fulfilment of the requirements
for the degree of Master of Applied Science

at

Dalhousie University
Halifax, Nova Scotia
March 2015

Table of Contents

List of Tables

List of Figures

Abstract

In recent years, studies have shown that substrate stiffness is a potent modulator of cellular function, gene expression, and morphology in many cell types. These observations may be of important relevance to asthma pathology as remodeling of the airway is thought to create a stiffer microenvironment for ASM cells. Indeed, ASM cells demonstrate a more contractile phenotype on stiffer substrates *in vitro*. However, the mechanotransduction process by which cells sense the external mechanical environment is an active system that relies on dynamic changes in cell tone, structure, and signaling pathways. Therefore, the ability of the cell to sense and respond to the stiffness of the external environment may be upset by other stimuli that affect external or internal mechanics. In the airway, ASM cells are constantly exposed to oscillatory strain due to breathing and in asthma, these cells also maintain higher tone. To better model the mechanical environment of the asthmatic airway, I attempted to integrate either chronic tone modulation or strain into the well-characterised polyacrylamide substrate stiffness model. The increase in contractile phenotype on stiff substrates was confirmed, and, for the first time, was shown to correlate with transcriptional regulation of smMHC. Interestingly, these effects were time-dependent and only observable after 7 days of cell culture. Strain was applied to the model by successfully binding PA gels to Flexcell silicone membranes. However, the inability to fully polymerise PA gels soft enough to accurately mimic the healthy airway environment, likely due to the use of oxygen plasma, prevented further use of this model. Chronic relaxation of ASM cells on PA gels had little effect on substrate stiffness-dependent changes, yet independently regulated transcription of SMA and Sm22. These results provide evidence for independent mechanotransduction pathways in ASM cells, implicating both airway remodeling and cell tone as necessary therapeutic targets in asthma.

List of Abbreviations Used

AFM	atomic force microscopy
AHR	airway hyperresponsiveness
AMPS	(3-aminopropyl)trimethoxysilane
APS	ammonium persulfate
ASM	airway smooth muscle
CSK	cytoskeleton
ECM	extracellular matrix
F-actin	filamentous actin
FBS	fetal bovine serum
FEV1	forced expiratory volume in 1 second
G-actin	globular actin
IT	insulin transferrin media
KCl	potassium chloride
MHC	myosin heavy chain
MLC_{20}	20kDa regulatory myosin light chain
MLCK	myosin light chain kinase
MLCP	myosin light chain phosphatase
MSC	mesenchymal stem cell
NHS	N-hydroxysuccinimide
NMM-II	non-muscle myosin
OMTC	optical magnetic twisting cytometry
PA	polyacrylamide
PDMS	polydimethylsiloxane
PKA	protein kinase A
qRT-PCR	quantitative real time polymerase chain reaction
RGD	arginine-glycine-aspartic acid motif
ROCK	RhoA associated kinase
SM	smooth muscle
Sm22	transgelin/ Sm22α

SMA	smooth muscle α-actin
smMHC	smooth muscle myosin heavy chain
SR	sarcoplasmic reticulum
SRF	serum response factor
Sulfo-SANPAH	sulfosuccinimidyl-6-[4′-azido-2′-nitrophenylamino]hexanoate
TcPM	3-(trichlorosilyl)propyl methacrylate
TEMED	tetramethylethylenediamine
TFM	traction force microscopy
TmPM	3-(trimethoxysilyl)propyl methacrylate
VIC	valvular interstitial cell
VSM	vascular smooth muscle
XPS	x-ray photoelectron spectroscopy

Chapter 1: Introduction

1.1 Thesis Overview

This thesis is organised into five chapters. Chapter one contains a literature review, the general hypotheses of the project, and outlines the two aims of this thesis. Chapter two consists of detailed descriptions of methodology that was common to all aims. Chapter three and four describe each thesis aim including the rationale, methods, results, and a discussion section. Chapter five consists of conclusions drawn from the thesis work, as well as future directions.

1.2 Asthma Pathology and Remodelling

Asthma is the most common respiratory disease in Canada, affecting approximately 3 million people nationwide, which includes 10% of the population of Nova Scotia (2). Current treatment options largely target the symptoms of this chronic disease rather than the underlying causes and can therefore be costly and frustrating for medical professionals and patients alike. For example, asthma is the most common chronic condition in children (1) and costs the nation more than $2 billion per year in health care costs (135). In adults, lung disorders are the leading cause of short term disability in Canada, adding loss of production to the cost of treatment (3). A better understanding of the underlying causes of lung disorders, such as asthma, would provide improved treatment targets in order to help reduce both the personal and societal burden of these chronic diseases.

Asthma pathology is characterised by airway hyperresponsiveness, chronic inflammation, and airway wall remodelling (101). Airway hyperresponsiveness (AHR) describes an excessive narrowing of the airways in response to a stimulus; it is mainly attributed to airway smooth muscle (ASM) dysfunction (6, 129) and is the principal functional defect in asthma. Some studies have shown that ASM from asthmatic airways have increased maximal shortening (133), shortening velocity (84), and sensitivity to contractile agonists (11) compared to healthy ASM. The resulting airway narrowing, known as an asthma attack, causes difficulty breathing, coughing, chest tightness, wheezing, and airway obstruction that can be life threatening if left untreated. Inflammation has traditionally been implicated as the major contributor to asthma pathology, however, inflammatory and allergenic characteristics have inadequate correlation with asthmatic symptoms (100). More recently airway remodelling and intrinsic changes of ASM cell function and phenotype have been implicated as instigators of AHR (20, 166) and may even precede symptoms (13). However, other studies have found a lack of functional differences in asthmatic ASM compared to healthy (155), and potential mechanisms responsible for ASM dysfunction leading to hyperresponsiveness are still debated (6, 101, 111).

The airway is a tube composed of multiple layers, including a layer of ASM that surrounds the airway circumferentially. The structural changes within these layers in asthmatic airways are referred to as airway wall remodelling. This remodelling phenomenon was first observed over 90 years ago as an increase in ASM mass (71) in asthmatic airways. More recently, more extensive structural changes throughout the airway have been posited as relevant disease factors. Within the inner most epithelial

layer, studies have found mucous gland and goblet cell hyperplasia (4), as well as other changes in epithelial cells (62). Additionally, there is an altered composition and increased density of extracellular matrix (ECM) components in connective tissue layers of the airway (109, 158), including thickening of the basement membrane, and within the ASM layer itself (9, 108). These structural changes surrounding the ASM may affect function and/or phenotype either via altered signaling or by altering the mechanical environment. Altered ASM inflammatory signaling has long been a focus in the framework of asthma research; however, much less is known about how the changes in the mechanical microenvironment of ASM cells might contribute to the disease. In recent years, research in other cell types has provided some compelling evidence that the mechanical environment exerts potent effects on cellular function and phenotype. The purpose of this thesis is to explore the still relatively unknown question: how does the mechanical environment affect ASM phenotype and function?

1.3 Cellular Mechanics

All cells have the ability to sense the external environment (outside-in signaling) and physically interact with it (inside-out signaling). This is done through a series of proteins that physically bind the external substrate to an internal cellular network: integrins, focal adhesions, adaptor proteins, and the cytoskeleton (CSK). These physical and biochemical connections throughout the cells provide a dynamic system through which the cell can sense and react to mechanical stimuli (Figure 1-1).

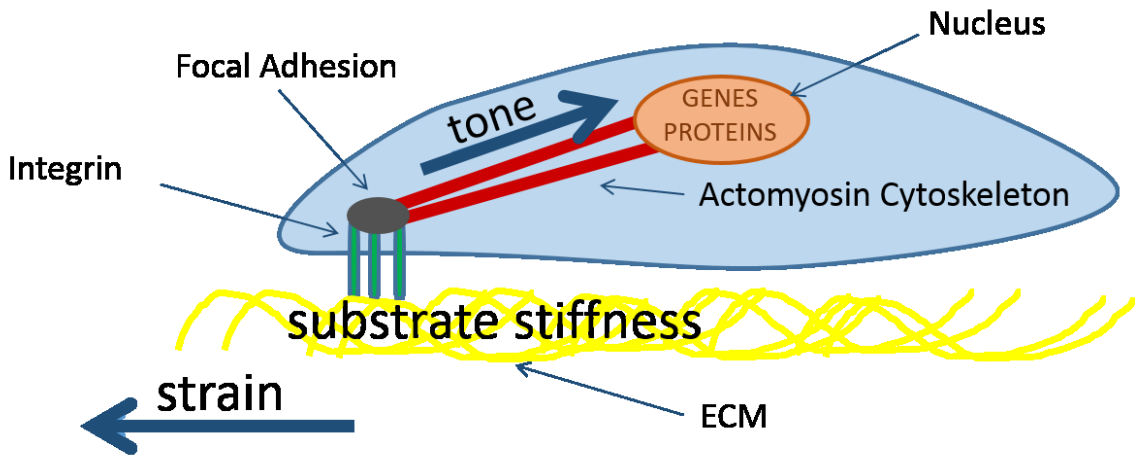

Figure 1-1. Representative diagram of mechanotransduction mechanisms. Internal and external cellular mechanics are physically and chemically linked. Integrins, focal adhesions, and the actomyosin cytoskeleton make up the basis for this system that regulates cell tone, and is integral to sensing the external mechanical environment including stiffness or the presence of strain.

Integrins are transmembrane proteins that bind specifically to components of the ECM, such as collagen, fibrin, or laminin (116). Inside the cell, integrins are physically linked to the CSK via a series of proteins called adaptor proteins that are often actively involved in mechanotransduction pathways. Thus, integrins can transmit information bidirectionally through the membrane; external cues can alter internal signaling, and internal cues can alter external interactions. It is this bidirectional property of integrins that allows cells to respond dynamically to the external mechanical environment and positions them as an important component of mechanotransduction pathways.

Upon changes in the mechanical environment of a cell, for example due to the presence of strain, or an increase in substrate stiffness, integrins and adaptor proteins bundle together to form focal adhesions (147). These are large, dynamic structures (115) that can quickly strengthen or weaken in response to mechanical changes (12, 32). It is through integrins, adaptor proteins, and focal adhesions that the CSK is then bound to the

external environment, allowing the transmission of mechanical information throughout the entire cell.

The CSK is a network of fibrillar proteins that span the entire cell, made up of actin filaments, intermediate filaments, and microtubules. While microtubules are thought to contribute to passive cell stiffness (147), the actin cytoskeleton is a major part of the contractile unit of the cell. Filamentous actin (F-actin) is composed of two coiled polypepetide strands of actin monomers (G-actin), creating a dynamic structure that can be quickly and easily assembled or disassembled. The actin CSK provides the framework for cell contraction while the biochemical interaction between actin and myosin contributes the necessary work. There are two major forms of myosin: type I, or unconventional myosin, and type II, or conventional myosin. Type II can be further subdivided into muscle and non-muscle myosin (NMM-II), each with multiple subtypes that are all made up of four light chains and two heavy chains (MHC). Due to inherent ATPase activity, it is the heavy chains that then bind to and move along actin fibrils, providing the molecular mechanism for cellular tone and contraction.

Contraction of the actomyosin CSK causes stiffening of the cell, allowing a cell to apply force to the substrate through focal adhesions, adaptor proteins, and integrins. It is through this application of tension, known as traction force, that the cell can sense the external mechanical environment. Traction force is calculated as the force the cell exerts on the substrate per unit area (35).

Outside-in signaling refers to a cell sensing external cues via integrins bound to the ECM, the transmission of this information through the membrane to adaptor proteins and the CSK, and a series of downstream signaling changes that lead to cellular

responses. These responses can be anything from acute responses due to changes in actin polymerization, or long term changes due to signaling events and alterations in gene and protein expression. In contrast, inside-out signaling is the reverse of these events; intracellular changes that can be initiated from any stimulus (mechanical, chemical etc.) and transmitted via the CSK, adaptor proteins, and integrins to affect how the cell interacts with the external environment either chemically, or physically. It is through these pathways that the cell can both sense and respond to changes in the mechanical environment.

1.4 Airway Smooth Muscle Function and Phenotype

Smooth muscle (SM) contraction occurs via actin-myosin interaction, similar to the mechanisms described above, and is therefore closely related to mechanosensing. This raises the question: if all cells can generate force, how are smooth muscle cells unique and specialised for contraction? The answer is not as clear as one might think and largely lies in the organisation of the contractile machinery and expression of specific isoforms of the proteins involved.

1.4.1 Characteristics of Mature ASM Cells

Contraction and force generation are classically regulated through similar mechanisms in both smooth muscle and adherent non-muscle cells. Upon an increase in internal calcium concentration, which can occur due to pharmacological activation or cellular depolarisation, calcium binds to calmodulin. This calcium-calmodulin complex then activates myosin light chain kinase (MLCK), which phosphorylates the myosin regulatory light chain (MLC_{20}). Phosphorylated myosin can then bind to actin to form

crossbridges, and the cycling of these crossbridge attachments leads to contraction and stiffening of the cell. Relaxation of the cell occurs upon dephosphorylation of MLC_{20} by myosin light chain phosphatase (MLCP), which stops crossbridge cycling. Therefore, the balance of myosin phosphorylation and dephosphorylation by MLCK and MLCP regulates cell contraction.

Smooth muscle is functionally unique in that it can create and sustain large forces while using small amounts of energy; the structure and variations in genes encoding contributing proteins are what determine this unique functionality. Although the mechanisms are similar, the contractile network in smooth muscle is a more organised structure compared to non-muscle cells and demonstrates some similarities to skeletal muscle. Actin and myosin filaments are organised into sarcomere-like structures that are bound together by dense bodies rich in α-actinin. Although these dense bodies are often compared to z-discs found in skeletal muscle, their function is still debated and may play a role in contractile characteristics that are unique to smooth muscle. Additionally, like skeletal muscle, smooth muscle cells have a sarcoplasmic reticulum (SR) that regulates intracellular calcium dynamics, although, by volume, the SR structure in smooth muscle is much less compared to skeletal muscle. Tonic smooth muscle, such as that found in the airway and much of the vasculature, is defined as cells that can sustain force for longer periods of time with minimal energy expenditure compared to skeletal muscle. Thus while smooth muscle machinery shares some characteristics with both non-muscle and skeletal muscle cells, it is functionally unique in the ability to generate large, sustained forces with little energy use.

Smooth muscle is also distinctive based on specific expression of contraction-related and structural genes. Mature smooth muscle cells cannot be identified by expression of a single gene, but instead by a profile of genes that encode contractile and/or cytoskeletal proteins including types of myosins, actins, MLCK, and others. All type II myosins have a similar structure that includes two heavy chains. Smooth muscle myosin heavy chain (smMHC) is encoded by a single gene (*MYH11*) while multiple genes encode NMM-II heavy chains. However, NMM-II is also present in smooth muscle and plays a role in the maintenance of muscle tone (96, 161). Additionally, there are multiple splice variants of smMHC and these may contribute to the contractile dynamics by changing the ATPase activity, allowing for slower crossbridge cycling and less energy use (75). There are multiple isoforms of actin that, in addition to quantity, dynamics, and localisation, may play a role in ASM force development (43, 163). The smooth muscle α-actin isoform (SMA) is specific to contractile cells and is used as a marker for myofibroblast differentiation, however ASM cells also express a contractile γ-actin in addition to the cytoskeletal γ-actin and β-actin (60). A single gene, *MYLK1*, encodes both non-muscle and smooth muscle MLCK; however, different promoter sites lead to three different transcripts and proteins of different sizes. The intermediate sized protein is attributed to smooth muscle MLCK, while the larger protein is considered the non-muscle form of MLCK (43).

Thus, although the contractile machinery is similar, there are important changes in protein expression and structural organisation that differentiates a smooth muscle cell from non-muscle or skeletal muscle cells, providing unique functionality. However, the phenotype and maturity of a smooth muscle cell is a continuum of functional, genomic,

and proteomic characteristics, complicated by the fact that other cell types can express smooth muscle specific genes in certain situations (132) and smooth muscle may not always express contractile genes. This ability to express a range of phenotypic characteristics, known as phenotypic plasticity, is itself an important characteristic of smooth muscle cells that will be discussed in the following section.

1.4.2 Airway Smooth Muscle Cell Plasticity

The chief function of smooth muscle cells is contraction, however, these cells are uniquely multifunctional and have the capacity for migration, proliferation, ECM synthesis, and growth factor/cytokine secretion (65). This functional diversity is achieved by both mechanical and phenotypic plasticity. In contrast to skeletal muscle, smooth muscle cells have been shown to adapt to changes in length and baseline tone to maintain the ability to generate the same magnitude of force (23, 106). The mechanisms for this mechanical adaptation are unknown, however, it may play a role in asthma by contributing to AHR (see chapters 1.6 and 1.7). On the other hand, phenotypic plasticity is a broader term that refers to an ever growing body of evidence that smooth muscle cells can change gene and protein expression in order to perform functions other than force generation. However, mechanical and phenotypic plasticity are likely integrated as they involve many of the same effector proteins.

The concept of phenotypic plasticity in ASM was first developed based on observations that canine ASM in culture demonstrated two divergent populations: long, spindle shaped cells that expressed an abundance of contractile proteins, and flat cells with a much lower expression of contractile proteins (86). Further studies showed that ASM cells in growth culture conditions naturally become less contractile and more

proliferative (30), a process termed “modulation”, and this could be partially reversed such that cells returned to a more contractile phenotype as they become quiescent (86), a process termed “maturation”. Thus it appears that smooth muscle cells are “quiescently differentiated”, suggesting that mature contractile smooth muscle is in G0 and can be induced to enter the cell cycle.

The phenomenon of phenotype switching has led to a list of ASM phenotypes, each one displaying a different functional profile including contractile, proliferative, secretory, and potentially hypercontractile (69). Although each phenotype is individually defined, a more appropriate picture would be to view ASM phenotype as a continuum of functional, and gene/protein expression profiles that may not be mutually exclusive. Although smooth muscle cells appear to have the ability to display the synthetic and proliferative phenotype both together and separately, here I will consider them as a single phenotype (referred to as proliferative from here) as they are not individually well defined.

The proliferative phenotype is demonstrated when ASM cells are cultured at subconfluence in the presence of a mitogen (30). This phenotype is chiefly defined by an increase in proliferative capacity and secretory function, as well as increases in synthetic organelles and a decrease in contractile function. Modulation also results in a change in gene and protein expression such that contractile genes are down regulated and synthetic genes are up regulated, thus the markers for this phenotype involve proteins such as non-muscle MHC, vimentin, and CD44 (64).

Maturation occurs when cells reach confluence and/or are serum deprived for prolonged periods (86). The contractile phenotype is defined by an increase in contractile

protein content, elongated morphology, as well as associated changes in protein expression. The markers for the contractile phenotype are proteins that are associated with smooth muscle contraction such as SMA, smMHC, and Sm22α (64).

Based on definitional descriptions of the synthetic and contractile phenotype, it appears that these phenotypes are functional, morphological, and genetic opposites. However, in asthma there is evidence that both proliferation and contractile function are increased in the airway. As discussed in section 1.2, asthmatic airway remodelling includes an increased mass of the ASM layer of the airways. This increased mass is due to both an increase in the size and mass (hypertrophy) (15) and number (hyperplasia) of ASM cells. Researchers have cultured ASM cells from both healthy and asthmatic airways and found that they are more proliferative in culture (74), but are also more contractile (85). Therefore, asthma, which is characterised by hyperplasia as well as hypercontractility, may involve cells that are either both more proliferative and more contractile, or the presence of two cell populations. This has led to the theory that "healthy" ASM is an intermediate phenotype that is quiescent, but can be driven to become more synthetic, proliferative, and/or contractile (159). Furthermore, studies have shown altered protein expression in asthmatic ASM (17) and both ASM hyperplasia (104) and altered phenotype (121) have been associated with decreased lung function. However, while many studies suggest inherent differences, others have shown that asthmatic ASM are not functionally or phenotypically different from healthy ASM (153). Thus, the question of whether AHR is caused by ASM cells that are unhealthy or by normal cells in an unhealthy environment is a subject of much debate (59). However,

exploring the mechanisms that contribute to phenotypic changes, such as the studies conducted in this thesis, may contribute to clarification of the issue.

1.5 Substrate Stiffness

As discussed in Chapter 1.2, components of airway remodelling, such as the thickened basement membrane and increased ECM deposition, are thought to contribute to a stiffer airway, and these changes are hypothesised to contribute to hyperresponsiveness by inducing changes in the ASM. An ever-growing body of evidence showing that substrate stiffness is a potent modulator of multiple cellular processes supports this hypothesis. Early observations that most cells only survived when attached to a substrate (88), and then later that epithelial cells only differentiated on soft floating collagen gels (37), suggested that the mechanical properties of the substrate play an important role in cell function. However, it was only in 1997 that Pelham and Wang developed a model that allowed for independent control of the elastic modulus of substrates (102). By altering the concentrations of acrylamide and bis-acrylamide, they were able to produce polyacrylamide (PA) gels that had a wide range of controllable stiffness, ranging from 150 Pa to more than 75 kPa (Young's Modulus). Polyacrylamide gels are ideal for use in cell culture studies as they provide the ability to isolate mechanical and chemical signals for independent control as neither cells nor proteins adhere to untreated gels.

Using PA gels, Pelham and Wang demonstrated that on softer substrates cells spread less, were irregularly shaped, and had weaker, transient focal adhesions (102), suggesting that cells can sense and respond to changes in substrate stiffness via

mechanotransduction machinery described in section 1.3. Over the next 10 years, responses, such as increased spreading, migration, and traction force on stiffer substrates were shown in many cell types (7, 38, 83). In 2006, an important study was published by Engler et al., showing that the modulus of the substrate not only determines CSK dynamics, but potently affects gene and protein expression (39). In this study, three ranges of substrate stiffness were chosen that mimic the physiological environment in which brain, muscle, and bone cells differentiate. On these stiffnesses mesenchymal stem cells (MSCs) began to take the shape of neurons, myoblasts, and osteoblasts respective to the substrate stiffness and, importantly, cells also began to express genes and proteins that were early markers of differentiation for each respective cell type. Interestingly, this effect could override biochemical signals that have been long known to determine differentiation. More evidence that substrate stiffness affects gene and protein expression is found in the proliferative response. Indeed, cells are less proliferative on soft substrates as compared to stiff substrates (95, 105, 141, 149).

Studies from our lab and our collaborators have shown that substrate stiffness also affects both the function and phenotype of ASM cells. Our collaborators found that ASM cells are more proliferative on stiff substrates as compared to soft substrates (95) and apply more traction force and demonstrate increased cell spreading (7). Other recent studies have shown that human lung fibroblasts grown on stiff substrates express more SMA mRNA along with increased levels of SMA protein and that this occurs via a serum response factor (SRF) mediated transcription pathway (70). Interestingly, when lung fibroblasts are explanted directly onto soft and stiff substrates, the substrate effect on SMA, proliferation, and contractility is maintained through multiple passages, even when

the cells are then subcultured onto the opposing stiffness (14). Although these studies are in fibroblasts, these results suggest that fibrosis may contribute to more contractile cells in the airways.

In our lab, we recently demonstrated that ASM cells have a higher baseline tone on stiff substrates and show an exaggerated response to a maximal dose of a contractile agonist (152). Furthermore, the expression of the contractile proteins smMHC and MLCK are increased, while MLCP is decreased (152). Taken together, this suggests that a stiff substrate would cause ASM cells to have more contractile phenotype. This implies a potential mechanism for ASM dysfunction contributing to AHR in asthma in which the increase in ECM components and connective tissue in the airways would lead to a stiffer substrate for ASM cells, causing these cells to be hypercontractile. However, although this evidence suggests that substrate stiffness alters the contractile phenotype of ASM cells via transcriptional regulation, changes in mRNA expression on different substrate stiffnesses has not been previously investigated. Additionally, any factor that alters inside-out and outside-in signalling, which govern the response to substrate stiffness, may affect the functional and phenotypic cellular response. Indeed, in asthma there are other mechanical factors that may influence cells differently, such as strain due to breathing, and baseline cell tone, and these must be considered when investigating how the mechanical environment affects ASM.

1.6 Strain

1.6.1 Deep Inspiration

Strain is an important factor to consider when discussing how the mechanical environment contributes to asthma not only because breathing is an obvious influence in the airways, but because asthmatic airways respond to strain differently than healthy airways. A deep inspiration that stretches the airways greater than tidal breathing can be a potent bronchodilator. Multiple studies, both clinical and *ex vivo*, show that after induced constriction, a deep breath (or large stretch) can soften the airways and reduce responsiveness for a short period of time (73, 99, 112). In addition to this bronchodilatory effect, a deep breath before induced bronchoconstriction can prevent airway stiffening, known as the bronchoprotective effect (26). However, both bronchodilatory and bronchoprotective effects are reduced, absent, or even reversed in moderate to severe cases of asthma (77, 80, 117).

1.6.2 Fluidization vs. Reinforcement

As briefly mentioned in Chapter 1.4, the contractile machinery in ASM cells is highly plastic and can adapt to mechanical changes, including stretch, due to the phenomenon of length adaptation. If an ASM cell is allowed to adapt to either an increase or decrease in length, the cell maintains the ability to generate the same maximal force as it did at the initial length (106). This length adaptation shows that strain can have important acute functional effects on these cells. The cellular response of ASM to strain is well studied, but has been contentious in recent years due to the observation of two seemingly opposing responses to stretch: reinforcement and fluidization. Early studies

showed that in tissue strip preparations, length oscillations caused sections of airway tissue to generate less force with increasing stretch (45, 58). More recently, cell culture techniques (traction force microscopy and optical magnetic twisting cytometry) have shown similar responses *in vitro* in individual cells. In response to an acute stretch, cells soften, but then recover stiffness over time (139). Interestingly, this immediate fluidization response is unaltered by pharmacological agents that affect signaling pathways, and along with an instantaneous time course, is evidence that fluidization is more of a material response, independent of chemical signaling pathways (31, 78, 139).

Reinforcement, the opposing response to stretch, has been characterised as a response to localised strain. In these studies a variety of methods are used for short applications (~minutes) of localised force to integrins, leading to formation and strengthening of focal adhesions, CSK remodelling and increased actin filaments, as well as an increase in cell stiffness (34, 48, 91, 147). Unlike the fluidization response, reinforcement is highly dependent on various signaling pathways and relies on the polymerization of actin (91, 143, 144).

Fluidization and reinforcement seem like opposing responses but are likely homeostatic opposites (31, 78, 139). Reinforcement appears to occur in response to localised strain to help the CSK bear increasing loads, whereas fluidization is thought to allow the cell to maintain function after cell wide stretches.

It is important to note, however, that all studies discussed so far have applied strain on a time scale of minutes to hours and focus on contractile properties of ASM. It is therefore difficult to draw any conclusions about how strain may affect the airway in chronic conditions, such as asthma. A series of studies from Smith et al. show that

chronic oscillatory strain has potent effects on ASM contractile properties, as well as other cellular responses. Chronic stretch leads to stiffer, more contractile cells (122, 126, 127) that are longer and more tubular in shape with a more organised CSK (123). In addition to these functional and structural changes, chronic stretch affects cell phenotype, increasing expression of the contractile proteins MLCK, smMHC, and desmin (125), and an increase in proliferation (124).

Although we are beginning to understand the acute response to stretch, the mechanisms responsible for chronic effects are still poorly understood and may be dependent on phenotypic changes. It is difficult to reconcile this stiffening response to chronic strain with the previous discussion of fluidization; however, some clues may be found in the recovery phase of the fluidization response. It appears that in all cases of acute whole cell stretch, cells do fluidise, but the recovery period can vary drastically depending on strain regimens. In some cases, cells recover stiffness that is up to 92% above baseline, therefore some cells eventually stiffen (78). It is noteworthy that previous exposure to chronic strain causes cells to recover to baseline stiffness faster than static cells (33). This may have important implications in asthma as the contractile response to an acute stretch can be altered by the presence of chronic strain. It is therefore possible that changes to the mechanical environment of ASM cells, whether it is a change in strain profile or substrate stiffness, could be contributing to the absence of relaxation in response to a deep inspiration.

It is interesting to note that at the integrin level, substrate stiffness and strain are studied using similar or identical techniques demonstrating the same reinforcement response (32, 142). Thus, it appears that at the molecular level, force has identical effects

whether it is applied externally to the cell, or through internal mechanisms (12, 48). What is still unknown, however, is how substrate stiffness and strain are mutually integrated as a cellular response. It becomes obvious that the internal tone or contractile force applied by the cell would alter this response. Therefore, cell tone must also be considered when discussing how substrate stiffness or strain affects ASM cells.

1.7 Cell Tone

The CSK of a cell and the contractile machinery provide both passive and active tension within the cell, which in turn contribute to the stiffness of the cell. In this thesis, cell tone is defined as the magnitude of active force generated at any given time within a cell. Changes in cell tone can be measured by changes in cell stiffness and can be altered by acute stimulation, such as administration of contractile agonists or relaxants.

In addition to the aforementioned length adaptation (chapter 1.6.2), there is a parallel plastic response to tone, which is known as force adaptation. In the presence of continuous tone elevation due to contractile agonists, ASM can increase the maximal force generated in response to repeated electrical stimulation (23), showing that these cells can adapt the maximal magnitude of force they generate to a higher baseline tone. Indeed, airway tone is an important factor in asthma pathology. Asthmatic airways have higher baseline tone compared to healthy airways that can be demonstrated by the standard diagnostic criteria for asthma. Asthma is diagnosed when there is more than 15% decrease in FEV1 upon administration of a relaxant agent (103). This means that in response to a bronchodilator, the airways relax and are thought to dilate to a larger extent than healthy airways, improving FEV1, and is associated with improvements in

breathing. The presence of high tone in asthmatic airways is also supported by evidence that endogenous contractile agonists, such as histamine and acetylcholine, are increased in asthmatic pathology (54, 156). Furthermore, clinical studies have shown that repeated increases in tone in asthmatic patients induces remodelling (55). Thus, clinical evidence suggests that high tone may contribute both directly to hypercontractiilty due to force adaptation and indirectly by inducing remodelling.

Such clinical evidence is also supported by other *in vivo* studies conducted in animal models. First, Gosens et al. showed that repeated administration of a bronchodilator reduces contractile function and contractile protein expression in a guinea pig model of asthma (50). Using an equine model of asthma, others found that treatments that increased baseline tone also caused an increase in airway resistance in response to methacholine, while agents that decreased tone demonstrated the opposite response (28).

Taken together, the *in vivo* evidence suggests that chronic increases in tone may lead to hyperresponsiveness, while chronic decreases may have the opposite effect. However, the *ex vivo* evidence exhibits a contradictory story. In a series of studies by Gosens et al. using smooth muscle tissue, they showed that while chronically reducing tone decreased contractile function and phenotype as expected (52), chronic increases in tone also decreased contractile function (51). Our lab has observed similar results in static ASM cultures where chronic increases in tone decreased both contractile function and MLCK expression (42).

The ASM tissue and cell culture experiments are at odds with both *in vivo* research and asthma pathology; if asthmatic ASM has higher tone and high tone actually reduces contractile function, then how does asthma even develop in the first place? Our

lab has demonstrated an intriguing answer to this question by showing that the presence of strain changes the effects of chronic tone modulation. In the presence of chronic oscillatory strain, cells with high tone have higher contractile function and phenotype, while cells with low tone show the opposite contractile response (42). Therefore, the true effect of chronic tone modulation may be entirely different under physiological strain conditions. This study also suggests that high tone in asthma, in the presence of strain, may contribute to hyperresponsiveness.

The evidence presented above suggests that high tone may contribute to asthma pathology, and this is supported further by *ex vivo* tissue strip studies showing that force and length adaptation are additive (24). Length adaptation can occur in the presence of force adaptation and vice versa, leading to ASM tissue which can generate higher forces and any length (24). Therefore, there appears to be no check or negative feedback mechanism on force-generation in ASM, which means that increases in tone could exaggerate the stiffening response to strain and contribute to airway narrowing. However, asthma is not a progressive disease with a runaway pathology that eventually causes airways to close all together, as this hypothesis would suggest, demonstrating the need for a better understanding of how ASM cells respond to mechanical cues.

1.8 Integrative Response

Thus far, I have discussed how substrate stiffness, strain, and tone in isolation each play an important role in asthma pathology. However, when discussing tone, it became clear that these factors interact as the presence of strain had a drastic effect on the cellular response to tone. If the mechanical environment is driving asthma pathology, then to

accurately model an asthmatic conditions, it is important to consider the interactions between contributing factors. The limited knowledge we have on mechanotransduction also highlights the importance of examining the interplay of mechanical factors as it is likely that there is a great deal of overlap and cross-regulation between sensing mechanisms.

The major barrier in examining substrate stiffness and strain in combination has thus far been the lack of, and difficulty in developing, appropriate models. Although there are well known, reliable models in isolation, they are difficult to combine due to the inherent inert nature of the materials. One method to study traction forces in response to strain and substrate stiffness in concert was developed by Krishnan et al., called Cell Mapping Rheometry (CMR) (78). This model makes use of the previously discussed PA gels developed by Pelham and Wang. Cells are grown on PA gels and biaxial strain is applied by lowering an annular punch to indent an area of cells, thus applying strain. Using this method, researchers showed that although there were differences in traction forces generated by cells on different substrate stiffnesses under static conditions, these differences disappeared after stretch was applied (78). This is interesting as it confirms that the presence of stretch can alter cellular responses, but is not applicable within the framework of asthma pathology. First, this method only tests the effect of acute transient stretch, while asthma is a chronic condition and requires the application of chronic oscillatory stretch. Second, this method only applies strain to a small population of cells, and although it is still possible to measure cell stiffness, it would be difficult to measure gene expression. Because the phenotype of ASM cells in asthma may be altered,

measuring gene and protein expression is integral for the investigation of asthma pathology.

Our collaborator, Dr. K. Billiar, has had some success in combining PA gels with the Flexcell Tension System to apply universal strain to a large population of cells for longer time periods. Using this model, they found some intriguing evidence that the presence of strain differentially affects the cell spreading response on soft and stiff substrates. On stiff substrates, 12 hours of 10% oscillatory strain reduced cell spreading, while on soft substrates, cells increased spreading in the presence of strain (134). Therefore, the presence of strain attenuated the cellular response to substrate stiffness (134) in these studies, but previous studies in our lab showed that strain exaggerated the cellular response to tone (42).

Based on this evidence, although it is obvious that both strain and substrate stiffness are important, it is difficult to predict how substrate stiffness in the presence of strain could alter ASM function, and how this may contribute to asthma pathology. This may be because the interaction of strain and substrate stiffness has been examined on a relatively short time scale (minutes to hours) and using non-ASM cells. In contrast, to elicit phenotypic changes in ASM cells, chronic strain is generally applied for 5-14 days.

In summary, previous studies in our lab show that the presence of strain exaggerates the contractile response to chronic tone modulation (42), while studies from other labs suggest that a stiff substrate along with chronic increases in tone also cause an exaggerated contractile response (94). Additionally, others have shown that force and length adaptation can occur cooperatively and can have an additive effect (24). Therefore, I hypothesize that the combination of stiff substrates with either physiological strain, or

high cell tone, would lead to extremely contractile and stiff cells. The combination of substrate stiffness, strain, and cell tone may be harmful to the airway and is a potential contributor to AHR.

1.9 General Hypothesis

The mechanical environment is an important modulator of many cell processes. It is well known that both substrate stiffness and strain can have potent effects on cells including changes in function, morphology, and gene and protein expression. However, the process in which external mechanical cues are translated into a cellular response is active and often depends on autoregulation of cell tone. In asthmatic airways, ASM is exposed to a stiffer environment, constant oscillatory strain due to breathing, and has higher cell tone. Therefore, it is possible that these changes in cellular airway mechanics may be driving changes in the ASM, contributing to the hyperresponsiveness that is characteristic of asthma pathology. Indeed, smooth muscle cells have shown remarkable functional and phenotypic plasticity and can easily display a more contractile phenotype in culture in response to many different chemical and mechanical cues (159). In culture, the contractile ASM phenotype is characterized by long cells with increased contractile function and increased expression of smooth muscle specific genes. Previous work by us (152) and our collaborators (125, 126) has shown that chronic strain and substrate stiffness in isolation can increase the contractile phenotype of ASM cells *in vitro*. However, we do not know how cells respond to the combination of these external mechanical cues. Additionally, we have previously shown that the addition of tone modulation alters this phenotypic response to strain (42), but we have not studied whether

the addition of tone would alter the phenotypic response to substrate stiffness in the same manner.

The governing hypothesis for my thesis is that changes in the mechanics of the airway on a cellular level induce the contractile phenotype in ASM cells and these contribute to hyperresponsiveness, the hallmark of asthma pathology. Based on previous work in our lab, I hypothesise that the presence of either cell tone or strain will alter the chronic functional and phenotypic response to of ASM cells to substrate stiffness.

The basic approach I have employed in this thesis to test this hypothesis was to culture human ASM cells on polyacrylamide gels that spanned the estimated range of healthy and pathological airways (22, 82, 89) and subject these cells to chronic oscillatory strain or chronic tone modulation with pharmacological agents. Using this approach, I attempted to mimic mechanical changes that are present in asthmatic airways, providing for a more accurate assessment of the cellular response to substrate stiffness.

This research is significant as it provides valuable information about possible mechanisms that might underlie asthma pathology and characterises cues and behaviour for cellular mechanotransduction. Current treatments for asthma target disease symptoms by inducing ASM relaxation or inhibiting inflammatory pathways, but do not specifically target causes of the development or progression of the disease. Understanding the underlying causes of AHR could lead to better therapeutic targets. Additionally, understanding how the cell responds to substrate stiffness and strain, and how this is influenced by cell tone, will contribute to a better understanding of mechanobiology.

1.10 Thesis Aims

In this thesis, I examined how mechanical factors affect ASM cells *in vitro* in two sets of experiments. The specific aims of my thesis address modeling the combination of mechanical changes observed in asthmatic airways.

1.10.1 Aim 1

Optimise the model developed by K.Billiar (134) with intent to subject cells cultured on soft and stiff PA gels to chronic oscillatory strain and assess changes in contractile phenotype.

1.10.2 Aim 2

Assess chronic changes in contractile phenotype of ASM cells cultured on soft and stiff PA gels with the addition of an increase or decrease in cell tone.

Chapter 2: Common Methodology

2.1 Cell Culture

For most experiments, primary cells were used. Human ASM cells were collected from resected bronchial tissue obtained by informed consent, as approved by Capital Health District Authority Ethics Review Board, from multiple donors undergoing thoracic surgery with no history of airway disease. Primary ASM cells were extracted from tissue explants as previously described (42) and stored in liquid nitrogen at low passage until use. Before seeding in experimental conditions, ASM cells were defrosted and cultured to confluence in standard feeder media made of DMEM/F12 (Invitrogen 11330, Burlington, ON) with 10% FBS (Invitrogen 12483, Burlington, ON) and 1% penicillin-streptomycin (Invitrogen 15140, Burlington, ON). In select experiments (see section 3.2.1.2) I used an immortalised human cell line, obtained as a generous gift from Dr. William Gerthoffer (University of South Alabama). This cell line, which has previously been characterised elsewhere (53), was immortalised by stable transfection with expression vectors containing human telomerase reverse transcriptase.

In all experiments, cells were kept at 37°C in a humidified incubator with 5% CO_2. Human ASM cells from passages 2-5 were used for all experiments.

2.2 Polyacrylamide Gel Fabrication

Polyacrylamide (PA) polymerisation is a free-radical chain reaction that creates growing chains of acrylamide monomers that are randomly cross-linked by bis-acrylamide. The stiffness of the resulting gel is controlled by the concentration of

acrylamide and bis-acrylamide according to the recipes in Table 2-1 (recipes provided in personal communication with Dr. Dan Tschumperlin based on Mih et al., 2011 (95)). For this study, an unpolymerised solution was made in 25ml glass beakers using an adjusted volume of 40% acrylamide (Bio-Rad, #161-0142, Mississauga, ON) and 2% bis-acrylamide (Bio-Rad, #161-0140, Mississauga, ON) with distilled water for a total volume of 5 mL. The solutions were stirred and degassed for 10 minutes to remove air bubbles, as the free radical polymerisation process is very sensitive to the presence of oxygen. To initiate polymerisation, standard amounts (Table 2-1) of tetramethylethylenediamine (TEMED) (Bio-Rad, #161-0800, Mississauga, ON) and ammonium persulfate (APS) (Bio-Rad, #161-0700, Mississauga, ON) were added. APS is the source of free radicals for the polymerisation process, while TEMED is a catalyst that speeds free radical formation from APS. A solution containing 1% APS in distilled water was made fresh directly before each experiment as the hygroscopic properties of APS cause it to lose reactivity quickly once dissolved in water. Once polymerisation was initiated, the gel solution was quickly added to the desired surface as polymerisation occurs within minutes. Throughout this thesis "stiff" gels refer to PA gels produced as per Table 2-1 using recipe 8 (PA#8) with a theoretical elastic modulus of 19.2kPa, while "soft" refers to gels produced with recipes 3 or 4 (PA#3 and PA#4) with theoretical elastic moduli of 600Pa and 1200Pa respectively.

Table 2-1. Polyacrylamide gel recipes. PA gel recipes were provided by Dr. Dan Tschumperlin. Numbers along the top demonstrate the labelling system used in our lab and others. Each number is a gel that has a doubled Young's modulus of the previous. The corresponding concentration of acrylamide monomer and bis-acrylamide are also listed in the top table. The bottom rows contain specific amounts (μL) of each component per 1mL total volume.

	1	**2**	**3**	**4**	**5**	**6**	**7**	**8**
E (Pa)	150	300	600	1200	2400	4800	9600	19200
% acrylamide	3	3	3	3	7.5	7.5	7.5	7.5
% bis	0.04	0.048	0.058	0.107	0.034	0.053	0.117	0.236

40% acrylamide	**75**	**75**	**75**	**75**	**188**	**188**	**188**	**188**
2% bis	**20**	**24.2**	**29.1**	**53.7**	**16.8**	**26.7**	**58.4**	**118.2**
water	**804**	**799**	**794**	**770**	**694**	**684**	**653**	**593**
TEMED	**1.5**	**1.5**	**1.5**	**1.5**	**1.5**	**1.5**	**1.5**	**1.5**
1% APS	**100**	**100**	**100**	**100**	**100**	**100**	**100**	**100**
Total	**1000**	**1000**	**1000**	**1000**	**1000**	**1000**	**1000**	**1000**

2.3 Collagen Coating

Polymerised PA is a relatively inert surface, which is advantageous as it is non-toxic for cell culture. However, this also makes it difficult to coat with ECM proteins. The most commonly used method employs the photoreactive heterobifunctional crosslinker sulfosuccinimidyl-6-[4′-azido-2′-nitrophenylamino]hexanoate (Sulfo-SANPAH). Upon exposure to UV light, the nitrophenyl azide group on Sulfo-SANPAH integrates with the PA gel, leaving an N-hydroxysuccinimide (NHS) ester that is amine reactive and facilitates crosslinking of sulfo-SANPAH to collagen (67).

A solution containing 0.5mg/ml Sulfo-SANPAH (ProteoChem, #c1111, Loves Park, IL, USA) in 50mM HEPES buffer (pH 8.5) was placed on the PA gel surface and activated under UV (UVP**,** UVM-57 #95-0104-01, λ_{UV}=302nm, Upland, CA, USA) for 5 minutes. The Sulfo-SANPAH step was repeated for another 5 minutes under UV for each PA gel before rinsing at least three times in HEPES buffer. All steps involving unactivated Sulfo-SANPAH were performed in the dark due to its light sensitivity. The HEPES was then replaced with 1 mL of 100 μg/ml collagen (Type I Rat Tail, BD Biosciences, #354326, Mississauga, ON) in PBS and incubated overnight at 4°C. Excess collagen was rinsed off with PBS, leaving a uniform collagen coating chemically linked to the PA gel with a collagen density unaffected by gel stiffness (95). The gels were sterilised under UV light for 20 minutes prior to cell culture.

.

2.4 Imaging and Histology

Fixed cells were imaged using a Leica DM IRB microscope and a 10x or 20x objective. Images were captured with a Sensicam CCD camera with custom software (Beadtracker software (42)). Cells were rinsed in cytoskeletal buffer (CB) and fixed in 4% paraformaldehyde in CB for 15 minutes at 4°C. Cells were then permeabilised with 0.3% Triton X-100 and 4% paraformaldehyde in CB for 5 minutes at 4°C and rinsed with CB. Fixed cells were stored in CB-TBS at 4°C prior to staining. Cell nuclei were stained with 0.5μg/ml DAPI (Invitrogen, D1306, Burlington, ON), which binds to DNA, in PBS at room temperature on a shaker for 30 minutes. Filamentous actin was stained with 3U of phalloidin-AF488 (Invitrogen, A12379, Burlington, ON) in PBS at room temperature

on a shaker for 30 minutes. Stained cells were rinsed and stored in PBS prior to mounting on glass microscope slides. PA gels, fabricated on silicone (Aim 1) or on glass (Aim 2), were gently placed face down in mounting media (ProLong Gold antifade reagent, Invitrogen, P36930, Burlington, ON) on a glass slide. The slides were air dried before they were sealed by painting clear nail polish around the edge of the glass or silicone.

2.5 Contractile Function Measurements

Optical magnetic twisting cytometry (OMTC) is a method used to measure cell stiffness and has been described in detail elsewhere (42). Briefly, 4.5 μm diameter ferrimagnetic beads (kindly provided by Dr. J.J. Fredberg, Harvard School of Public Health, Boston, MA) were coated in Arg-Gly-Asp (RGD)-containing peptide (Peptite 2000, Integra Life Sciences, San Diego, CA, USA), which allows the beads to bind to integrins. In all experiments, ASM cells were serum deprived for 24 hours in IT media media consisting of DMEM/F12 (Invitrogen #11330, Burlington, ON) with 5.8 μg/mL insulin (Sigma-Aldrich # I1882, Oakville, ON) and 1.0 μg/mL transferrin (Sigma-Aldrich # T4382, Oakville, ON) prior to OMTC as proliferative cells may be less contractile (65). Beads were added to confluent ASM cell cultures and allowed to adhere for 20 minutes at 37°C. Any unbound beads were removed with gentle rinses in IT and incubated for another 20 minutes. The culture dish was mounted onto a custom microscope stage and the beads were magnetized twice in the horizontal field. A sinusoidal magnetic field at 0.5 Hz applied torque to the beads, causing them to twist. The bead displacement was tracked using a CCD camera (SensiCam, Cooke, Auburn Hills, MI) and was then used to calculate cell stiffness.

The torque applied to each bead (T) is determined by the amplitude of the applied magnetic field. A complex modulus (G^*) is calculated using the Fourier transform of the torque and the displacement of each bead as in equation 2.1, where f is the twisting frequency and i is the unit imaginary number $\sqrt{-1}$. The complex modulus is composed of a real component (G'), which is a storage modulus, and an imaginary component (G''), which is a loss modulus. The storage modulus (G') is a measure of cell stiffness with units of Pa/nm and has been shown to be proportional to other measures of cell elasticity (131). The median G' from well of cells (40-150 beads) is then used to calculate the mean from multiple wells for each group. There is a known skewness in the distribution of stiffness calculated for each bead, thus the median was used as it is less influenced by skewness compared to the mean. Beads that have a G''/G' ratio of less than 0.02 are discarded as these beads are likely not bound to cells. Contractility was measured as the change in cell stiffness in response to a maximal dose (80mM) of isotonic KCl (Sigma-Aldrich, Oakville, ON) to cause maximal contraction.

$$G^*(f) = \frac{\tilde{T}(f)}{\tilde{d}(f)} = G'(f) + iG''(f) \qquad (2.1)$$

Chapter 3: Substrate Stiffness and Strain Model

3.1 Rationale

The asthmatic airway wall is stiffer compared to healthy airways and this change in mechanical environment may contribute to AHR. Recently, we have found that cells cultured on substrates that have a Young's modulus in the range of the estimated stiffness of fibrotic airways are more contractile and express more contractile proteins compared to cells cultured on less stiff substrates (152). However, mechanotransduction pathways for strain and substrate stiffness are closely related and overlap, as discussed in chapter 1. Thus the presence of strain due to breathing in the airway may affect how these cells behave on substrates of physiological stiffness. Indeed, it has previously been shown that the presence of strain alters the contractile response of ASM cells to tone modulations (42). Therefore, my first aim was to determine whether the presence of strain also changes how cells respond to substrate stiffness. For this reason I attempted to develop a model to allow for chronic culture of ASM cells in the presence of strain while simultaneously exposed to substrates of physiological stiffness in order to simulate airway fibrosis in the presence of tidal breathing

In order to accomplish this, a model that includes substrates with tunable stiffness that can also be stretched for relatively long periods of time (>24 hours) was required. We have previously studied independent effects of strain and substrate stiffness in isolation using two separate systems: polyacrylamide gels and the Flexcell Tension System. Therefore, the most obvious solution was to combine these two familiar and reliable systems. Recently, a method that binds PA gels to Flexcell BioFlex plates was

published, demonstrating feasibility and experimental data on the combined effects of substrates stiffness and strain in valvular interstitial cells (134). Polyacrylamide gels, as described in chapter 1, are hydrogels that can be manipulated to have a Young's modulus from 150Pa to 76 800 Pa (95). In the Flexcell Tensions System, cells are cultured in six-well culture plates with silastic membranes and computer controlled vacuum pressure is applied underneath, imparting cyclic strain on the cells. Using these two methods, Throm Quinlan et al. (107) developed a method in which a silane is used to chemically bind PA gels to the Flexcell silicone membranes, allowing cells to experience strain while cultured on different substrate stiffnesses (Figure 3-1). In addition the development of the protocol, this study also characterised the strain profile that the cells experience on the PA gel while bound to the silicone membrane (134). This model, referred to as "Flexwells" for the remainder of this thesis, was chosen as an ideal starting point for our investigation of substrate stiffness and strain in ASM cells.

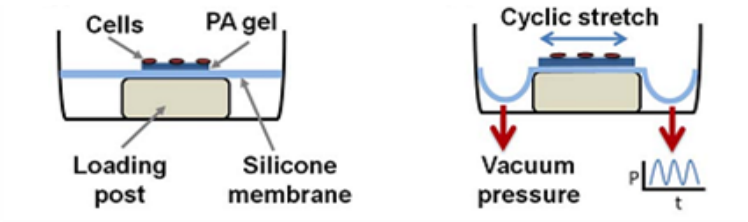

Figure 3-1. Schematic design of Flexwells. PA gels are chemically bound to silicone membranes in Bioflex silicone plates. Once cells are cultured on the gel, the plate is loaded into a gasket within an incubator. Vacuum pressure is applied underneath the plate and cells experience stretch. The set up shown here uses loading posts that produce biaxial strain. From: Throm Quinlan et al., 2011. (134)

Although the main purpose of this aim was to assess cellular response, optimisation of the model proved more difficult than initially anticipated. Therefore, this chapter largely focuses on the 4 approaches I used to develop a reliable model for assessment of the cellular response to chronic strain and substrate stiffness: characterisation of original

Flexwell model, alterations to original protocol, development of alternative protocols, and characterisation of surface chemistry.

3.2 Characterisation of the Original Flexwell Model

The model developed by Throm Quinlan et al. (107) combines substrate stiffness and strain using PA gels and the Flexcell Tension System, which are both well characterised methods that have been previously used in our laboratory. This Flexwell model would allow for the application of a characterised strain field to cells cultured on a range of substrate stiffnesses. However, in order to address phenotypic changes in ASM cells in response to substrate stiffness and strain characterisation of the model was necessary to confirm the ability to meet criteria specific to our needs (Table 3-1). First, because asthma is a chronic condition, we needed to confirm that the model could withstand strain of at least 3 days as Throm Quinlan *et al*. reported strain up to only 12 hours. Second, cellular responses were characterised using porcine valvular interstitial cells (VICs) or human mesenchymal stem cells (hMSCs), while we are interested in the response of human ASM cells. Thus, we needed to confirm that these cells could survive under physiological strain imposed by the model for at least 3 days. We also needed to ensure that cells could reach near-confluence, as this is required to measure contractile function using OMTC and to ensure sufficient RNA could be collected from a minimal number of wells. Additionally, these cells needed to reach this level of confluence while being serum deprived for 24 hours before OMTC measurements are be taken.

Table 3-1 Flexwell model requirements. Flexwell model as developed by Throm Quinlan et al. (134) compared to requirements necessary for Aim 1 of this thesis.

	Throm Quinlan et al.	Aim 1 Requirements
Model Durability	up to 12 hours 10% strain	at least 3 days 4-10% strain
Cell Type	porcine VICs and human MSCs	human ASM cells
Cell Survival	up to 6 hours	at least 3 days
Cell Population	sparse seeding to evaluate individual cells	at least 80% confluence required for OMTC and feasible RNA extraction
Serum Conditions	15% FBS	24 hours serum deprivation required for contraction

I hypothesised that the Flexwell model developed by Throm Quinlan et al. (107) could be used to meet all necessary criteria to investigate the chronic effects of substrate stiffness and strain on contractile phenotype of human ASM cells.

3.2.1 Methods

3.2.1.1 Flexwell Fabrication

The initial protocol for creating Flexwells was developed by Angela Throm-Quinlan in Dr. Kristen Billiar's Lab at the Worcester Polytechnic Institute (134). Throughout the initial stages of my project, I made many adjustments to the protocol and these will be described throughout this chapter. Here I will briefly describe the major steps and basic chemistry involved in the original protocol as obtained from Dr. Billiar.

The BioFlex silicone (BioFlex® Culture Plates, Flexcell Int. Corp., McKeesport, PA) was first treated with oxygen plasma using the SPI Plasma-Prep™ II Plasma Etcher at full power for 2 minutes to create hydroxyl groups on the surface. The surface was

then treated with 3-(trichlorosilyl)propyl methacrylate (TcPM) (Sigma-Aldrich # 64205, Oakville, ON). This silane is highly reactive due to the chlorinated silicon, therefore, a glass syringe was used to add 20µl of TcPM to a 1:4 mixture of CCl_4 (Sigma-Aldrich # 319961, Oakville, ON) and heptane (Sigma-Aldrich, # 246654, Oakville, ON) that was made anhydrous using 1g of molecular sieves (Sigma-Aldrich, #69839, Oakville, ON). Approximately 3ml of the TcPM solution was immediately added to each well of the BioFlex plate for 5 minutes and each well was then rinsed with hexane (Sigma-Aldrich, #296090, Oakville, ON). The plates were then dried and reshaped under vacuum for 5 minutes, which was necessary due to membrane swelling caused by the solvents. To maintain a low oxygen environment for PA polymerisation, the vacuum chamber was sealed and only opened once a steady flow of nitrogen had been established. The PA polymerisation solutions were then prepared as described in chapter 2.2. Immediately after initiator addition, 50µL of the appropriate PA mixture was added to each membrane and covered with a 22 mm glass coverslip (VWR, #48382 063, Mississauga, ON) that was pre-treated to be hydrophobic (see Appendix A.3.1). Gels were polymerised under nitrogen for at 45 minutes. The coverslips were then removed and the gels were collagen coated as described in chapter 2.3. A step-by-step summary of this protocol can be found in Figure 3-2.

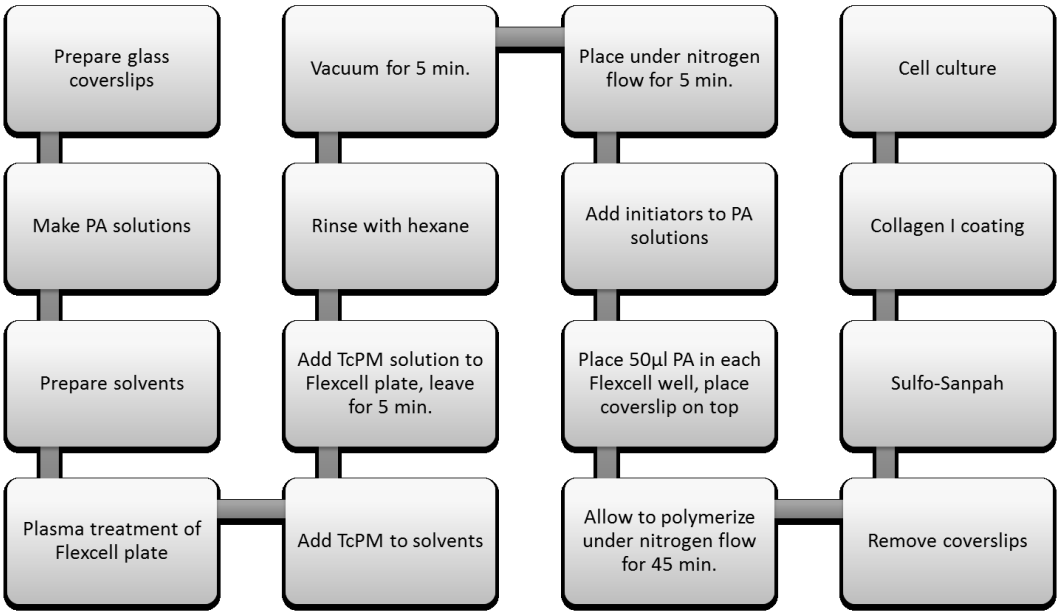

Figure 3-2. Step-by-step flowchart of the complete Flexwell protocol (134) showing the timing of each step of the protocol.

3.2.1.2 Strain Regimen

Initial experiments to determine the durability of the Flexwell model and survivability of cells were conducted using the Flexcell® FX-4000™ Tension System to impart oscillatory strain at 0.25Hz with physiological (5% biaxial) or supraphysiological (20% complex) magnitude. Static controls were prepared alongside experimental plates and placed in the same incubator beside the baseplate. Model testing experiments were carried out for three days with a covering amount of PBS in each well to maintain hydration. Human ASM cells were cultured on collagen coated Flexwells for 24 hours in standard feeder media containing 10% FBS before initiating strain and media was replaced every 24 hours throughout the strain regimen. In order to control for cell cycle progression and serum induced phenotype changes, standard OMTC protocols call for serum deprivation for 24 hours before measurement. Therefore, survivability under

different serum conditions was tested in standard feeder media containing 10% serum for all three days, or in 10% serum media for 2 days and one day in IT media. Contractility and stiffness measurements were performed with OMTC (as described in chapter 2.5) on membranes that were punched out of each well and affixed to a 35ml petri dish using vacuum grease. In OMTC experiments, an immortalised cell line of human ASM cells was used, as described in section 2.1.

3.2.1.3 Atomic Force Microscopy

Atomic force microscopy (AFM) has previously been used to measure the Young's modulus of PA gels (95) and is the most accurate method that is readily available. Dr. Laurent Kreplak (Department of Physics, Dalhousie University) provided access to equipment in his lab, and his student Sam Baldwin performed the measurements. Atomic force microscopy can be used as a microindentation method when used in the force-volume mode to generate force-indentation curves. The force curve is then fit to the Hertz sphere model to calculate the Young's modulus (36). Samples on silicon were prepared using the basic Flexwell protocol described above. The silicone membranes were then cut out of the Bioflex plate and placed in glass dishes used for AFM measurements. All samples were kept fully hydrated in PBS.

Measurements were taken using cantilevers with a spring constant of 0.134 N/m or 0.284 N/m with a 6.62 μm diameter borosilicate spherical tip. Force curves were generated at an indentation speed of 20 μm/s or 1.6 μm/s. The first 5 nm of the force curve was discarded and the Hertz sphere model was used to fit within the first 100 nm of the curve. Curve fits that have an R^2 value of less than 0.97 were discarded.

3.2.2 Results

Using the Flexwell protocol developed by Throm Quinlan *et al.* (107), Flexwells using PA recipes 6 and 8 (PA#6 and PA#8) were produced relatively quickly and easily (Figure 3-5A). These gels were generally fully polymerised and well bound to Flexcell silicone membranes, although consistency of success was poor at times.

Flexwell gels made using PA#6 or PA#8 withstood supraphysiological complex oscillatory strain of 20% for 3 days with minimal deformation. ASM cells cultured on Flexwells survived and grew to confluence under supraphysiological and physiological strain conditions for 3 days (Figure 3-3). Additionally, cells grew to confluence under all serum conditions. Contractility was assessed using OMTC after 24 hours of serum deprivation or in 10% serum media and under static or strain (5% biaxial) conditions. Although these cells did contract after 3 minutes of 80mM KCl there was a great deal of variability between wells (Figure 3-4B). The baseline stiffness of the cells was also extremely high (Figure 3-4A), likely due to the use of the immortalised cell line as these cells tend to be stiffer in culture. Regardless, this experiment demonstrates feasibility in using the Flexwell model to measure contractile function of ASM cells using OMTC.

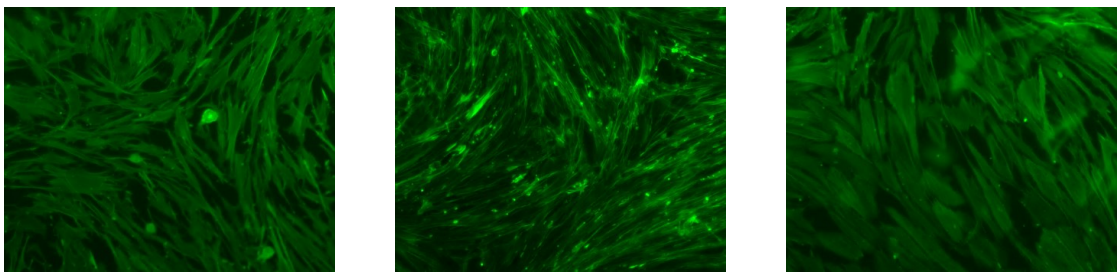

(A) (B) (C)

Figure 3-3 ASM cells survive on Flexwells under strain. Representative pictures of human ASM cells on stiff substrates after 3 days in static conditions (A) or with 5% (B) or 20% (C) strain.

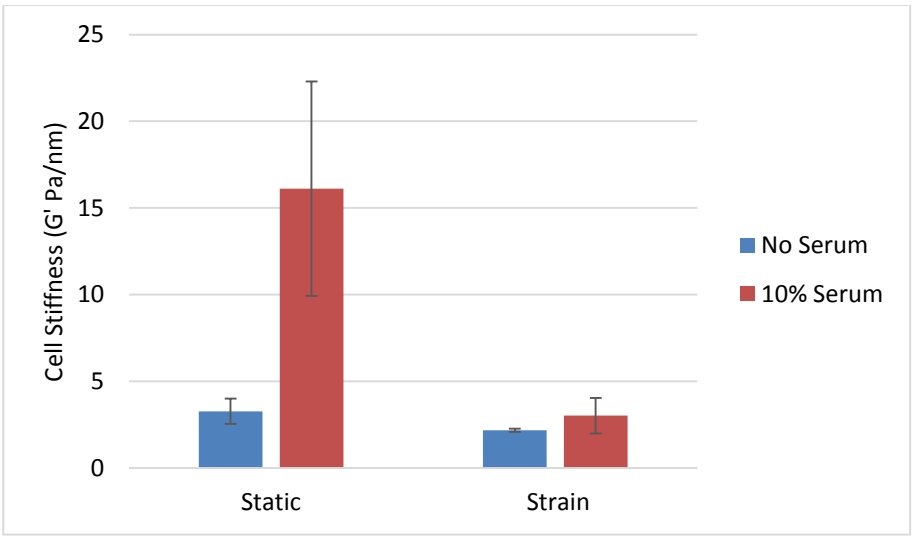

(A)

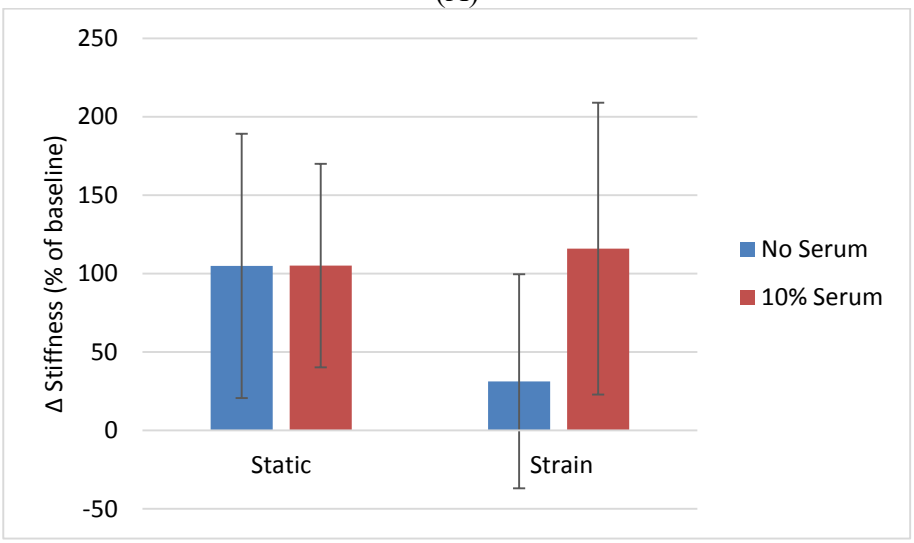

(B)

Figure 3-4 Flexwell contractile function demonstration. Immortalised human ASM cells were cultured for 3 days in 10% serum media (red bars) or for 2 days in 10% serum media and switched to IT media for the last 24 hours (blue bars). Baseline stiffness (A) was extremely high in these experiments. Generally, cells did contract in response to 3 minutes in 80mM KCl, but the variability was extremely high (B). Values are the means ± SE of wells within each group (n=3).

However, using the published protocol, gels softer than PA#6 were difficult to produce. Softer gels (PA#4 and PA#2) form either rings that have no gel in the centre, or very patchy gels (Figure 3-5B and C).

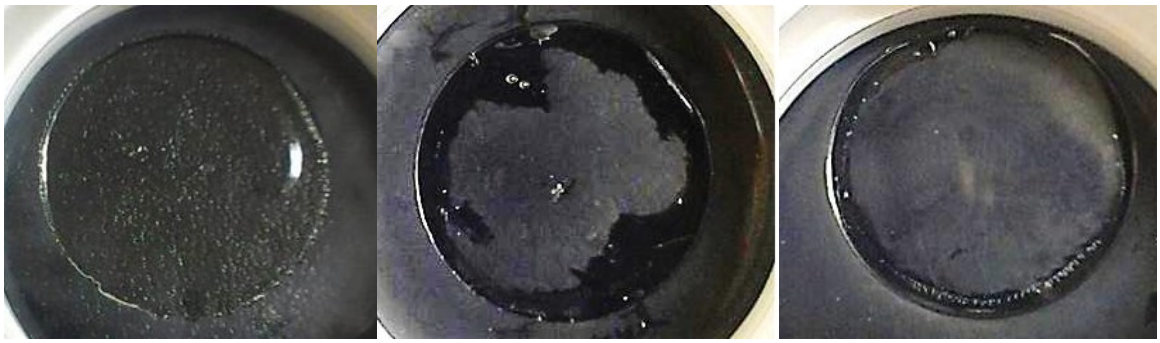

(A) (B) (C)

Figure 3-5 PA gels prepared using the original protocol from Throm Quinlan *et al.* (107). Representative pictures of complete PA#8 stiff gels (A, theoretical Young's modulus of 19.2kPa) and incomplete soft PA#4 (B, theoretical Young's modulus of 1.2kPa) and PA#2 (C, theoretical Young's modulus of 300Pa). Contrast has been adjusted in order to visualise incomplete gels.

The Young's modulus of fully or partially formed (in the case of PA#4 gels) PA gels bound to Flexcell silicone were very close to theoretical values (Figure 3-6).

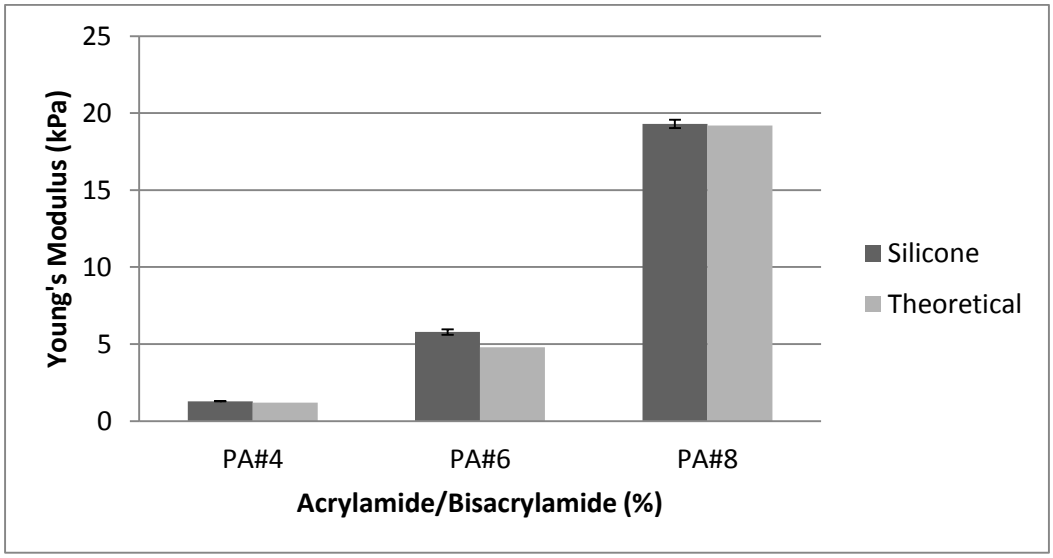

Figure 3-6 Measurement of Flexwell Young's modulus. Young's modulus calculated from AFM indentation curves of the first 100nm of PA gels bound to silicone membranes. These data are compared to theoretical values based on the acrylamide and bis-acrylamide concentrations (Table 2-1). Values are means of the Young's modulus calculated from multiple force curves on a single sample ± SE.

3.3 Alterations to the Original Protocol

The inability to consistently produce softer Flexwells (PA#4 gels with a Young's modulus of 1.2kPa and below) was unexpected. Therefore, I hypothesised that relatively simple modifications to the protocol, which would ensure proper function of key materials and equipment, would allow for more consistent production of soft Flexwells. I then identified critical steps in the protocol and divided these into four categories: hydrophobicity of the glass top coverslip, PA polymerisation solution, PA polymerisation environment, and the PA-silicone interaction.

3.3.1 Methods

3.3.1.1 Modification Details

Modifications to the protocol were divided into four categories based on the critical steps identified above. Modifications made in each category are briefly outlined below. A more detailed description of materials and methods used can be found in Appendix A.

Hydrophobicity of glass coverslip:

The glass coverslip (top slip) is placed on top of the polymerisation solution and wicks the liquid into a circular shape to ensure uniform thickness and a smooth surface. The coverslip must be hydrophobic so that it can be easily removed without detaching the gel from the silicone. In softwell fabrication, RainX, a commercial product designed to repel rain from automotive windshields, is used. However, the Flexwell protocol used SurfaSil Siliconizing Fluid (Thermo Scientific, #TS-42800, Bellefonte, PA, USA) for this

purpose. These two products were tested with different methods of application to ensure that soft gels were not sticking to the top slip.

PA polymerisation solution:

The polymerisation of PA is sensitive to inhibitors, particularly oxygen. Therefore, modifications were made to exclude as much oxygen as possible from the pre-polymerisation solution by placing the solution under vacuum or by bubbling nitrogen through the solutions. Additionally, due to polymerisation kinetics, gels with lower concentrations of acrylamide take longer to polymerise and are more affected by inhibitors. Therefore, gels were left to polymerise overnight to ensure complete polymerisation and TEMED was increased, which would theoretically increase the polymerisation rate.

PA polymerisation environment:

Polymerisation inhibitors may have also been introduced in the surrounding environment. To prevent any atmospheric oxygen getting trapped between the glass and the gel, coverslips were "rinsed" with high pressure nitrogen immediately before placing on the gels. The original Flexwell protocol calls for the BioFlex plates to be placed under vacuum and then under nitrogen flow and is required to dry and remove solvents from the membranes as well as removing oxygen from the polymerisation environment. Different vacuum chamber set-ups were used to ensure maximal vacuum strength. Additionally, in some trials, the nitrogen was replaced with less reactive argon gas, and in other trials polymerisation was attempted under vacuum pressure instead of under constant gas flow.

PA and silicone interaction:

Finally, the treatment of the silicone membrane itself was modified to have a longer exposure to oxygen plasma. Additionally, in the original protocol, the TcPM solution, which includes heptane and CCl_4 is rinsed off with hexane. This rinse step was repeated once or removed to test the inhibitory effect of these solvents on polymerisation.

3.3.2 Results

3.3.2.1 Hydrophobicity of Glass Coverslip

All SurfaSil methods allowed for stiff gels to form completely. However, PA#6 Flexwells did not fully polymerise using RainX alone.

3.3.2.2 Polyacrylamide Polymerisation Solution

Polymerisation of bulk PA gels using PA#4 and PA#2 recipes were tested. I hypothesised that increasing initiator concentrations would decrease polymerisation time, thus allowing for more complete polymerisation of soft gels. A single experiment was conducted in which polymerisation time and stiffness of the gels was measured. The control gels based on the PA#2 recipe did take nearly 4 times as long to polymerise as the PA#4 gels. However, increasing TEMED and/or APS 2x or 5x in PA solutions did not lead to any apparent change in polymerisation time. Additionally, an increase in initiator did seem to decrease the stiffness of the gels. This was especially apparent in the PA#2 gels, which became too soft to measure stiffness with any increase in initiator. Due to limitations of the methods used to measure polymerisation time and stiffness of the gels, in addition to the apparent lack of effect on polymerisation time, these experiments were

not repeated. Details of the specific methods used and results can be found in Appendix A.

Although the bulk gel experiments were inconclusive, I did attempt to increase the initiator concentrations in the Flexwell protocol. Neither a 5x increase in TEMED in the PA#4 recipe nor a 2X increase in the PA#2 recipe produced fully polymerised gels. Additionally, when the Flexwells were left overnight to increase polymerisation time, the gels were still not fully polymerised.

Methods used to reduce the amount of oxygen within the unpolymerised solution generally did not produce fully polymerised soft Flexwells. A single experiment in which nitrogen was bubbled through the unpolymerised solution to exclude oxygen produced fully polymerised PA#4 Flexwells, however, this success was not reproducible. Additionally, because temperature and pH are known to inhibit PA gel polymerisation, we confirmed PA gel solutions were at room temperature and measured the pH to be ~8.5 in all solutions.

3.3.2.3 Polyacrylamide Polymerisation Environment

Methods used to optimise oxygen removal from the environment surrounding the PA gels during polymerisation generally did not produce fully polymerised soft Flexwells. However, the success rate of stiff Flexwells was improved by using thicker tubing to connect the vacuum to the vacuum chamber, and by using a plastic vacuum chamber instead of glass, as well as "rinsing" the glass coverslips with nitrogen gas directly before placing them on the unpolymerised solution. For softer Flexwells, although some of these methods produced fully polymerised PA#4 Flexwells in single experiments, none

were reproducible. Additionally, there were a few experiments where the vacuum chamber was not closed properly, allowing large amounts of oxygen in. In these experiments, neither soft nor stiff gels polymerised.

3.3.2.4 Polyacrylamide Gel and Flexcell Silicone Interaction

The final critical step that was identified was treatment of the Flexcell silicone itself. Although removing the hexane wash step, along with increasing plasma time, was successful in a single experiment, it was not reproducible. A summary of these attempts and outcomes is presented in Figure 3-7.

Coverslip Hydrophobicity																		
Undiluted Surfacil - wipe + RainX	x					x	x		x	x	x		x	x	x	x	x	x
Diluted Surfacil - soak + 24 hr dry + RainX		x										x						
Diluted Surfacil - soak + 2 hr dry			x					x										
Diluted Surfacil - soak + 2hr dry + RainX				x								x						
RainX alone					x													
PA Polymerisation Solution																		
2x TEMED						x												
5x TEMED							x											
Overnight polymerisation								x										
Vacuum PA solution	x	x	x	x	x	x	x	x			x	x	x	x	x	x	x	x
No vacuum of PA solution									x									
Nitrogen bubbled through PA										x								
PA Polymerisation Environment																		
Polymerisation under vacuum											x							
Nitrogen "rinse" of coverslips	x	x	x	x	x	x	x	x	x	x	x	x	x	x	x	x	x	x
Increased membrane vacuum time												x						
Plastic chamber + thin tubing	x	x	x	x	x	x	x	x			x	x						
Glass vacuum chamber									x	x			x	x			x	x
Argon gas														x				
Plastic chamber + thicker tubing															x	x		
PA gel/Silicone Interaction																		
2x hexane wash																	x	
No hexane wash																		x
Longer plasma time																		x
																		Stiffness
																		PA#2
																		PA#4
																		PA#6
																		PA#8

Figure 3-7. Summary of modifications made to the original Flexwell protocol. Green squares represent PA gels that formed completely and were well bound to the silicone membrane while red squares represent incomplete gels. Although some modifications did produce fully polymerised PA#4 gels, these results were not reproducible.

3.4 Development of Alternative Protocols

Although some modifications to the protocol produced successful gels using the PA#4 recipe, none of these methods allowed for consistent production of the soft gels, continuing to limit use of this model for Aim 1 of this thesis. I then began to explore alternative methods to combine substrate stiffness and strain. The original protocol relied on the silane TcPM to bind the PA gels to the surface of plasma treated Flexcell silicone. This silane posed two potential problems to the protocol. First, TcPM is a chlorosilane, which is highly reactive and readily loses reactivity easily upon exposure to water and oxygen. This posed the constant possibility that individual experiments were not successful simply due to progressive loss of reactivity of the silane. Additionally, this silane requires harsh solvents for dilution and it was hypothesised that residual solvents may inhibit PA polymerisation. The second potential problem with TcPM was the propyl methacrylate R group. The presence of the vinyl group on the propyl methacrylate allows for the silane to be incorporated into the free-radical polymerisation process. As stated in section 3.3.2.2 (and detailed in Appendix A), I observed a potential change in stiffness and polymerisation time with changes to the polymerisation conditions (increased initiators), suggesting that small changes to PA chemistry may affect polymerisation.

Therefore, I developed alternative protocols that would avoid the potential problems that TcPM use presented by either using different silanes (TmPM and amino protocols), different methods of silane deposition (vapour deposition), or avoiding the use of silanes altogether (benzophenone protocol). The first alternative replaced TcPM with the less reactive TmPM. The second alternative, the amino protocol, was based on the method used to make softwells, which are PA gels bound to glass coverslips (detailed

protocol can be found in chapter 4.2.1). This method requires the silicone surface to be coated with amino groups and then uses glutaraldehyde to cross-link the amino group in acrylamide to the silicone. I hypothesised that this would be advantageous as the amino group on acrylamide is not involved in the polymerisation process, thus separating the chemical processes that bind the PA to the silicone and cause polymerisation. I also tested vapour deposition methods to apply silanes to Flexcell silicone, thus preventing the use of solvents. I additionally attempted a recently published protocol that does not require the use of silanes and instead uses benzophenone to bind PA to polydimethylsiloxane (PDMS).

3.4.1 Methods

For all alternative protocols plasma treatment was performed as per the original protocol (see chapter 3.2.1.1) and polyacrylamide gel preparation was performed as described in chapter 2.2. All alternative protocols differ in the method used to chemically bind PA gels to a silicone surface, thus, unless otherwise noted, steps after surface treatment are the same as the original protocol (see chapter 3.2.1.1).

3.4.1.1 Amino Protocol

There were a few variations of this protocol. First, an amino-functionalised surface was obtained either with BioFlex plates (BioFlex® Culture Plates, Flexcell Int. Corp., McKeesport, PA) that were pre-coated with ProNectin (#BF-3001P) or amino groups (#BF-3301A). Alternatively, uncoated BioFlex plates (#BF-3001U) were treated with oxygen plasma followed by 150µl of undiluted (3-aminopropyl)trimethoxysilane (AMPS) (Sigma-Aldrich, #281778, Oakville, ON). Excess AMPS was rinsed off with distilled

water, leaving amino groups chemically bound to the BioFlex membranes. The amino-functionalised membranes (pre-coated or AMPS treated) were then soaked in 0.5% glutaraldehyde in PBS for 30 minutes and rinsed in distilled H_2O before continuing as per the original Flexwell protocol.

3.4.1.2 Vapour Deposition and Alternative Silane

Based on recommendations from Dr. David Juncker (McGill University, Associate Professor, Biomedical Engineering), a specialist in surface chemistry, I developed protocols that made use of a less reactive silane and alternative deposition methods. I first tried replacing the TcPM with 3-(trimethoxysilyl)propyl methacrylate (TmPM), which is an identical silane with the exception of having three methoxy groups bound to the silicon instead of chlorine groups. The switch of chlorine with methoxy causes TmPM to be much less reactive, requiring less harsh solvents compared to TcPM dilution. Although ethanol does cause swelling of silicone based materials, the effect is drastically reduced compared to the harsher solvents used in the original Flexwell protocol. I then tried to exclude the use of solvents altogether by using a vapour deposition method to coat the silicon with either TcPM or TmPM.

For wet TmPM deposition, 125µl of TmPM (Sigma-Aldrch, #M6514, Oakville, ON) and 750µl of 10% acetic acid were added to 25 ml of ethanol, as recommended by the manufacturer. The BioFlex wells were soaked in the TmPM solution for 5 minutes and then rinsed in ethanol. For vapour deposition a glass pipet was used to place a few drops of the silane (TmPM or TcPM) on a glass microscope slide, which was then placed in a desiccator alongside an oxygen plasma treated BioFlex plate. The desiccator was then placed under vacuum for 24 hours.

3.4.1.3 Benzophenone

This new method uses the UV activated chemical benzophenone instead of silanes to bind PA gels to a silicon material (120). In this method, 10%wt/vol benzophenone was dissolved in a 35% acetone solution and placed on the membranes for 1 minute. The acetone swells the membrane, allowing the benzophenone to be impregnated within the surface of the silicone. The membranes are then rinsed with methanol and dried under vacuum then nitrogen flow until the PA solutions are added to each well as per the original Flexwell protocol. Instead of polymerising under nitrogen flow, the plates were then removed from the desiccator and placed under UV light (UVP**,** UVM-57 #95-0104-01, λ_{UV}=302nm, Upland, CA, USA), which initiates benzophenone attachment to the PA as it polymerises.

3.4.2 Results

The initial attempts to make Flexwells using pre-coated amino or ProNectin BioFlex plates did allow for full polymerisation of PA gels. However, due to the hydrophobic nature of the silicone, the gels did not wick under the entire area of the glass coverslip and formed very thick, uneven gels. These gels were also poorly bound to the silicone and were easily removed. Plasma etching the silicone before treatment, creating a more hydrophilic surface, allowed the gel to fully spread and polymerise. Although the gels appeared to be bound to the silicone upon stretching, the PA gels peeled off when left under static conditions in PBS overnight. Additionally, when the same method was applied to uncoated Flexcell plates (no amino groups), the gels polymerised and appeared to bind to the silicone, but similarly peeled when left overnight in PBS.

I used AMPS to coat untreated Flexcell plates with amino functional groups as an alternative to the amino coated BioFlex plates. Flexwells made using this method produced patchy gels that were unpolymerised in some areas while areas that were polymerised were poorly bound to the silicone. Wet TmPM deposition generally produced fully polymerised stiff gels, but softer PA#4 gels still did not polymerise. Similarly, vapour deposition of either silane produced polymerised stiff Flexwells, although this was inconsistent, and polymerised soft gels remained elusive.

Using the benzophenone method, both PA#8 and PA#4 gels formed on PDMS, although they were not well bound to the surface and could be easily pulled off. Since the protocol did not call for plasma treatment, the hydrophobicity of the PDMS caused irregularly shaped gels, similar to previous experiments. Therefore, untreated Flexcell plates were treated with oxygen plasma before benzophenone treatment, however, even PA#8 gels did not fully polymerise in this experiment.

3.5 Analysis of Surface Chemistry

The process of making Flexwells using any protocol requires many steps, making it difficult to determine which parts of the protocol were failing. Thus, in a final attempt to understand why none of the protocols produced fully polymerised soft Flexwells as expected, I analysed the surface chemistry of the Flexcell silicone that had been treated as per the original protocol, as well as some of the alternatives. Specifically, x-ray photoelectron spectroscopy (XPS) was used to quantify elements present on the surface. I hypothesised that the amount of silicon, oxygen, carbon, chlorine, and nitrogen would change with chemical treatment of the silicone.

3.5.1 Methods

3.5.1.1 X-ray Photoelectron Spectroscopy

X-ray Photoelectron Spectroscopy (XPS) is a surface analysis technique that can be used to quantify the elemental make-up of the surface of a material. In this technique, a material is irradiated with an X-ray and due to the photoelectric effect, electrons are ejected from atoms on the surface of the material. The kinetic energy level at which an electron is ejected is related to its initial binding energy within the atom, and therefore, can be related to specific elements and chemical groups. An electron energy analyser counts how many electrons are ejected at different kinetic energy steps. This data is plotted as the number of electrons versus binding energy and peaks occur that correspond to specific elements. These peaks are then curve fit and the area under these curves provides a quantitative analysis of the elements present on the surface of the material. I calculated the atomic percent of each element measured (nitrogen, oxygen, carbon, chlorine, and silicone), assuming that these were the only elements present in any detectable amount at critical steps in the original protocol.

All XPS analysis was performed by Andy George with equipment provided by Dr. Ted Monchesky (Department of Physics, Dalhousie University). Bioflex plates were prepared for each condition as per previously described methods in the original Flexwell protocol for plasma treated and TcPM samples (see chapter 3.2.1.1) and alternative methods for TmPM and AMPS (see chapter 3.4.1 TcPM wet protocol and amino protocol). A sample ~ 1 cm in diameter was cut out from each membrane in an argon filled vacuum bag and placed in a vacuum chamber for transport.

Silicone samples were irradiated with monochromatic X-ray source (Al Kα 1486.6 eV) operated at 14.7 kV with a 26 mA emission current. Samples were mounted on stainless steel stubs using adhesive carbon tape and then loaded into a thermal evaporator. A 1mm diameter gold dot was deposited on the centre of the silicone sample, which was used to calibrate the energy scale as silicone is an insulating material and considerable charge can accumulate during irradiation. Samples were then loaded into the XPS load lock held at ~$2x10^{-7}$ torr and transferred one at a time to the analysis chamber, where pressure was held between $1x10^{-8}$ and $1x10^{-9}$ torr. A survey scan of each sample was performed at a resolution of 1 eV and a pass energy of 50 eV. High resolution (0.1 eV) survey spectra of the Au4f, C1s, O1s, Si2p, N1s, and Cl2p peaks were performed at 30 eV pass energy.

The XPS peaks were processed using CasaXPS software with the Shirley background correction method and peaks were fit using a Guassian/Lorentzian function. The area under each curve was corrected using sensitivity factors and the transmission function of the analyser. The atomic percent of each element was calculated as the ratio of the corrected area under all curves for that element to the total area.

3.5.2 Results

The untreated BioFlex silicone surface was composed of 42.3% carbon, 35.3% oxygen, and 22.4% silicon. Oxygen plasma treatment decreased the relative carbon content on the silicone surface to 20.9% and increased oxygen to 55.1%, leaving silicone relatively unchanged (23.9%) (Figure 3-8A). The narrow scans for C1s, O1s and Si2p showed that oxygen plasma treatment did not cause a chemical shift of the carbon or oxygen peaks, although the carbon peak may be slightly narrower. However, the silicon

peak shifted to a higher binding energy with the peak at 103.5eV compared to the untreated silicon peak at 101.9eV (Figure 3-8B). The untreated, oxygen plasma, TmPM, and TcPM samples all had undetectable levels of chlorine and nitrogen.

Treatment with TcPM decreased surface carbon content and increased oxygen (50.3% and 32.8%) by a large amount, and slightly decreased the silicon content (16.9%) (Figure 3-8A). In contrast, TmPM treatment had little effect on the relative surface content of carbon, oxygen, and silicon (25.3%, 51.5%, and 23.1%) compared to the plasma treated sample (Figure 3-8A). The narrow scans show that although the oxygen and carbon content differ in magnitude, the peaks for TmPM and TcPM samples are very similar, peaking at approximately 531 eV and 283.4 eV (oxygen and carbon respectively), which is slightly lower than the untreated and oxygen plasma samples that have carbon peaks at approximately 531.6 eV and oxygen peaks at approximately 284 eV (Figure 3-8B).

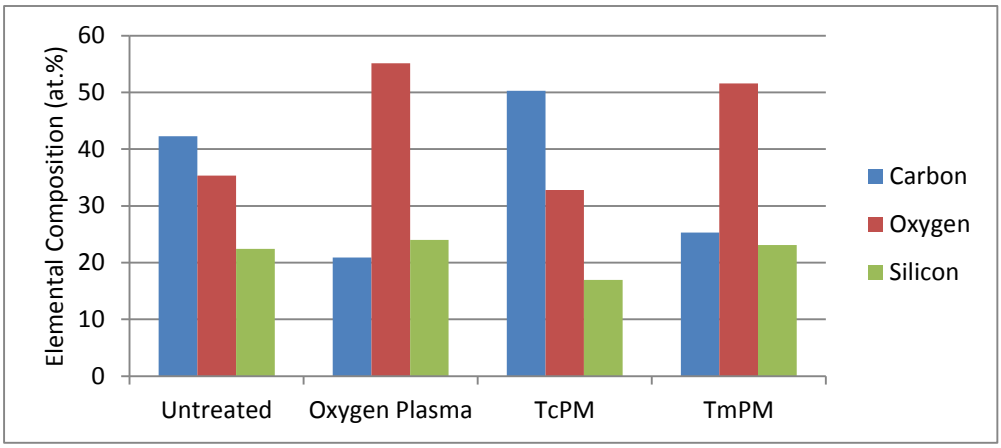

(A)

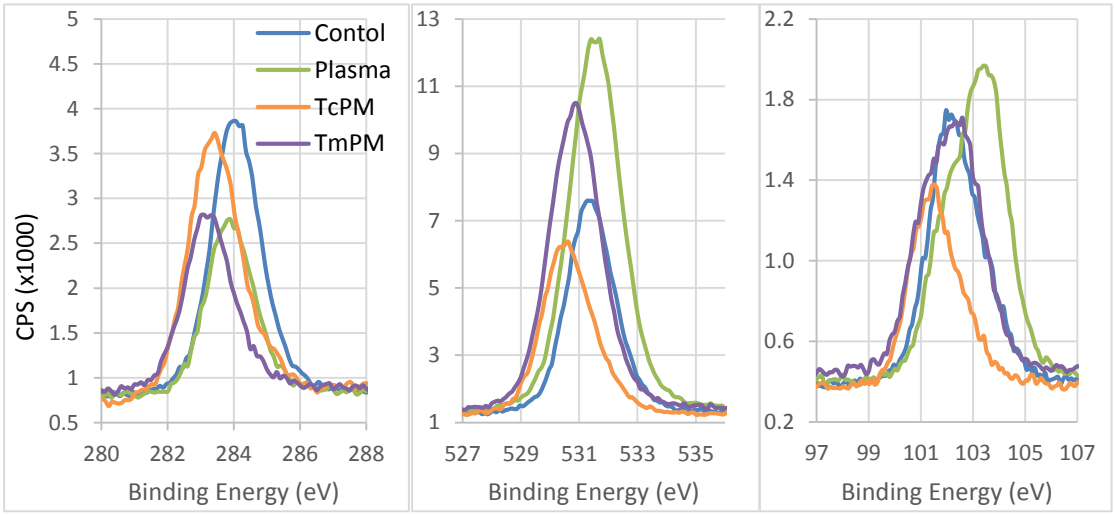

(B)

Figure 3-8 XPS data for steps of original Flexwell protocol. A: percent composition of carbon, oxygen, and silicon, as measured by XPS of silicone treated at different stages of the original Flexwell protocol. Silicone samples are from untreated Bioflex plates (control), 2 minutes of oxygen plasma (plasma), or silane treated by described protocols (TcPM or TmPM). Error bars are absent as these data were collected from single samples. B: narrow scans of each silicone sample for C1s (280-288eV), O1s (527-535eV), and Si2p (97-107eV).

The pre-coated BioFlex amino plates had a very similar surface make-up compared to the uncoated BioFlex plates (43.7% carbon, 34.6% oxygen, and 21.6% silicon) and no detectable amount of nitrogen on the surface. In contrast, silicone treated

with AMPS has 5.53% nitrogen on the surface. The AMPS treated samples also had increased carbon content (35.1%) and decreased oxygen (39.7%) and silicon (18.2%) compared to the oxygen plasma samples. The narrow scans show that both the BioFlex amino and AMPS treated samples have very similar carbon (peak at approximately 284eV) and oxygen (peak at approximately 531eV) curves compared to untreated, with the AMPS sample showing a very slight upward shift of the silicon peak (102.6eV) compared to untreated (102.0eV).

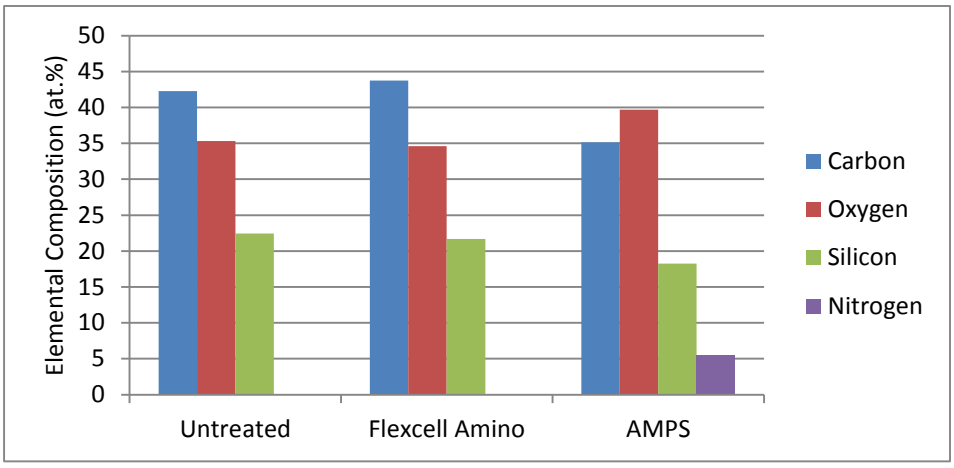

(A)

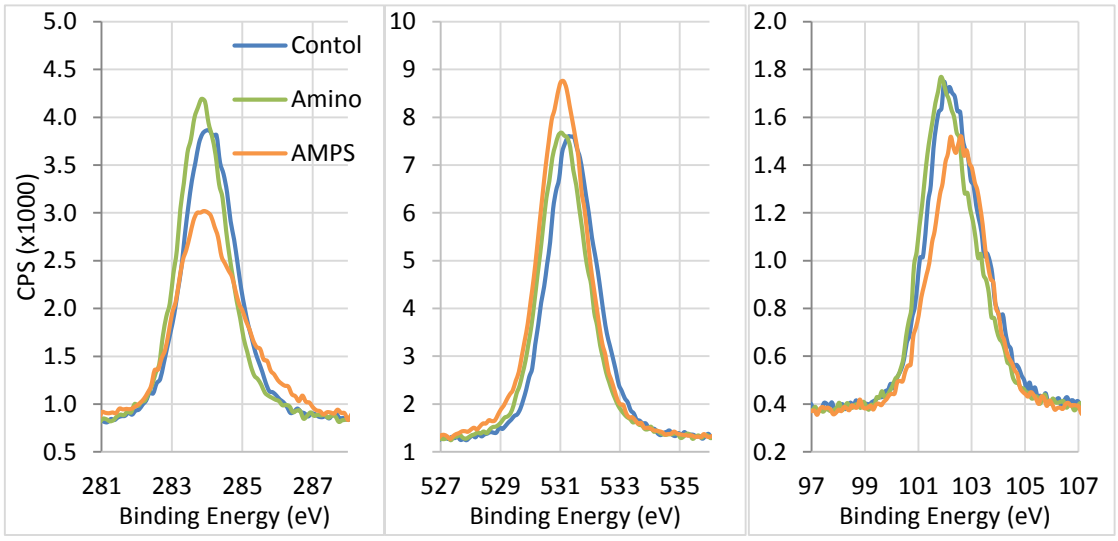

(B)

Figure 3-9 XPS data for steps of alternative amino protocols. A: percent composition of carbon, oxygen, and silicon, as measured by XPS. Silicone samples are from untreated Bioflex plates (control), from pre-coated amino Bioflex plates (amino), or silane treated by described protocols (AMPS). Error bars are absent as these data were collected from single sample. B: narrow scans of each silicone sample for C1s (280-288eV), O1s (527-535eV), and Si2p (97-107eV).

3.6 Overall Conclusions and Discussion

Flexwells developed using the original protocol as per Throm Quinlan et al. (134) could withstand chronic oscillatory strain of varying magnitude and cells survived under

chronic physiological strain conditions with serum deprivation. Therefore, this model met almost all necessary requirements to study the chronic effects of substrate stiffness and strain on ASM phenotype. However, the inability to generate Flexwells with substrate stiffnesses less than 4.8kPa (PA#6) was a major barrier. Although it is difficult to measure the stiffness that ASM cells experience *in vivo*, it is estimated that healthy airways have a Young's modulus of less than 3kPa, while fibrotic lungs are above 8kPa (22, 82, 89). Additionally, previous work in our lab shows that cells are only significantly more contractile on substrates of 19.2kPa (PA#8) and above compared with 1.2kPa (PA#4) and below (Figure 3-10). These ranges also apply to baseline stiffness and expression of contractile proteins of cells in culture (152). Therefore, it is unlikely that there would be significant differences between 4.8kPa Flexwells and 19.2kPa. Additionally, using a 4.8kPa Flexwell as a healthy substrate stiffness model may be slightly higher than estimated physiological values. Therefore, it was thought to be important to consistently produce Flexwells as low of at least 1.2kPa in order to use this model to cover previously established stiffness ranges for cellular responses under static conditions and to target estimated conditions of the healthy and asthmatic mechanical microenvironment.

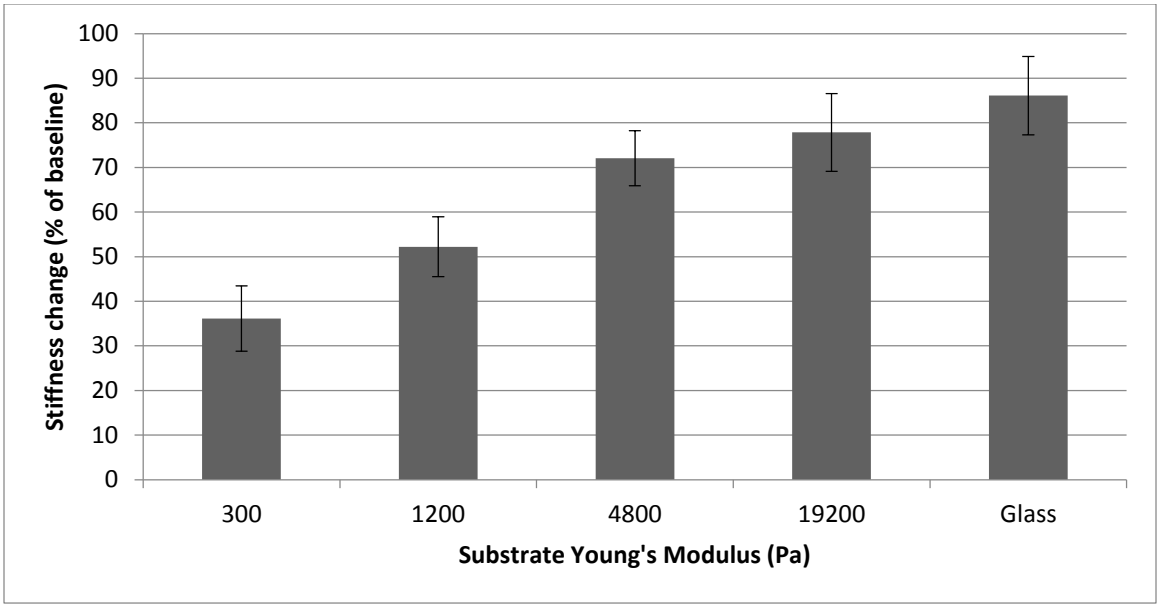

Figure 3-10. Contractile function of ASM cells cultured on different substrate stiffnesses. Primary ASM cells cultured for seven days on PA gels ranging from 300 Pa to 19 200 Pa and on glass coverslips. Contractile function is measured as percent change in stiffness after treatment with 80mM KCl for 3 minutes. Cells on the softest substrates are significantly less contractile than those cultured on the stiffest substrate and on glass. Values are means ±SE, n≥18 from 8 donors, *p<0.0001, 1-way ANOVA. Unpublished data collected by Dr. Adrian West

The inability to produce Flexwells with softer PA gels is unexpected as Throm Quinlan *et al*. reported producing Flexwells with a shear storage modulus (G′) of 0.3kPa to 50 kPa, which would correspond to a Young's modulus (E) of 0. kPa and 150kPa respectively. These measurements were performed using a rheometer and bulk gels, thus the actual stiffness of the gels once polymerised on Flexcell silicon may be different. Additionally, the acrylamide/bisacrylamide concentrations reported were 3%/0.058% for the low stiffness gels and 7.5%/0.117% for the high stiffness gels. Mih *et al.* measured the stiffness of PA gels bound to glass dishes using AFM and found that these same acrylamide and bis-acrylamide concentrations resulted in a Young's modulus of approximately 0.6kPa and 10kPa for the lower and higher stiffness respectively (95). Additionally, although slightly different recipes were used, the range of stiffness measured by Engler et al. using AFM (140) is close to the values obtained by Mih et al.

(95). In this thesis, partially or completely polymerised Flexwells made using PA gel recipes obtained from the Mih lab group (Dr. Dan Tschumperlin, Harvard School of Public Health, Boston, MA) had Young's moduli very close to these published values (95). Therefore, the PA gel stiffnesses used by Throm Quinlan *et al.* may have been misreported, making it difficult to determine the stiffness of the softest gels based on the original publication. However, personal communication with this lab confirmed that Flexwells using PA#3 and #4 recipes (Table 2-1) are possible, though successful production is inconsistent.

Although the original purpose of Aim 1 was to use the Flexwell model to examine the effects of substrate stiffness and strain on ASM cells, the inability to produce softer Flexwells led to a shift in goal of this aim, instead exploring potential reasons and solutions for the failure of soft Flexwells. In the end, I did not find a solution to the problem, although the work presented here provides some important insight into the Flexwell methodology. Here I will discuss theories and the supporting evidence to explain why the original protocol did not work, why alternative protocols developed to solve these problems may not work, and finally suggestions on resolving the problem in the future.

3.6.1 Free Radical Polymerisation Kinetics

In order to examine the reasons for the failure of soft Flexwells, it is helpful to understand some basics about the chemical processes involved. The discussion that follows includes some basic polymerisation kinetics principals and an overview of this material, including the equations that follow, can be found in Introduction to Polymers by Young and Lovell (160).

Polyacrylamide is formed through the process of free radical polymerisation. This is a well-characterised polymerisation chemistry in which a free radical attacks the double bond on the acrylamide monomer, linking the molecules together and creating another radical that allows for subsequent reactions with more monomers (Figure 3-11). Free radical polymerisation has three stages: initiation, propagation, and termination. In the initiation stage, a free radical must first be generated from another molecule called the initiator. In polyacrylamide polymerisation, the initiator is APS, which divides into two free radical containing persulfate groups in aqueous solution. These radical persulfates then generate the first acrylamide monomer radicals, known as active centres, by reacting with the vinyl group on the acrylamide monomer (Figure 3-11). Once an active centre is created on the acrylamide, the propagation stage begins and acrylamide chains are formed (Figure 3-11).

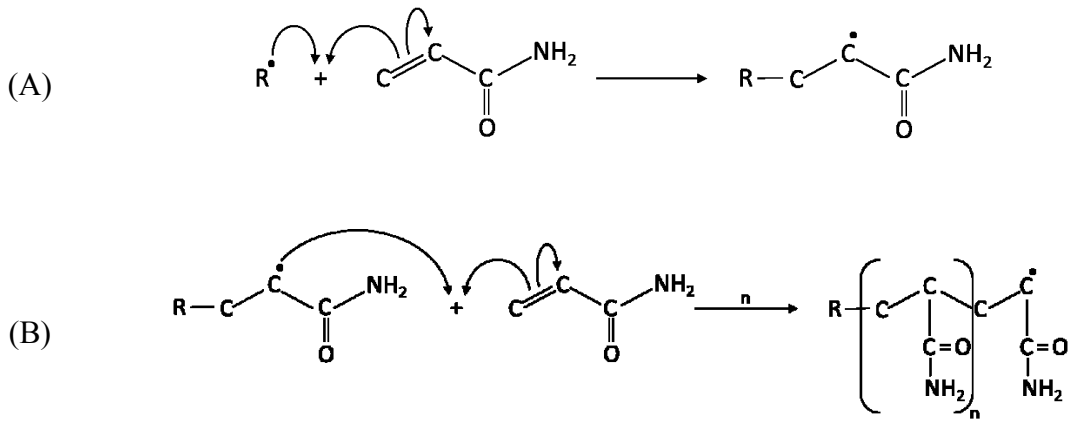

Figure 3-11 Polyacrylamide polymerisation reaction. Free radical initiation (A) and propagation (B) of acrylamide polymerisation. The "R" represents the initiator radical, which would most likely be a persulfate molecule.

The growth of the polymer chain is eventually stopped through a number of potential termination reactions. Combination termination occurs when two active centres on growing polymer chains couple to form a single C-C bond, thus no free radical is

generated and polymerisation stops. Disproportionation termination occurs when the active centre of a growing polymer chain abstracts a hydrogen atom from the penultimate carbon on a growing chain, creating two polymer chains one ending in a hydrocarbon and the other with a vinyl group, but no free radical to continue the reaction. The final termination reaction is chain transfer, which importantly provides an opportunity for contaminants to affect polymerisation. In chain transfer reactions the active centre abstracts an atom (usually a hydrogen or halogen) from another molecule, creating a polymer chain that ends in a carbon bonded to the atom and a free radical is generated on the other molecule. The other molecule may be an acrylamide monomer, in which case another polymer chain would begin, or it may be an initiator molecule, which would again form a new polymer chain. However, the other molecule may be a contaminant, such as a solvent, in which case the free radical generated may not be reactive enough to continue polymerisation.

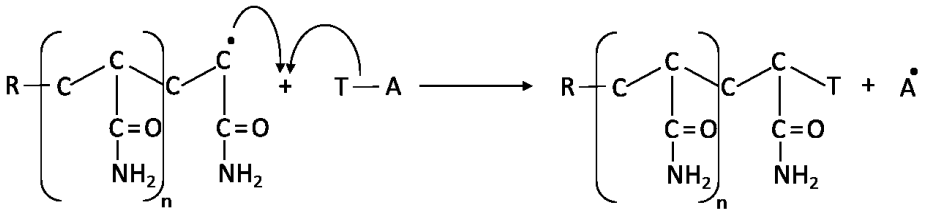

Figure 3-12 Termination of acrylamide free radical polymerisation by chain transfer to a solvent. The "T" is usually a hydrogen or halogen and the "A" is any atom. The radical generated from the solvent atom may not be reactive enough to continue propagation, thus terminating the chain reaction.

Although calculating the rate of polymerisation is beyond the scope of this thesis, there are some useful relationships in a simplified rate equation. The rate of polymerisation equation (equation 3.1) contains terms from each of the three stages: the rate coefficients for initiator dissociation (k_d), propagation (k_p), and termination (k_t). This equation assumes the reaction is at steady state and does not include factors that would

represent the catalyst activity of TEMED or the presence of the bis-acrylamide cross linker. None the less, this set of equations provides insight into the relationship between the rate of polymerisation and important variables such as the initiator concentration ([*I*]), the initiator efficiency (*f*), and the monomer concentration ([*M*]). The rate coefficient for termination (k_t) is the sum of the rate coefficients for disproportionation and combination, however, chain transfer termination is not included in this equation.

$$R_p = -\frac{d[M]}{dt} = k_p \left(\frac{f k_d}{k_t}\right)^{1/2} [M][I]^{1/2} \qquad (3.1)$$

In addition to the rate of polymerisation, polymerisation kinetics can also affect the structure of the resulting polymer as shown in the Mayo-Walling Equation (equation 3.2). The simplest example of this can be observed in the number-averaged degree of polymerisation ($\bar{x}_n$), which is representative of the average length of polymer chains formed. Similar to polymerisation rate, the structure of the polymer formed is dependent on the kinetics of each stage of polymerisation as it includes the rate coefficients for each. However, this equation also takes chain transfer termination into account and includes constants that are the ratios of chain transfer to monomer (C_M), initiator (C_I), and solvent (C_S) to the polymerisation rate coefficient (k_p). A term is also included that represents the fraction of termination reactions that occur by combination and disproportionation (q). When q=1, termination occurs only by disproportionation and $\bar{x}_n$ is equal to the chain length. However, when q<1, some termination is attribute to combination, meaning that chain length is doubled in these termination reactions. Chain transfer is not included in the rate equation because rate would be unaffected by most chain transfer reactions as propagation is continued with chain transfer to monomer, initiator, or a reactive radical is

generated on the solvent molecule. However, it should be noted that if a reactive radical is not generated, the polymerisation rate would be decreased.

$$\frac{1}{\bar{x}_n} = \frac{(1+q)(fk_dk_t)^{1/2}[I]^{1/2}}{k_p[M]} + C_M + C_I\frac{[I]}{[M]} + C_s\frac{[S]}{[M]} \qquad (3.2)$$

3.6.2 Potential Causes of Soft Flexwell Failure

Although consistent production of soft Flexwells was not achieved, the process of troubleshooting provides some insight as to why the protocol was problematic. First, the fact that the stiff gels did consistently polymerise and were chemically bound to the Bioflex silicone surface shows that all steps of the protocol do function under these conditions. Therefore, it is likely that plasma etching introduces reactive groups on the silicone surface, the silane binds to these groups, and polyacrylamide polymerisation is initiated, incorporating the propyl methcrylate group into the gel, attaching the gel to the membrane.

The XPS results presented here also support the theory that the steps leading up to polyacrylamide addition are functioning as we expected. Oxygen plasma treatment caused an increase in overall surface oxygen content and a decrease in carbon content, similar to changes in oxygen and carbon content obtained by others using XPS to measure oxygen plasma treated PDMS (16, 68, 110, 119). Oxygen plasma contains highly energised oxygen species including ions, electrons, radicals, and photons. This highly energised mixture bombards surface of the silicone and breaks organic bonds, which is the BioFlex silicone in this case. The energy from the plasma dissipates into the surface of the silicone causing surface degradation, deposition of the oxygen species on the surface, and/or functionalization. Thus, the increase in oxygen is likely due to

oxygenated species of carbon or silicon on the membrane surface, while the decrease in carbon would be due to the removal of adventitious carbon.

In addition to changes in the atomic percent of carbon and oxygen, previous studies using XPS analysis shows that oxygen plasma introduces oxygenated carbon species in the form of alcohol/ether, carbonyl, and carboxylic acid/ester groups onto the surface of PDMS (110, 119). The chemical environment of an atom causes a change in binding energy which in turn causes a shift in the XPS peak and shape of the curve when comparing the narrow scan of an element from two different samples. For example, a carbon that is bound to oxygen will have a higher binding energy than a hydrocarbon species (119). Thus the C1S peak should shift to the right upon plasma treatment due to the introduction of oxygenated carbon species, however, this was not observed. This does not necessarily mean that these oxygenated species are not present as the exact chemical structure of the BioFlex silicone is proprietary, and therefore unknown. If the silicone was pure PDMS, based on stoichiometric ratios, the untreated surface would be made up of 50% carbon, 25% silicon, and 25% oxygen. This ratio is closely reflected in previous studies that used XPS to measure untreated PDMS (110, 119, 151), however, the untreated BioFlex silicone measured here had a higher oxygen content. It is therefore plausible that BioFlex silicone has some oxygenated carbon species instead of, or in addition to, the methyl side chains in PDMS. This may have resulted in a broader C1S peak for untreated BioFlex silicone that obscured the chemical shift due to oxygen plasma. Thus, based on the XPS data presented here, the exact make-up of oxygenated species on the plasma treated BioFlex silicon surface remains unknown, although there is clearly an increase in oxygen content.

Although many studies have investigated the effect of oxygen plasma on silicone, the characteristics of the resulting surface are still debated. Many studies have shown that oxygen plasma increases oxidised silicon species on the surface potentially creating a brittle glassy siloxane layer. Increasing the time and strength of oxygen plasma may create more oxidised silicon and a thicker siloxane layer, estimated to be up to 10nm thick (46). Here, I found that in addition to an increase in overall oxygen content, oxygen plasma treated BioFlex had a Si2p peak that was shifted to the right compared to the untreated sample. This is similar to studies conducted on silicone that concluded that a shift to a higher binding energy is evidence for an increase in SiO_x species (68, 97), which would form hydroxyl groups upon air exposure, creating an ideal surface for silane binding.

Silanes all contain a silicon group on one end that covalently bind to surface hydroxyls through hydrogen bonding and condensation reactions. The silane used in the original protocols (TcPM) has a chlorinated silicone group. Unlike the less reactive (m)ethoxysilanes, chlorosilanes do not require hydrolysis in order to react with hydroxyl groups, allowing for direct reaction at room temperature. After TcPM treatment, the oxygen and carbon content returned to similar ratios as were observed on the untreated silicone, along with a small decrease in silicon content. This decrease in silicon is characteristic of silane coated silicone (79, 110, 119) and suggests that less of the bulk silicone material is measured by XPS due to surface silane coating. Additionally, successful stiff Flexwells withstood supraphsyiological strain, high temperatures, and storage in solution for up to 3 days, suggesting that polymerised gels are indeed chemically bound via TcPM. Therefore, success of stiff Flexwells and supporting XPS

data suggest that the steps of the Flexwell protocol are functioning as expected up to the addition of polyacrylamide.

By process of elimination, this leaves the polymerisation of the polyacrylamide itself as the most likely problem area. The shape of the failed soft Flexwells in which gels formed in rings (Figure 3-5) suggests that polymerisation was initiated, but did not continue to completion. Free radical polymerisation can be inhibited by a number of factors as anything that reacts with, or rapidly produces excess free radicals can affect the polymerisation process. Based on equations 3.1 and 3.2, it is obvious why inhibition of polymerisation at any stage would affect soft gels more than stiff. Soft gels contain less acrylamide monomer, which is directly proportional to both the rate of polymerisation and the polymer chain length. Thus, termination (or prevention of initiation) of the same number of polymer chains would result in proportionally more inhibition in the soft gels compared to stiff, and thus have a more drastic effect on the already longer polymerisation time.

The most commonly discussed inhibitor of free radical polyacrylamide polymerisation is molecular oxygen, which is known as a free radical sink as it readily reacts with other radicals. The resulting oxygen radical is more stable and may not be reactive enough to initiate more polymer chains. Therefore, polyacrylamide protocols generally include a vacuum step to remove molecular oxygen from the unpolymerised PA solution. One of my original hypotheses was that molecular oxygen was inhibiting polymerisation of soft gels on silicone. However, the data presented here does not support oxygen contamination as the sole cause of soft gel failure. First, PA polymerisation does occur with some oxygen present as demonstrated in the production

of softwells (PA gels on glass, see chapter 4.2.1 for full protocol), which polymerise on the bench top where they are exposed to atmospheric oxygen. The Flexwell protocol, however, takes even more steps to exclude oxygen as the system is prepared and polymerised in a vacuum chamber under the flow of nitrogen. Second, the shape of the failed soft gels suggests that polymerisation is initiated at the edges, where we would expect the most oxygen exposure. Finally, steps taken to exclude oxygen from the surrounding environment such as vacuuming the BioFlex plates for a longer time, using equipment that ensures a lower vacuum pressure, and polymerising gels under vacuum did not allow for consistent soft gel polymerisation. Thus, it is unlikely that the presence of molecular oxygen in the surrounding environment is inhibiting polymerisation. However, it may be that molecular oxygen is present elsewhere in the system, likely within the polymerisation solution itself. Forcing oxygen out by bubbling nitrogen directly through the polymerisation solutions did create successful soft gels once, but was not reproducible. Taken together, this evidence suggests that there are likely other factors inhibiting polymerisation that may make the system more sensitive to the presence of molecular oxygen in solution, but oxygen presence alone cannot explain soft gel failure.

Another possibility is that species created on the silicone surface are acting as inhibitors. PA gels are easily polymerised on glass coverslips in our hands (softwells), suggesting that perhaps the silicone itself is inhibiting polymerisation. It is interesting to note that failure of some of the alternative protocols was due to poor gel attachment, but did in fact result in fully polymerised soft gels. Generally, successful soft gel polymerisation was correlated with protocols that did not involve plasma treatment, such as the amino protocol using pre-coated BioFlex plates. Even more compelling is that soft

gels polymerised using the benzophenone protocol on non-plasma treated PDMS, but did not polymerise on plasma treated BioFlex plates. As previously discussed, oxygen plasma may introduce a variety of oxygenated carbon and silicon species, along with the silanol functionalities necessary for silane binding. It is possible that these species are inhibiting polymerisation through chain transfer termination mechanisms (Figure 3-12). As discussed in the previous chapter on polymer kinetics, when chain transfer occurs to a solvent (or contaminant) molecule and the resulting free radical is more stable, both the rate of polymerisation and the polymer structure may be affected. The magnitude of the effect on chain length is dependent on the ratio of the chain transfer constant for the solvent to the polymerisation rate coefficient ($C_s = \frac{k_{trS}}{k_p}$), which is a measure of the reactivity of the contaminant, as well as the ratio of the concentration of solvent to monomer (equation 3.2). Thus, high solvent concentration and/or a solvent with a high chain transfer coefficient may cause a significant decrease in chain length, which may result in complete inhibition of polymerisation. This would be especially significant if the monomer concentration is low as the concentration of monomer is included in every term of equation 3.2, supporting the theory that the soft gels are more sensitive to inhibition due to the lower concentration of monomer.

The Mayo-Walling equation (equation 3.2) shows that solvents need to be considered as potential inhibitors. It is possible that the solvents required for the TcPM solution and rinsing (heptane, hexane, and carbon tetrachloride) are acting as chain transfer agents. Indeed, halogens are commonly discussed as chain transfer agents and have relatively high chain transfer constants. However, the presence of CCl_4 is not likely enough to completely inhibit polymerisation as the XPS results show that there were no

detectable levels of chlorine on the BioFlex surface after TcPM application. Additionally, the vapour deposition protocol, which excluded the use of all solvents, still resulted in soft gels that were not fully polymerised, suggesting that the solvents are not solely responsible for failed soft gels.

Finally, it is necessary to consider the effect that the silane itself may have on PA polymerisation. As previously described, silanes vary based on the side groups on the silicon end of the molecule, as well as the reactive group. The silane used in the Flexwell protocol has three chlorines bound to the silicon, and a propyl methacrylate reactive group. In contrast, the silane used in the softwell protocol has three methoxy groups on the silicone and an amino reactive group (Figure 3-13). As previously discussed, the differences between the silicon side groups determine the solvents that are necessary, but it is unlikely that solvents would be solely responsible for polymerisation inhibition. This leaves the possibility that the reactive group may be affecting polymerisation and the use of different reactive groups involves two completely different PA binding chemistries (Figure 3-13).

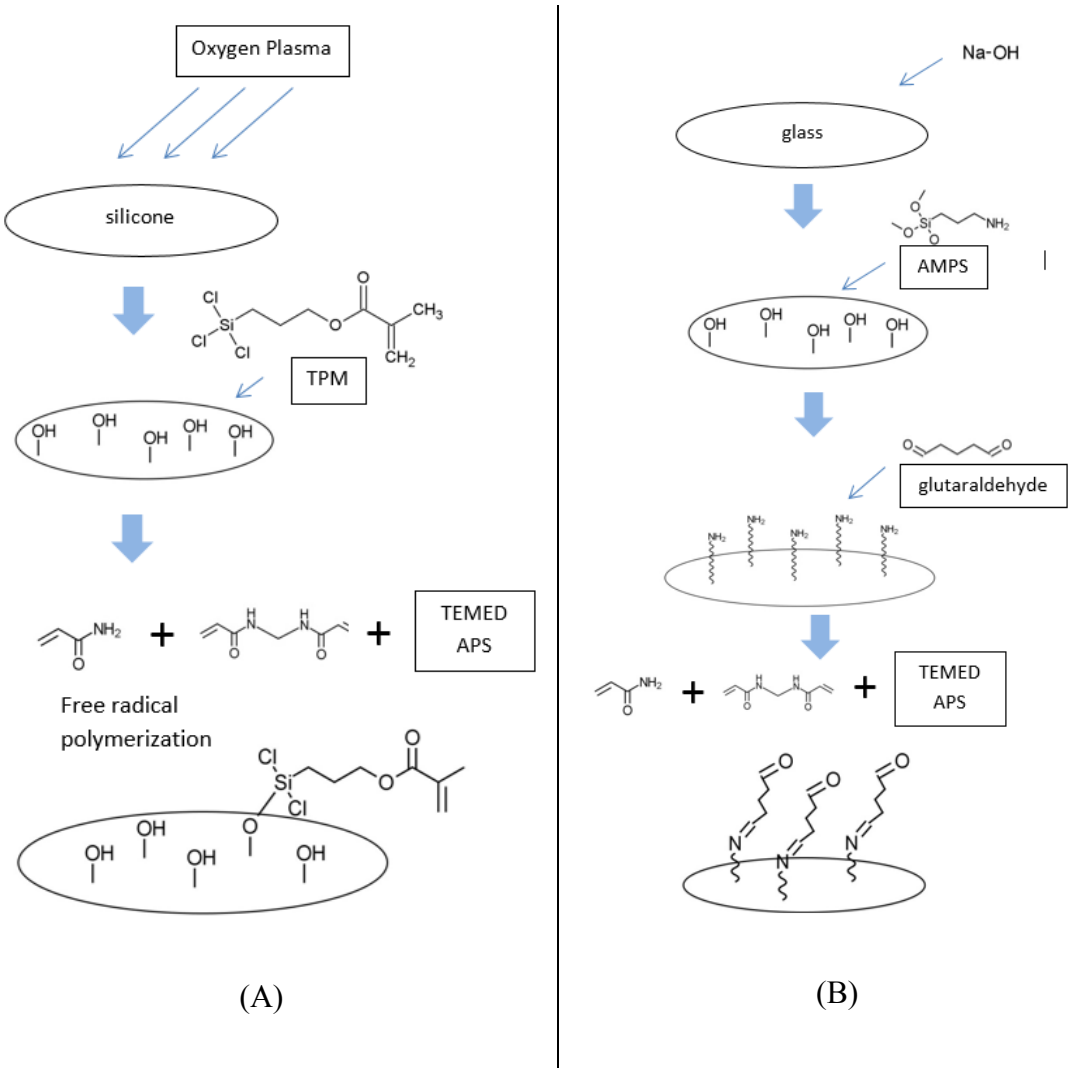

Figure 3-13 Original Flexwell protocol chemistry (A) compared to softwell chemistry (B).

In the Flexwell protocol, as previously described, the vinyl group in the propyl methacrylate can be made into a free radical, thus inserting itself directly into the backbone of the acrylamide polymer chain. In contrast, the softwell protocol uses glutaraldehyde, an amino cross linker, to bind the amino reactive group on the silane to the amino groups on acrylamide molecules. The amino group in the acrylamide monomer is extraneous to the polymerisation reaction, therefore, the softwell protocol chemically segregates the reactions involved in polymerisation and binding the gel to the surface. In the Flexwell protocol, however, both gel binding and gel formation depend on free

radical polymerisation reactions. Upon reaction with a free radical, the vinyl group in the propyl methacrylate of TcPM and TmPM would create a new reactive free radical and would be included within the polymer chain. Thus, inclusion of a propyl methacrylate may be more akin to an increase in monomer than introduction of a contaminant. An increase in monomer concentration proportionally increases both the rate of polymerisation and the degree of polymerisation (equation 3.1 and 3.2). Therefore, if anything, the presence of propyl methacrylate molecules on the silicone surface would help polymerisation by increasing the reaction rate.

Although TcPM is not likely a contributor to polymerisation inhibition, the presence of propyl methacrylate in the polymer backbone may change the polymer structure, and therefore would also change the mechanical properties of the resulting gel. However, when the Young's modulus of Flexwell gels that were made using TcPM was measured using AFM, the values were very close to theoretical measurements based on polymerisation on glass surfaces (Figure 3-6) (95). This suggests that the number of propyl methacrylate molecules involved in the polymerisation reaction is not enough to significantly alter the structure of the polymer at the surface of the gel. However, the Young's modulus is not necessarily representative of changes to the polymer structure. In order to fully understand whether any molecule, including silanes, functionalities introduced by oxygen plasma, solvents, or other contaminants are affecting the polymer structure it would be necessary to perform more in depth experiments that directly measure the length of resulting polymer molecules.

In conclusion, the data shown here suggest that failure of the soft Flexwells is likely due to inhibition of PA polymerisation. Based on correlational observations of

polymerised soft gels, the most likely inhibitor is some species introduced or produced or exposed on the silicone surface during oxygen plasma treatment. However, due to the sensitivity of the soft gel polymerisation system, it is possible that small amounts of inhibitors from multiple sources accumulate to impede complete gel formation. Additionally, it is important to note the limitations of conclusions drawn from XPS measurements. Although this method is highly accurate using the methods presented here, single samples were tested and therefore the data does not account for inter-sample variability. Additionally, XPS analyses a very small area of the silicone surface and does not account for variations in distribution across the membrane.

3.6.3 Flexwell Solutions

In this aim, I explored multiple potential solutions for the probable polymerisation inhibition that was causing failure of soft Flexwells. If the source of inhibition accumulated over time (such as in the case of atmospheric oxygen exposure), then increasing the polymerisation rate would also reduce inhibition. I expected that increasing the initiator concentration in soft gels would increase the rate of polymerisation, but would also affect the stiffness of the resulting gels as initiator concentration affects chain length (equation 3.2). Surprisingly, it was found that in bulk gels the initiator concentration had a small and variable effect on polymerisation time, while the gel recipe had a much larger effect on polymerisation time (Appendix A). In contrast, the initiator concentration appeared to have a larger effect on gel stiffness (Appendix A). This suggests that it may be possible to use a stiff gel recipe with a fast polymerisation time and use an increase in initiators to reduce gel stiffness while maintaining the polymerisation rate. However, this hypothesis is based on an incomplete data set due to

lack of accurate measurement techniques of polymerisation time and gel stiffness. Additionally, changing gel recipes may change structural properties of the gel beyond the stiffness, such as porosity. Therefore, without the proper techniques and theoretical knowledge, finding the optimal concentration of acrylamide, bis-acrylamide, APS, and TEMED would be an impractical approach to solving the polymerisation inhibition problem presented in this aim.

The second method to reduce polymerisation inhibition was to develop alternative chemistries that would exclude potential sources of inhibition. The most important finding here was that soft gels did polymerise in protocols that did not require oxygen plasma treatment, however, these did not appear to be chemically bound to the silicone. The first of these protocols was the amino protocol using BioFlex plates that were pre-coated with amino groups. It was surprising that this method was unsuccessful, as this chemistry works well in making PA gels on glass (softwells). However, XPS analysis revealed that there was no detectable nitrogen on the surface of the amino-coated BioFlex plates, explaining the poor gel attachment. In contrast, using AMPS to introduce amino functionalities on the uncoated BioFlex plates resulted in 5% nitrogen on the surface, which is comparable to protocols using similar techniques on PDMS (110, 151). However, this protocol still required oxygen plasma treatment and resulted in incomplete polymerisation of soft gels.

The second protocol that did not require plasma treatment was a recently published protocol (120) that used solvents to impregnate benzophenone directly into the surface of the surface, circumventing the need for plasma treatment. The main problem with this protocol is Simmons *et al.* do not address the natural hydrophobicity of PDMS,

which prevents the unpolymerised solution from spreading out and creates irregularly shaped gels. This hydrophobicity may contribute to the lack of chemical bonding to the PDMS. I therefore exposed BioFlex plates to oxygen plasma before applying benzophenone. Although this did increase the hydrophilicity of the silicone membrane and allowed the PA solution to spread evenly under the glass coverslip, these gels did not polymerise, further supporting the hypothesis that oxygen plasma inhibits polymerisation. Furthermore, the softest gels produced by Simmons et al. were 6kPa, which is stiffer than the PA#6 gels. Therefore, it is unknown whether softer gels would be compatible with this protocol.

3.6.4 Future Directions

Thus far I have shown the most likely problems within the original Flexwell protocol and discussed attempts to solve them. Although we have learned a great deal about the chemistry involved in the Flexwell protocol, consistent production of fully polymerised soft Flexwells remains elusive. Moving forward, I think that there are three possible avenues to explore that may significantly improve the protocol.

First, since oxygen plasma appears to be the top candidate for polymerisation inhibition, removing this step from the protocol would be beneficial. However, some method to functionalise the surface of the silicone membrane is still required. One option may be to simply use a different type of plasma. Others have used water, argon, nitrogen, and ammonia plasma to modify the surface of PDMS and all treatments induced a more hydrophilic surface (79, 157), similar to oxygen plasma. Water and argon plasma both have similar effects as oxygen plasma, increasing the oxygen content on the surface and introducing oxygenated carbon species (79, 157). Although the chemical groups that may

responsible for polymerisation inhibition are unknown, argon or water plasma may be capable of creating the necessary silanol groups while reducing polymerisation inhibition. Another option may be to introduce amine groups directly on the surface of PDMS using nitrogen or ammonia plasma (157). The presence of amine functionalities on the surface would present the opportunity for many chemical strategies, including direct crosslinking with amine side chains in PA using glutaraldehyde, similar to the softwell and amino protocols.

The second suggestion for protocol improvement is to functionalise the surface of PDMS instead of the unknown BioFlex silicone. This would be possible by either developing a method to manufacture plates that work with the Flexcell Tension system, or by simply coating BioFlex wells with PDMS (79). Working with PDMS would remove unknown variables from future experiments as the chemical make-up pf PDMS is well known and this material has been the basis for much of the literature exploring silicone surface modification. Additionally, the polymerisation process of PDMS may allow for other avenues of surface modification.

The final suggestion for future work would be to explore different hydrogels. Other hydrogels such as poly(ethylene)glycol (PEG) (98, 105, 136) or alginate (10, 21) would present opportunities to develop other chemical strategies to bind a substrate with tunable stiffness to a silicone surface. Both PEG and alginate polymerise via non-free radical processes, can be produced with elastic moduli below 1kPa (21, 136), and have functional groups within the polymer structure that offer opportunities for chemical linkages. Therefore, these gels may be less sensitive to the inhibitors introduced in the Flexwell protocol as well as provide opportunities for development of protocols based on

alternative chemistries. Additionally, it may be possible to use PDMS itself as a model for substrate stiffness. The main barrier to this material is that it is difficult to make PDMS that is soft enough for our purposes (25), thus most studies that use PDMS as a substrate stiffness model use much higher stiffness ranges (56, 72). However, in a recent study, researchers produced PDMS with a Young's modulus as low as 0.1kPa (138) showing that this may be the simplest solution to the problem presented by the Flexwells.

Chapter 4: Manipulation of Substrate Stiffness and Cell Tone

4.1 Rationale

In addition to the aforementioned stiffening of the ASM environment due to remodelling, the cells themselves may experience higher tone in asthmatic airways (103). Chronic increases in tone have been shown to cause remodelling in the airway (55) and increased contractility (28) *in vivo*. However, *in vitro* tone appears to have inconsistent effects. In a series of studies by Gosens et al. (51, 52), chronic decreases in tone decreased contractile phenotype, while chronic increases also decreased contractile phenotype. We have previously shown that while ASM cells demonstrate a more contractile phenotype in response to strain, this can be augmented or diminished by an increase or decrease in cell tone respectively (42). Based on these studies, it appears tone only has consistent effects on ASM in the presence of strain, either due to *in vivo* tidal breathing, or induced *in vitro*. As discussed in chapter 1.3, mechanosensing of substrate stiffness and strain depend on similar molecular signaling pathways and on cellular autoregulation of tone. Therefore, my second aim was to determine whether, like strain, the response to substrate stiffness would also be affected by an increase or decrease in cell tone. This response not only includes an increase in contractile function, but evidence suggests that functional differences may be due to changes in contractile proteins (152). As discussed in chapter 1.4.2, ASM cells *in vitro* show remarkable phenotypic plasticity, displaying a more contractile phenotype characterised by elongated cells with increased contractile function and expression of smooth muscle specific genes. To fully understand

the changes that occur due to mechanical stimulation in the asthmatic environment, it is therefore important to measure both contractile function and changes in gene expression.

The integrated effect of substrate stiffness and cell tone has been investigated in fibroblasts (94). While cell morphology, traction force, and proliferation are often considered clustered responses and change in predictable ways in reference to each other, this study demonstrated that these responses can be uncoupled when cellular mechanics are manipulated.

In this aim, I measured cell phenotype using contractile function, morphology, and gene expression assays in cells cultured on different substrate stiffnesses with the addition of tone modulating drugs. In this study, I elected to measure contractile phenotype expression at the mRNA level as there is strong evidence that many of these genes are under transcriptional control via the serum response factor (SRF) pathway (93). Although previous work in our lab has shown that contractile proteins increase on stiff substrates, we have not confirmed an accompanying transcriptional increase in the same genes. I expected to see a more contractile phenotype in cells on stiff substrates with higher tone.

4.2 Methods

4.2.1 Softwell Fabrication

Softwells consist of PA gels of different stiffnesses polymerised on 18mm glass coverslips (VWR, #48382 041, Mississauga, ON) that fit comfortably in 12-well plates. Glass coverslips were cleaned in methanol and dried before use to prevent dust contamination. The glass coverslips were activated with oxygen plasma in the SPI

Plasma-Prep™ III Plasma Etcher at 50 watts for 30 seconds, or by dipping in methanol and briefly placing in a flame. Activated coverslips were then transferred to glass plates in a laminar flow hood to prevent dust contamination and treated with 40 µl of 0.1M NaOH for 10 minutes. Excess NaOH solution was aspirated from the surface after 10 minutes and the coverslips were allowed to air-dry completely. Once dry, 40 µl of (3-aminopropyl)trimethoxysilane (AMPS) (Sigma-Aldrich, #281778, Oakville, ON) was placed on the surface of each coverslip for 5 minutes. For both the NaOH and AMPS treatment, a cell scraper was used to ensure the solution covered the entire surface of the coverslip. The plasma etching step helped to make the cell scraper less necessary as oxygen plasma renders the surface more hydrophilic, allowing the solution to spread across the surface naturally. The coverslips were then transferred to a 12 well plate and rinsed and soaked in distilled water on a shaker for 15 minutes to ensure complete removal of AMPS residue. The water was then replaced with 500 µl of 0.5% glutaraldehyde (Sigma-Aldrich, #G7776, Oakville, ON) in PBS and placed on a shaker at room temperature for 30 minutes. The coverslips were rinsed with distilled water to remove excess glutaraldehyde and allowed to air-dry before PA gel polymerisation.

A second set of coverslips (top slips) were prepared by cutting a small notch in them. These top slips were made hydrophobic by soaking them in RainX for 10 minutes and were then carefully dried to remove residue. PA gel solutions were made in bulk as described in chapter 2.2 and 20 µl was placed on each coverslip. Before the solution was able to polymerise one of the top slips was carefully placed on top, wicking the PA gel solution into uniform layer sandwiched between the two coverslips. The coverslip sandwiches were allowed to polymerise for at least 30 minutes before the top slip was

removed using a razor blade wedged under the notch in the top slip. The PA gels bound to glass coverslips were rinsed in HEPES before functionalization with sulfo-SANPAH and collagen coating as described in chapter 2.3. Primary human ASM cells were then seeded onto the collagen coated softwells in standard media containing 0.5% serum. The density at which the cells were seeded was determined by the type of experiment and the measurement time points (Table 4-1) to control for confluence. In initial contractile function experiments cells were seeded on "soft" PA gels at 1200 Pa and "stiff" at 19.8 kPa (PA#4 and #8 recipe as per Table 2-1). In later morphology, gene expression, and adjusted contractility experiments, the "soft" substrates were adjusted to be 600Pa (PA#3 recipe as per Table 2-1).

Table 4-1. Cell seeding density (cells/mm^2) for different experimental conditions. Cells densities were chosen to obtain near confluence for contractile function and gene expression studies, while morphology studies required visualisation of individual cells.

Experiment Type	Substrate Stiffness	Day 0 (4 hrs)	Day 1 (24 hrs)	Day 3 (up to 5 days in OMTC experiments)	Day 7
Initial Contractile Function	Soft and Stiff	600	360	180	N/A
Gene Expression/Adjusted Contractility Experiments	Soft and Stiff	360	360	180	120
Morphology	Soft	60	60	30	15
Morphology	Stiff	60	30	15	7.5

4.2.2 Cell Tone Modulation

Pharmacological agents and doses used to modulate tone were selected based on previous work in our lab (42) and related studies in other labs (94). Three different

relaxants (forskolin, blebbistatin, and Y277632) and two contractile agents (histamine and cantharidin) were initially tested, however, only forskolin and histamine were used in the following experiments. The pharmacological signaling pathways for each of these drugs is summarised in figure Figure 4-1. Briefly, Forskolin acts by increasing intracellular cAMP, which decreases both MLCK phosphorylation and intracellular calcium. Previous work in our lab shows that forskolin chronically affects ASM cell tone and contractility at a concentration of 5 and 10μM (42). Blebbistatin acts by directly inhibiting NMM-II at low doses but only inhibits SM myosin at very high doses (81). The final relaxant used was Y27632, a ROCK inhibitor that decreases tone in most cell types by increasing MLCP activity through the Rho/ROCK pathway.

Histamine activates specific g-protein coupled receptors located on the surface of ASM cells that ultimately act to increase intracellular calcium concentrations. Increased calcium increases MLCK activity and therefore causes an increase in cell tone. Finally, cantharidin acts on contractile pathways by inhibiting MLCP.

In all experiments, except dose experiments, forskolin, blebbistatin, Y27632, and histamine were administered at 10μM and cantharidin was administered at 1μM. The experimental design including the media used, dosing and culture time points, and drugs used varied depending on the type of experiment and are detailed in the following sections.

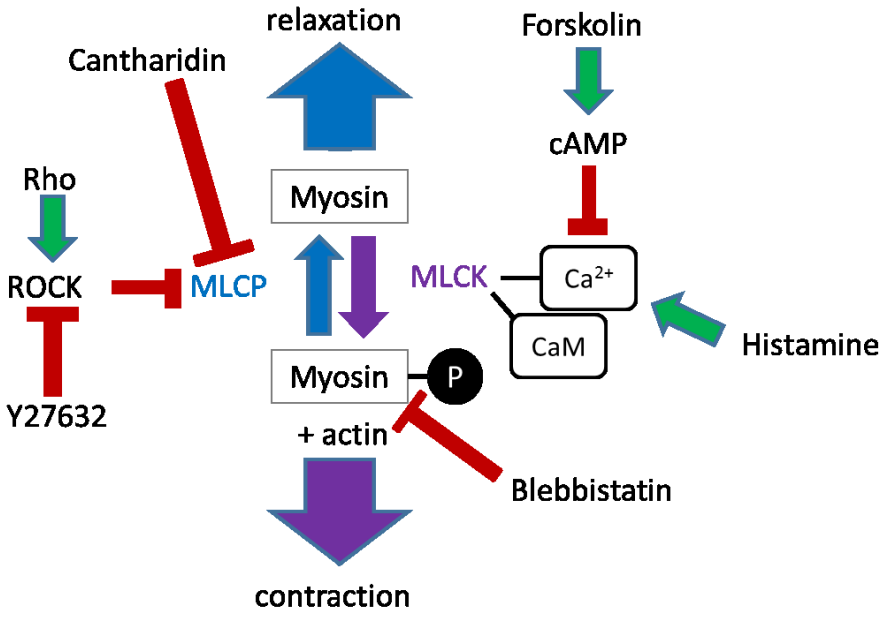

Figure 4-1. Diagram of contractile pathways and signaling pathways of various pharmacological agents. In ASM cells contraction is initiated by phosphorylation of myosin that can then interact with actin to increase cell tension. Phosphorylation of myosin, and therefore contraction, is chiefly regulated by MLCK and MLCP. MLCK interacts with calcium and calmodulin in order to phosphorylate myosin, while MLCP is regulated by the Rho/ROCK pathway. Pharmacological agents used in Aim 2 affect various steps of these pathways. Contractile agents either increase calcium (histamine) or inhibit MLCP (cantharidin), ultimately increasing the MLCK:MLCP ratio and driving the pathway towards contraction. Relaxant agents either inhibit calcium by increasing intracellular cAMP (forskolin), or inhibit ROCK (Y27632) thereby decreasing the MLCK:MLCP ratio and driving the pathway towards relaxation. An additional relaxant (blebbistatin) directly inhibits myosin leading to decreased cell tone.

4.2.3 Cell Morphology Measurements

Pictures of each region of interest were taken with a 10x objective using the appropriate fluorescent filters and images were captured with a Sensicam CCD camera with custom software (Beadtracker software (42)). Two images for each region were generated, one of DAPI stained nuclei and another of phalloidin stained f-actin filaments, which was used to estimate the 2 dimensional projection of cell shape. Images were analysed using Cell Profiler software (29) with a custom pipeline (Figure 4-2). In this pipeline nuclei were first identified from the DAPI image using a stringent background thresholding method, which discarded very large or very small objects to prevent artifacts

from being counted as cell nuclei. The next step used the nuclei image to identify cells in the phalloidin image. Any cells that were touching the edge of the image were discarded in this step. A composite image was then created and used to calculate cell dimensions such as cell area, cell length (long and short axis), and cell perimeter. The median of the length and shape factor (Equation 4.1) from each picture were calculated and then used to calculate group means. Although cell area is commonly measured in substrate stiffness studies, cell length and shape factor are more relevant morphological measures for ASM cells as the contractile phenotype is defined by cell elongation and cell length may play a role in contractile function. Shape factor is a calculation of 2D roundness, representing the ability of a cell to spread out on a given surface. A high shape factor is indicative of a very rounded and compact shape, while a low shape factor indicates an irregularly shaped cell with more appendages. When ASM cells were first seeded, they were a rounded shape, and within hours resembled a more fibroblastic shape, eventually lengthening. Therefore, cell length and shape factor were more descriptive of the shape changes that occur in these cells compared to just cell area.

$$Shape\ Factor = \frac{4\pi Area}{Perimeter^2} \qquad (4.1)$$

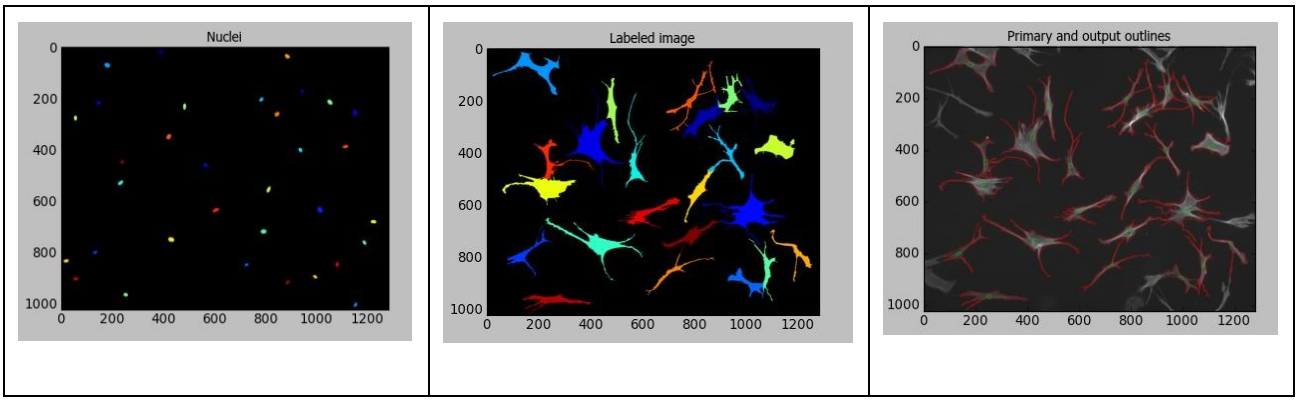

Figure 4-2. Representative image of results of three steps of the custom designed CellProfiler pipeline. The first image was generated after stringent background thresholding was applied to the DAPI image to identify cell nuclei. The second image was generated using cell nuclei from the first image to identify individual cells in the F-actin image. The final image is the composite showing the outlines of each cell and its nucleus.

The distribution of morphological measurements for individual cells within each well often demonstrated non-normal distributions (bimodal, skewed, and/or outliers). Therefore, the median length and shape factor within each image was used as this measure of central tendency is less sensitive to non-normality. For each well, three images were taken to obtain a representative sample of the distribution of morphologies across the well. The median of each image was averaged to obtain the well mean. Three wells from each donor for each experimental group were averaged to obtain group means.

Differences between the means of the three donors (n=3) from each group were tested using a series of two-way ANOVAs. Although the distribution of morphologies across an individual well may be non-normal, there is no reason to assume non-normality within the donor population. To the best of my knowledge, donors were selected randomly from the population, and therefore, the morphological response was assumed to be normally distributed. Therefore, even though the samples size was small, parametric analysis was used. Two-way ANOVAs were first performed for each morphological measure to assess the main effect of time and substrate stiffness, followed by a two-way ANOVA at each time point to assess the interaction of substrate stiffness and tone

treatment. Specific differences between substrates, between time points, or in tone treatment groups compared to vehicle were assessed using a Bonferroni correction for multiple comparisons.

4.2.4 Gene Expression Measurements

The change in ASM phenotype due to substrate stiffness or tone modulation was tested by measuring changes in expression of genes of interest that are involved in contractile mechanisms or mechanotransduction including *myh11* (smMHC), *mypt* (MLCP), *mylk* (MLCK), *acta2* (SMA), and *tagln* (Sm22) by qRT-PC.

First, RNA is extracted using the Qiagen RNeasy Mini Kit. In the initial lysis step of RNA extraction, cells grown on softwells of each group will be pooled into a single sample. Ethanol is then used to bind RNA to the silica membrane in RNeasy Spin Columns. Using spin technology, RNA is separated from contaminants and other cell materials and eluted using RNase free water. Eluted RNA is stored in -80°C until use. A small amount is used to calculate total RNA in each sample by spectrophotometry. The Qiagen QuantiTect Reverse Transcription Kit is used to generate cDNA from the RNA samples. Genes are then amplified and quantified using the Qiagen QuantiTect SYBR Green PCR Kit and the Mx3000P thermal cycler.

Total RNA was isolated from cells at each time point using the Qiagen RNeasy Mini Kit. To ensure that enough RNA was obtained, cells grown in 6 wells (same donor, same group) were pooled in the initial lysis step and treated as a single sample for the rest of the experiment. Total RNA concentration for each sample was obtained using the FLUOStar Omega microplate reader in the spectral mode to obtain UV absorbance at

260nm and 280nm. I used a two-step qPCR protocol and used the Qiagen QuantiTect Reverse Transcription Kit to generate cDNA from the RNA samples prior to PCR amplification. Each gene was amplified using 300mM primers for three candidate reference genes and five genes of interest (Table 4-2). Primer sequences were designed using commercial software and were tested for efficiency and dynamic range using a standard curve assessing five-fold dilutions of calibrator RNA across three orders of magnitude. The Qiagen QuantiTect SYBR Green PCR Kit and the Mx3000P thermal cycler were used to amplify 30ng of cDNA from each sample in duplicate. Each plate contained experimental samples, calibrator samples, and no-template controls in duplicate. Calibrator samples were cDNA reverse transcribed from pooled RNA extracted from multiple cell donors grown in plastic culture flasks.

The crossing threshold of each sample was determined using Stratagene MxPRo v4.1 software. The most stable reference gene was YWHAZ, as determined by Bestkeeper and Normfinder software (Appendix C). The efficiency of each gene was estimated using LinReg PCR software, which uses the linear region of amplification curves from all samples to estimate amplification efficiency. Gene expression was calculated relative to YWHAZ and the calibrator sample using the efficiency-corrected $\Delta\Delta$Ct method. The expression of each gene was normalised to the mean of the three donors from the soft substrates at day 0.

Similar to methods used for morphological analysis, differences between the means of the three donors (n=3) were compared as there was no reason to assume non-normality within the donor population. To the best of my knowledge, donors were selected randomly from the population, and therefore, expression of genes is assumed to

be normal. Therefore, group means were compared using a series of two-way ANOVAs and parametric multiple comparisons with Bonfferroni correction. However, for all genes, except smMHC, substrate stiffnesses were pooled because there was no main effect in any test and cells on soft and stiff substrates followed nearly identical trends. This allowed for analysis of the interaction between tone treatment and time using a two-way ANOVA. Since the changes in gene expression within the first 24 hours varied a great deal between genes, the day 0 time point was removed to better observe the general trends over time.

Table 4-2. Primer sequences and common names for all genes measured.

Common Name	Gene Code	Primer Sequence (FWD/REV)
Smooth muscle myosin heavy chain (MHC)	MYH11	5'-ATCGGGAGGACCAGTCCATT-3' 5'-GCTCTCCCGTGATACTTGTGT-3'
Myosin light chain kinase (MLCK)	MYLK	5'-CTGCTGCCTGACCACGAATA-3' 5'-CATCCTTCGGCTCTTCAGGT-3'
Myosin light chain phosphatase (MLCP)	MYPT1	5'-TGCTGCAGCTTCTACCACAACCC-3' 5'-TGAGGTATGATCTGCGTCTCTCCCT-3'
smooth muscle α-actin (SM actin)	ACTA2	5'-TAAGACGGGAATCCTGTGAAGC-3' 5'-TACAGAGCCCAGAGCCATTG-3'
Sm22α	TAGLN	5'-ATCATAGTGCAGTGTGGCCC-3' 5'-CAGCTTGCTCAGAATCACGC-3'
Ubiquitin C (UBC)	UBC	5'-ATAAGGACGCGCCGGGTGTG-3' 5'-GCATTGTCAAGTGACGATCACAGCG-3'
Glyceraldehdye 3-phosphate dehydrogenase (GAPDH)	GAPDH	5'-CTGCTGATGCCCCCATGTTCGT-3' 5'-TGGTGCAGGAGGCATTGCTGATG-3'
Phospholipase A2 (YWHAZ)	YWHAZ	5'-CGCTGGTGATGACAAGAAAGGGAT-3' 5'-GGGCCAGACCCAGTCTGATAGGA-3'

4.2.5 Contractile Function Measurements

Cell stiffness and contractile function was measured using OMTC. A detailed description of OMTC methodology can be found in chapter 2.5. Initial contractility experiments included four different designs that differed in substrate, drug dosing time points, and cell growth time points, as well as different serum conditions and tone modulating agents. Results from these experiments were variable, however, we did observe a general increase in baseline stiffness and contractility over time (see Appendix B). The results from these early experiments suggested that longer culture times might be necessary to observe significant effects of tone and substrate stiffness, providing the basis for the adjusted contractile experimental design described below.

Adjusted Chronic Contractility Experiments

Based on observations made during cell morphology and gene expression experiments, the chronic contractility experiments were repeated with an adjusted design to better match this data. Cells were seeded on soft and stiff substrates at cell densities listed in Table 4-1 in standard feeder media containing 0.5% serum. The media was replaced after 4 hours with 0.5% serum media containing forskolin (10μM), histamine (10μM), or vehicle (1% DMSO). Control measurements were taken after the initial 4 hours, before any drug containing media was added, and measurements were taken at 1, 3, and 7 days for experimental time points. For all experimental time points media was switched to IT media containing drug 24 hours before baseline measurements. Beads were added and baseline stiffness and contractility measurements were performed as described in chapter 2.5.

In the analysis of the earlier contractile function data, there appeared to be more variability between wells than there was between donors. Therefore, the number of wells measured was used as the sample size for statistical analysis as this was likely the largest source of variability. Due to unequal sample sizes between different time points, one-way ANOVAs within each tone treatment and substrate stiffness group were used to compare means across time. Because the distribution stiffness measured within wells is known to be skewed, it is possible that the distribution of the stiffness of the wells is also non-normal. Therefore, due to the combination of unequal and small sample sizes across time, non-parametric Kruskal-Wallis post-hoc analysis was employed to evaluate specific differences across time. This was followed by a two-way ANOVA to confirm the main effect of time, and to measure main effects of substrate stiffness or any interactions. A Bonferroni post-hoc analysis was used to confirm significant differences between time points found with the Kruskal-Wallis test, evaluate the effect of substrate stiffness, and to ensure appropriate consideration of multiple comparisons. This was followed by two-way ANOVAs at each time point to examine the main effects and interactions of substrate stiffness and tone treatment. A Bonferroni post-hoc analysis was used to compare forskolin and histamine group means to vehicle, and examine specific effects between soft and stiff substrates when there was a main effect of these variables.

4.2.6 Statistical Analysis

Statistical significance was assessed using GraphPad 4.0 software with $p<0.05$ considered statistically significant. Specific statistical tests are detailed in the methods sections for each measure.

4.3 Results

4.3.1 Development of the Protocol

I first attempted to generate dose response curves for the contractile response to chronic dosing for each drug (Appendix B:). However, the inherent variability in OMTC and large number of experimental groups made complete dose response curves very time consuming. I additionally carried out acute dose response experiments on cells cultured on glass under different serum conditions to confirm the acute contractile or relaxant response of ASM cells to the candidate pharmacological agents under different serum conditions (Appendix B:). Based on these experiments, I was not confident in the effects of Y27632 or cantharidin on ASM cells and did not use these agents as tone modulators beyond the initial contractile function experiments. Based on evidence from these experiments and published literature (42), I selected histamine and forskolin at a concentration of 10μM to chronically increase and decrease tone respectively in ASM cell culture in the following experiments.

4.3.2 Cell Morphology

To allow for a more direct comparison to previous work that examines the effect of substrate stiffness and changes in contractile phenotype, 2D cell morphology was analysed in primary ASM cultures. We found that at all time points, vehicle treated cells on stiff substrates had increased cell length (Figure 4-3) and a lower shape factor (Figure 4-4) than cells cultured on soft substrates ($p<0.05$). Cell shape was differentially affected by both time and drug treatment on stiff versus soft substrates.

On stiff substrates, cell length almost doubled over time (124±2 μm at day 0) in both vehicle (225±4 μm) and histamine (249±26 μm) treated cells ($p<0.001$) (Figure 4-3). In contrast, forskolin treated cells did not lengthen as much over time (171±15 μm), and were shorter than vehicle treated cells by day 7 ($p<0.05$, Figure 4-3). Unlike cell length, shape factor of cells on stiff substrates did not change over time or between treatment groups (Figure 4-4).

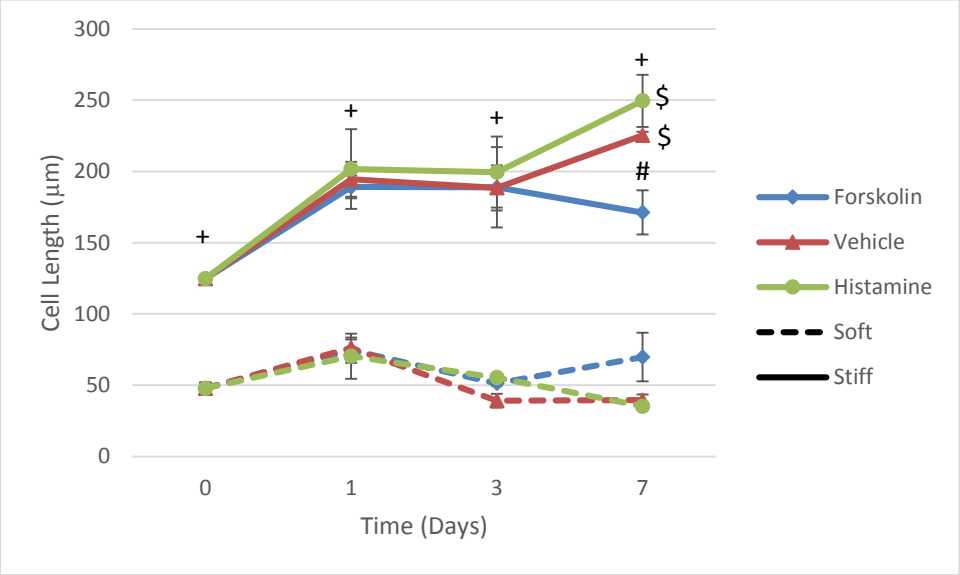

Figure 4-3 Length of cells cultured on soft or stiff substrates and treated with vehicle, forskolin (10μM), or histamine (10μM) for 7 days. At all time points and within all drug treatment groups, cells were significantly longer on stiff substrates than on soft (+$p<0.05$, 2-way ANOVA of time and substrate stiffness within each treatment group with Bonferroni post-hoc). On stiff substrates, cells were significantly longer at day 7 compared to day 0 in both the histamine and vehicle treated cells ($p<0.001, 2-way ANOVA of time and substrate stiffness within each drug treatment with Bonferroni post-hoc compared to day 0). This lengthening effect over time was not observed in the forskolin treated cells on stiff substrates, resulting in significantly shorter cells at day 7 (#$p<0.05$, 2-way ANOVA of substrate stiffness and drug treatment at day 7 with Bonferroni post-hoc compared to vehicle). All groups had three donors (n=3) that were the means of at least 4 wells. Error bars represent SEM.

In contrast, it was shape factor, but not length, that was affected by both time and tone treatment in cells cultured on soft substrates. Similar to changes in cell length on stiff substrates, shape factor increased over time on soft substrates in vehicle (0.57±0.06 AU) and histamine (0.55±0.04 AU) treated cells ($p<0.05$, Figure 4-4). Again, forskolin

inhibited this increase over time and these cells had a lower shape factor at day 7 (0.29±0.06 AU) compared to vehicle treated cells ($p<0.01$, Figure 4-4).

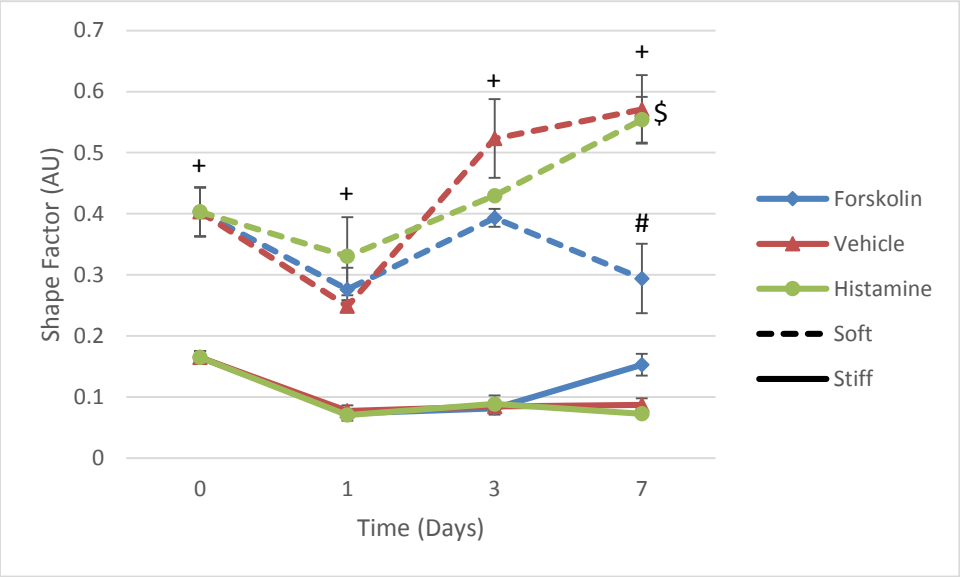

Figure 4-4. Shape factor of cells cultured on soft or stiff substrates and treated with vehicle, forskolin (10μM), or histamine (10μM) for 7 days. On soft substrates, cells had a higher shape factor at day 7 compared to day 0 in vehicle and histamine treated cells ($\$p<0.05$, 2-way ANOVA of time and substrate stiffness within each drug treatment with Bonferroni post-hoc compared to day 0). Shape factor did not increase over time in forskolin treated cells, resulting in a significantly lower shape factor in forskolin treated cells compared to vehicle at day 7 ($\#p<0.01$ 2-way ANOVA of substrate stiffness and drug treatment at day 7 with Bonferroni post-hoc compared to vehicle). Substrate stiffness was a significant effect in all treatment groups and at all time points ($+p<0.05$, 2-way ANOVA of time and substrate stiffness within each treatment group with Bonferroni post-hoc). All groups had three donors (n=3) that were the means of at least 4 wells. Error bars represent SEM.

These data show that cells lengthened on stiff substrates and were more compact on soft substrates, creating very different morphologies by day 7 (Figure 4-5 B). However, forskolin treatment had opposing effects on soft and stiff substrates resulting in cells with similar shapes on soft and stiff substrates after 7 days (Figure 4-5 A).

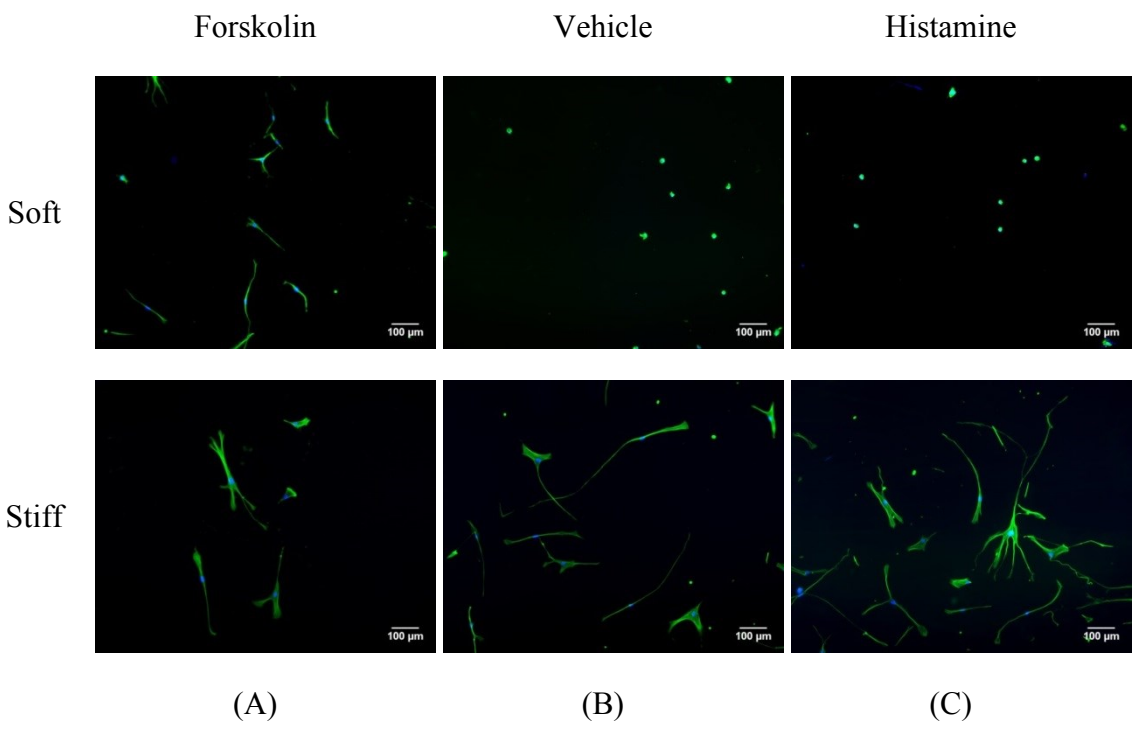

Figure 4-5. Representative pictures of cells stained for nuclei (blue, DAPI stain) and F-actin (green, phalloidin stain) after 7 days of culture on soft or stiff substrates in forskolin, vehicle, or histamine supplemented media. Contrast has been digitally enhanced to allow for qualitative assessment.

4.3.3 Contractile Gene Expression

To assess whether cell phenotype was indeed changing due to substrate stiffness or tone, it was necessary to examine changes in genes related to contractile phenotype and function. Initial analysis of vehicle treated cells using a 2-way ANOVA of substrate stiffness across time showed that substrate stiffness altered expression of smMHC ($p<0.05$), but surprisingly had no effect on expression of SMA ($p=0.26$), Sm22 ($p=0.51$), MLCK ($p=0.94$), or MLCP ($p=0.17$) and no significant interaction was found between substrate stiffness and time (Figure 4-6). However, expression of all genes, with the exception of MLCP, changed over time. Although changes from day 0 to day 1 were different between genes, a similar trend of increasing expression over time was observed. Expression of Sm22 decreased within the first day by more than 70% (soft=0.24±0.005,

stiff=0.29±0.003, $p<0.05$) and increased to 60% of baseline by day 7 (soft=0.60±0.07, stiff=0.65±0.1, $p>0.05$). A similar trend was observed in SMA with expression initially decreasing and then exceeding baseline by day 7 (soft 1.35±0.12, stiff=1.61±0.08, $p>0.05$), although post-hoc analysis was not significant. Expression of MLCK did not have the initial decrease like Sm22 and SMA, but steadily increased over time by more than 250% by day 7 (soft=2.99±0.23, stiff=2.48±0.13, $p<0.001$). Similarly, smMHC expression increased to almost 300% of baseline by day 7, but only on stiff substrates (2.98±0.47, $p<0.05$). On soft substrates, smMHC expression was unchanged over time (1.26±0.18, $p>0.99$).

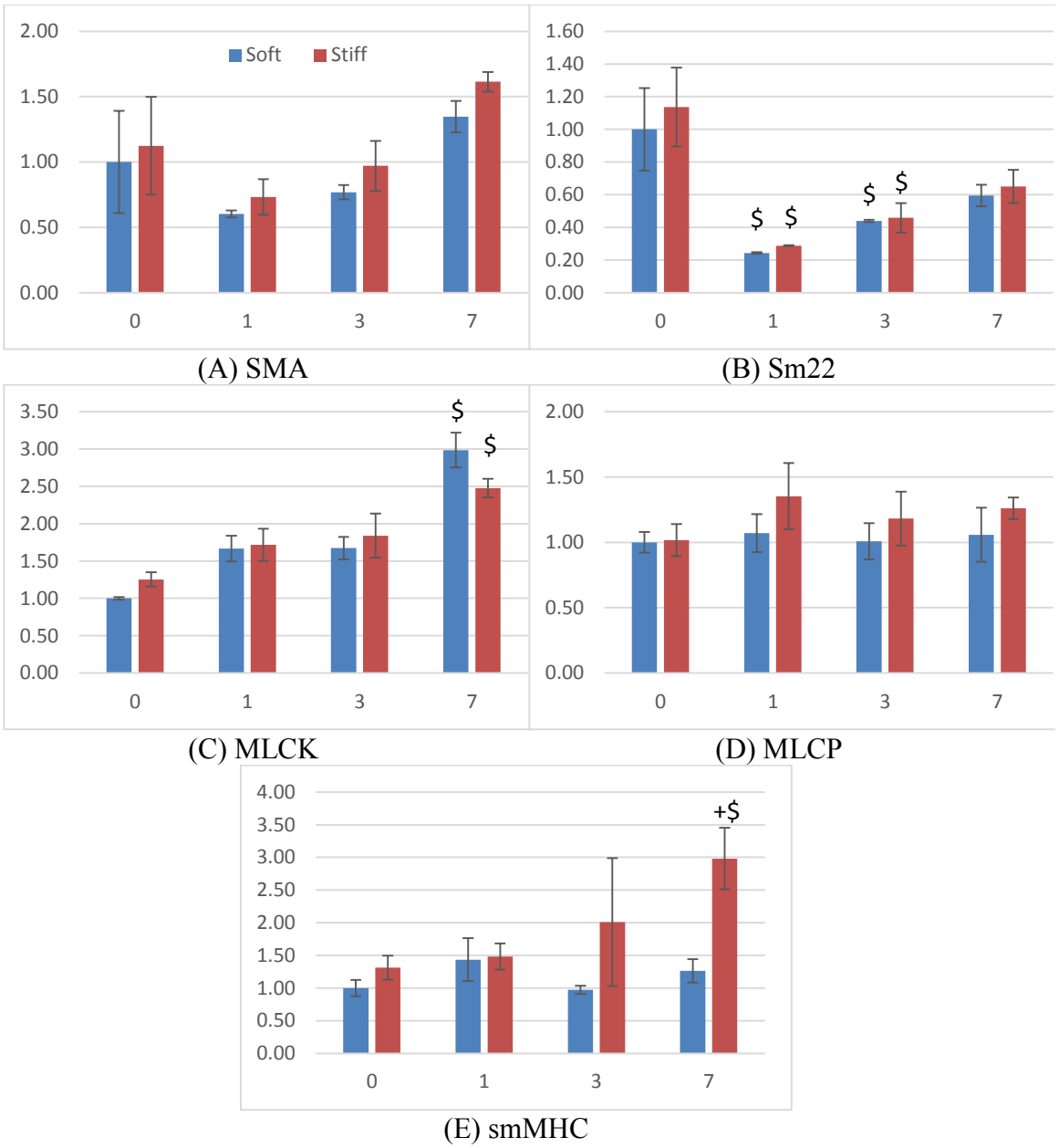

Figure 4-6 Gene expression over time of ASM cells cultured on soft or stiff substrates in vehicle media. Graphs show data from 5 genes of interest SMA (A), Sm22 (B), MLCP (C), MLCK (D), MHC (E) analysed using the efficiency corrected method of quantification against a stable reference gene YWHAZ and normalised to soft substrates at day 0. Statistical analysis was performed using a 2 way ANOVA with Bonferroni post-hoc where +$p<0.05$ compared to soft substrates and \$$p<0.05$ compared to day 0. All groups consist of three donors (n=3) that contain RNA pooled from at least 6 wells. Error bars represent SEM.

Since substrate stiffness contributed little variability to any treatment or time point and gene expression followed very similar trends on both soft and stiff substrates for most genes measured, groups were pooled for subsequent analysis of all genes except smMHC. Histamine had no effect on expression of any gene at any time point or on any

substrate stiffness and generally followed similar expression trends as vehicle treated cells (Figure 4-7). In contrast, forskolin treatment had a moderate effect on expression of SMA and Sm22. The increase in expression of both Sm22 and SMA in vehicle treated cells over time was inhibited with forskolin treatment, resulting in lower expression compared to vehicle treated cells by day 7 ($p<0.0001$) (Figure 4-7 A and B). Expression of MLCP and MLCK did not change significantly with any tone treatment (Figure 4-7 C and D). Interestingly, although smMHC expression was regulated by substrate stiffness, tone treatments had little effect on expression in cells cultured on either soft or stiff substrates (Figure 4-7 E and F).

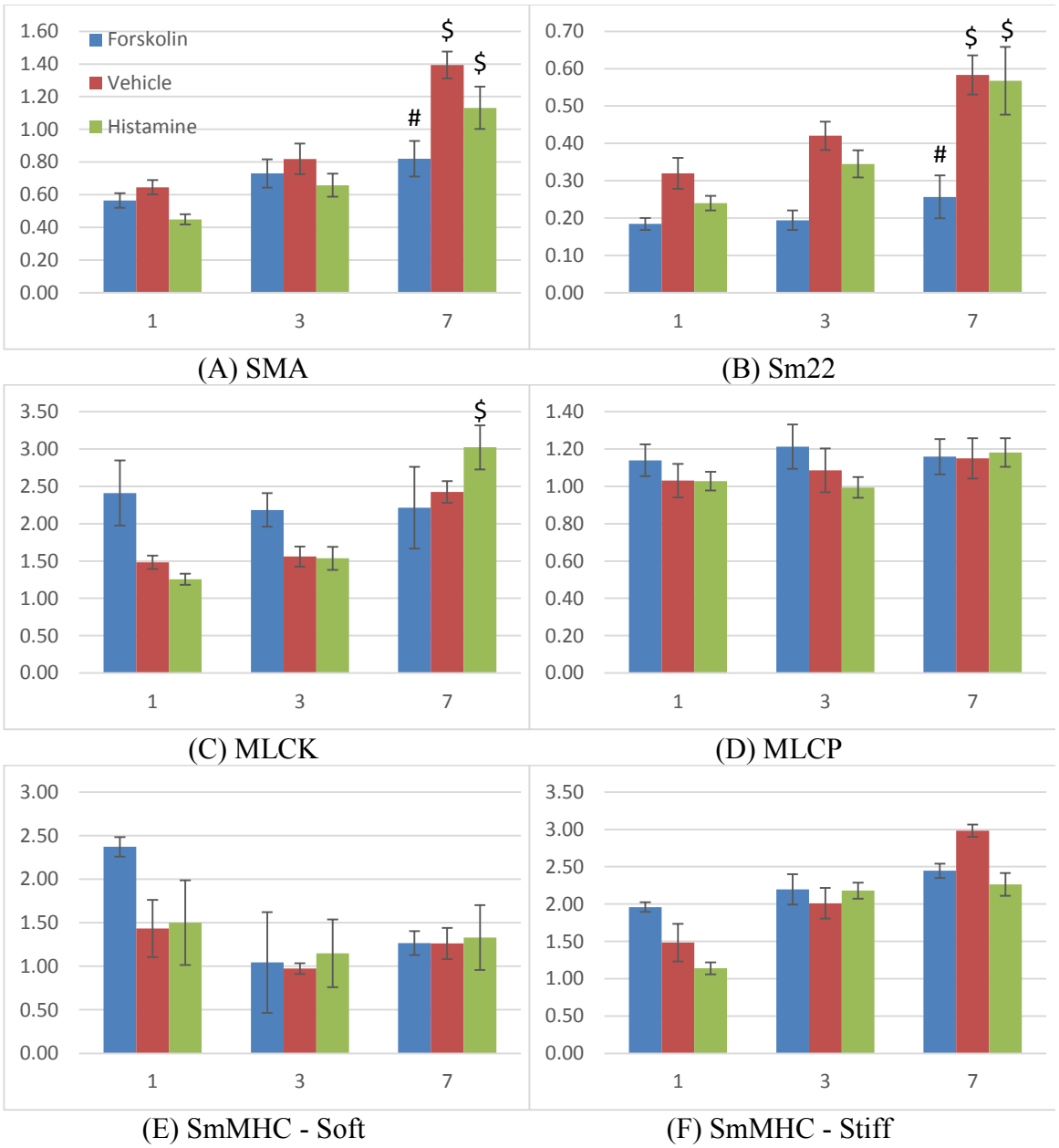

Figure 4-7 Gene expression over time of ASM cells cultured on any substrate and treated with vehicle, forskolin (10µM), or histamine (10µM) for 7 days. Graphs show data pooled from both soft and stiff substrates from 4 genes of interest SMA (A), Sm22 (B), MLCP (C), and MLCK (D) normalised to pooled cells at day 0. Each group consists of three donors from each substrate (n=3) with RNA from at least 6 wells per sample. Expression of smMHC is divided into soft (E) and stiff (F) substrates with the same treatment groups and normalised to day 0 within each substrate. All data were analysed using the efficiency corrected method of quantification against the reference gene YWHAZ. Statistical analysis was performed using a 2-way ANOVA of time and treatment with Bonferroni post-hoc where #$p<0.05$ compared to vehicle treated cells within each time point and \$$p<0.05$ compared to day 1 within each treatment. Error bars represent SEM.

4.3.4 Adjusted Contractile Function Experiments

The intriguing results obtained from morphology and gene expression studies motivated further experiments in contractile function to provide a more complete data set to match these studies. Therefore, contractile function experiments were repeated and re-analysed to include the same time points (0, 1, 3, and 7 days) using the same tone modulation procedures (10μM histamine or forskolin, or vehicle media containing 0.5% serum) on soft and stiff substrates (E_{soft}=600Pa; E_{stiff}=19.2kPa). Similar to previous experiments in this thesis, there appeared to be an increase in baseline stiffness over time from day 1 (G'_{soft}=0.27±0.07 Pa/nm and G'_{stiff}=0.18±0.03 Pa/nm) to day 7 (G'_{soft}=0.64±0.07 Pa/nm and G'_{stiff}=0.50±0.06 Pa/nm) in vehicle treated cells, although these differences only reached significance on soft substrates ($p<0.05$) (Figure 4-8B). Similarly in histamine treated cells, baseline stiffness increased ($p<0.05$) over time on soft and stiff substrates (Figure 4-8C). Interestingly, the increase over time was not observed in forskolin treated cells (Figure 4-8A).

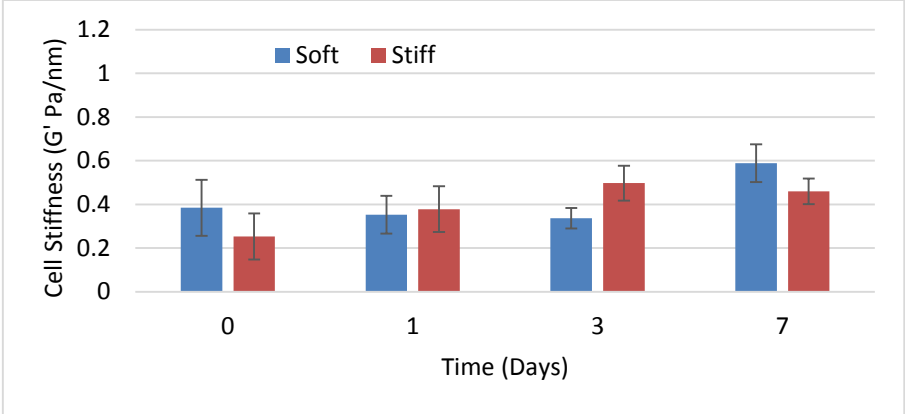

(A)

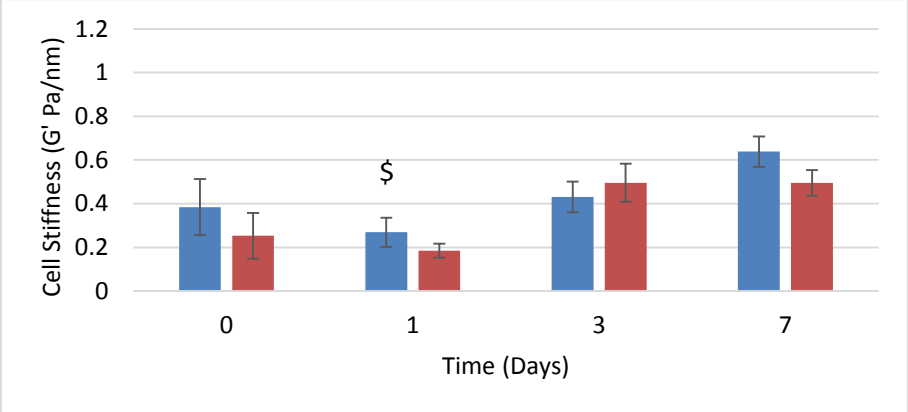

(B)

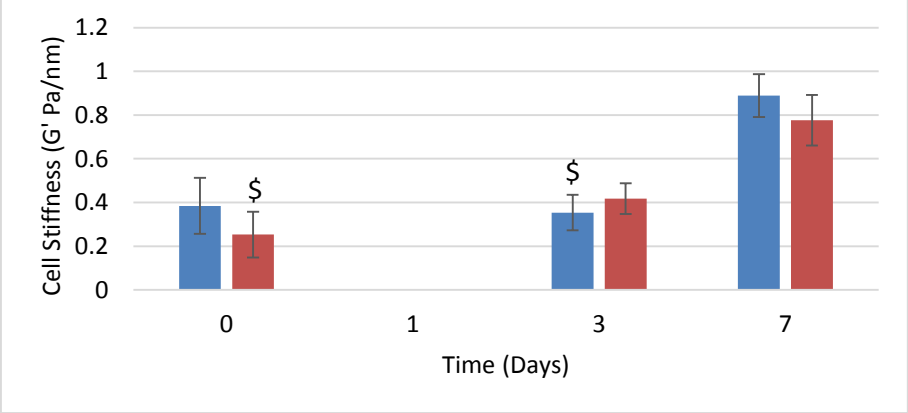

(C)

Figure 4-8 Baseline stiffness of cells over time. Primary ASM cells cultured for 4 hours (Day 0), 1 day, 3 days, or 7 days on soft (600 Pa) or stiff (19 200 Pa) PA gels. Cells treated with forskolin (10 µM) (A) showed no change in stiffness over time due to substrate stiffness. Cells treated with vehicle media (B) or histamine (10 µM) (C) were less stiff at day 1 (vehicle) or day 3 (histamine) compared to day 7 ($ $p<0.05$) on both soft and stiff substrates. Data for histamine treated cells is incomplete and is missing measurements for the day 1 time point. Values are means ± SEM, n=4 from one donor for day 0, n=7-8 from 2 donors for day 1, n=12-16 from 4 donors for day 3, and n=21-24 from 5 donors for day 7. Statistical differences over time were evaluated using a one-way ANOVA with non-parametric Kruskal-Wallas post-hoc analysis. A two-way ANOVA with Bonferroni post-hoc confirmed statistical differences over time and demonstrated significant differences between soft and stiff substrates.

Vehicle treated cells also demonstrated an increase in contractile function over time, however, this effect was only observed on stiff substrates ($p<0.05$) while there was no significant change in contractile function on soft substrates over time (Figure 4-9B). This stiffness dependent increase over time resulted in cells with higher contractile function on stiff substrates (58.99±7.68%) compared to soft (29.73±7.10%) ($p<0.05$), confirming the previous hypothesis that longer time points are necessary to observe the effect of substrate stiffness on contractile function. In contrast to changes in baseline stiffness over time, forskolin did not inhibit an increase in contractile function over time and cells on both soft and stiff substrates demonstrated an increase ($p<0.05$) from day 1 (-14.74±7.08% on soft and -0.99±5.98 on stiff) to day 7 (47.13±12.198% on soft and 74.48±14.88 on stiff) (Figure 4-9A). In contrast, although there appears to be a trend of increasing contractile function over time, there were no changes due to substrate stiffness or time in histamine treated cells (Figure 4-9C).

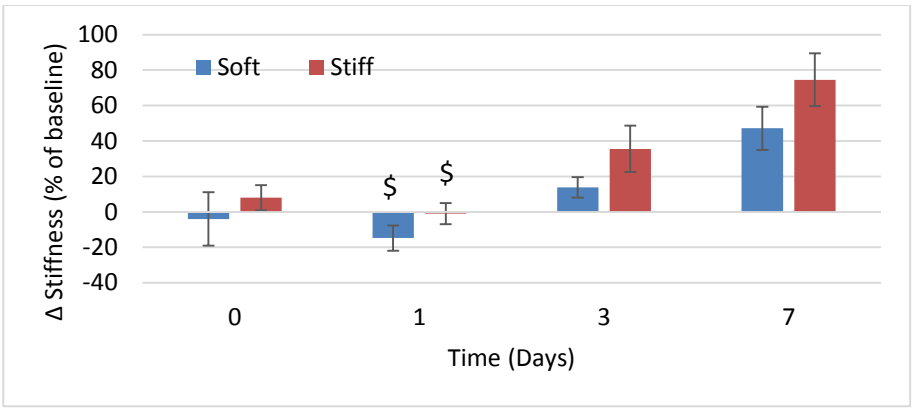

(A)

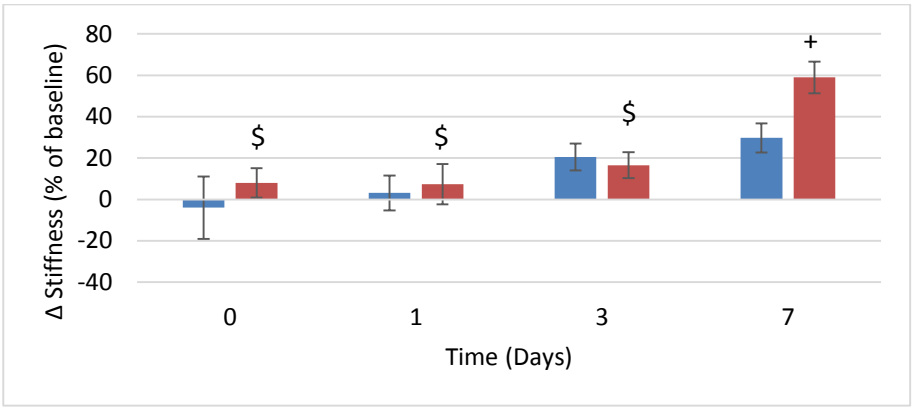

(B)

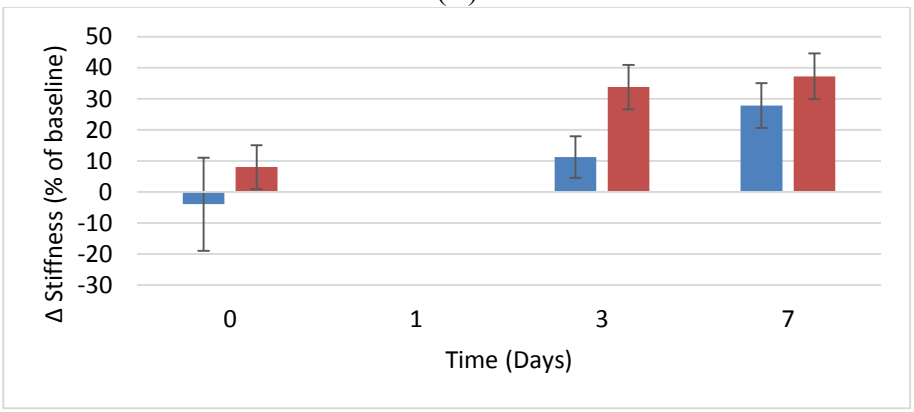

(C)

Figure 4-9 Contractility of cells over time. Primary ASM cells cultured for 4 hours (Day 0), 1 day, 3 days, or 7 days on soft (600 Pa) or stiff (19 200 Pa) PA gels. Cells treated with forskolin (10 µM) (A) were more contractile after 7 days in culture ($p <0.05 compared to day 7) on both soft and stiff substrates. Cells treated with vehicle media (B) were more contractile at day 7 only on stiff substrates ($ p<0.05 compared to day7). Cells were more contractile on stiff substrate compared to soft (+ p<0.05) after 7 days in culture when treated with vehicle (B). Cells treated with histamine (10 µM) (C) showed no change in contractility due to culture time or substrate stiffness. Data for histamine treated cells is incomplete and is missing measurements for the day 1 time point. Values are means ± SE, n=4 from one donor for day 0, n=7 or 8 from 2 donors for day 1, n=12 to 16 from 4 donors for day 3, and n=21 to 24 from 5 donors for day 7. Statistical differences over time were evaluated using a one-way ANOVA with non-parametric Kruskal-Wallas post-hoc analysis. A two-way ANOVA with Bonferroni post-hoc confirmed statistical differences over time and demonstrated significant differences between soft and stiff substrates.

Similar to morphology and gene expression studies, the effects of tone modulation on baseline stiffness and contractility were only observed after 7 days, with no significant differences between treatment groups at day 1 or 3 (Figure 4-10).

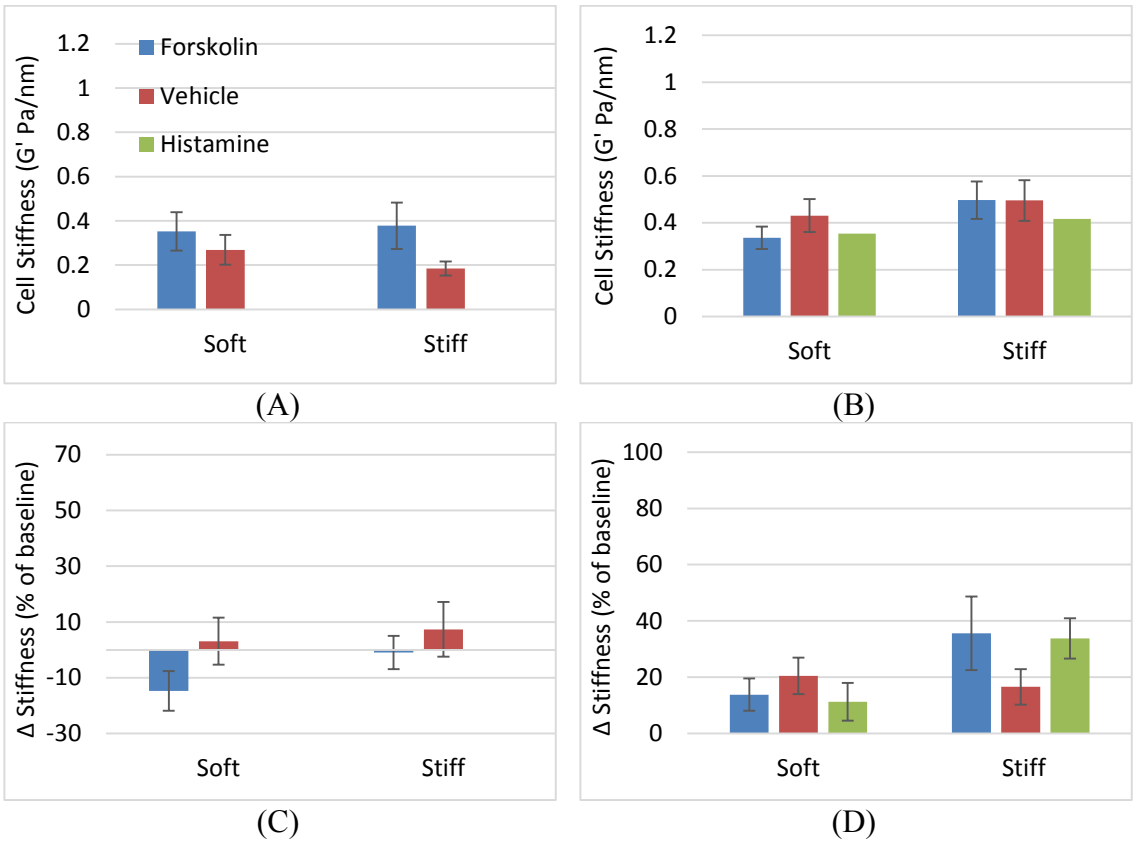

Figure 4-10. Baseline stiffness and contractility with tone modulation at earlier time points on soft and stiff substrates. After 1 day (A and C), there were no significant differences in baseline stiffness (A) or contractility (C) between vehicle and forskolin treated cells or between soft and stiff substrates. The data set for histamine treatment is incomplete and therefore, there is no data baseline stiffness or contractility data for histamine treatment at 1 day. After 3 days of treatment (B and D), there were no significant differences in baseline stiffness (B) or contractility (D) between vehicle and forskolin treated cells or between soft and stiff substrates. Statistical differences were evaluated with a two-way ANOVA of substrate stiffness and tone treatment at each time point. Values are means ± SE, n=7 or 8 from 2 donors for day 1, n=12 to 16 from 4 donors for day 3.

At day 7, histamine treated cells appeared to have a higher baseline stiffness on both soft and stiff substrates (Figure 4-11), but were not significantly different from vehicle. Interestingly, it was the forskolin treated cells that seemed to have increased contractile function, although again this was not significant different from vehicle (Figure 4-11B). Because the stiffness of the histamine treated cells was higher at baseline (Figure 4-11A), even though the contractile function appeared to be decreased, the absolute stiffness of the histamine cells after KCl treatment was still higher. There were no significant differences in post KCl absolute stiffness due to treatment or substrate stiffness (Figure 4-11C).

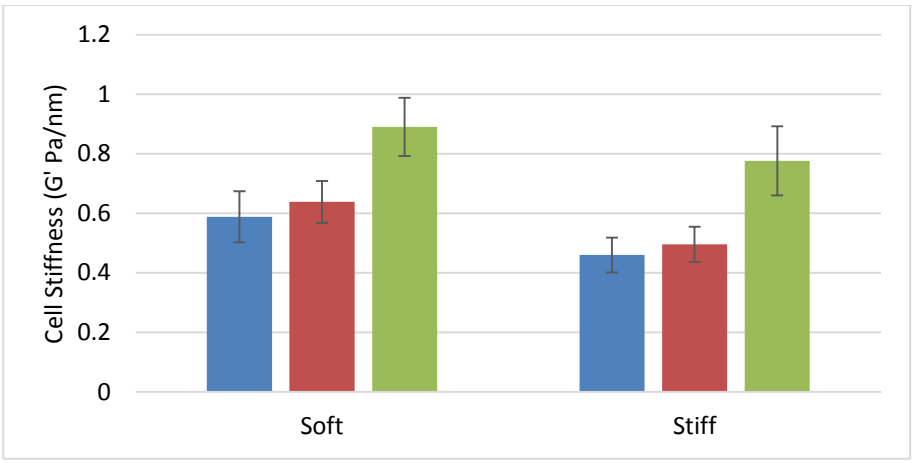

(A)

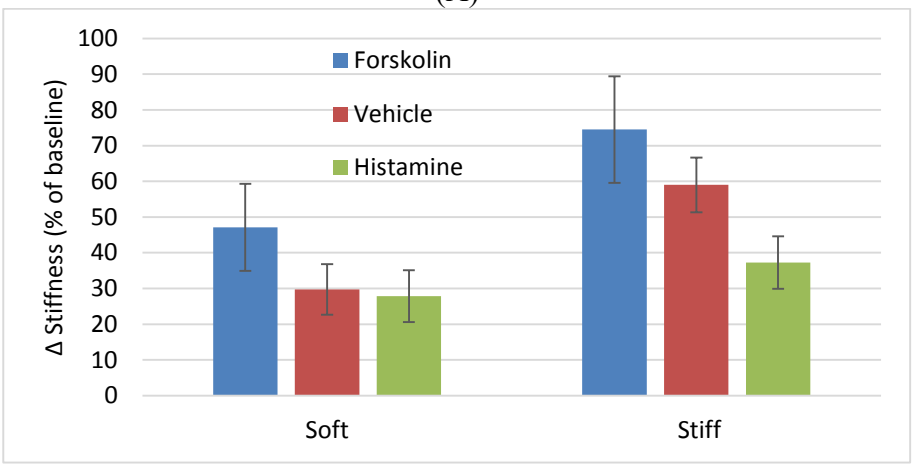

(B)

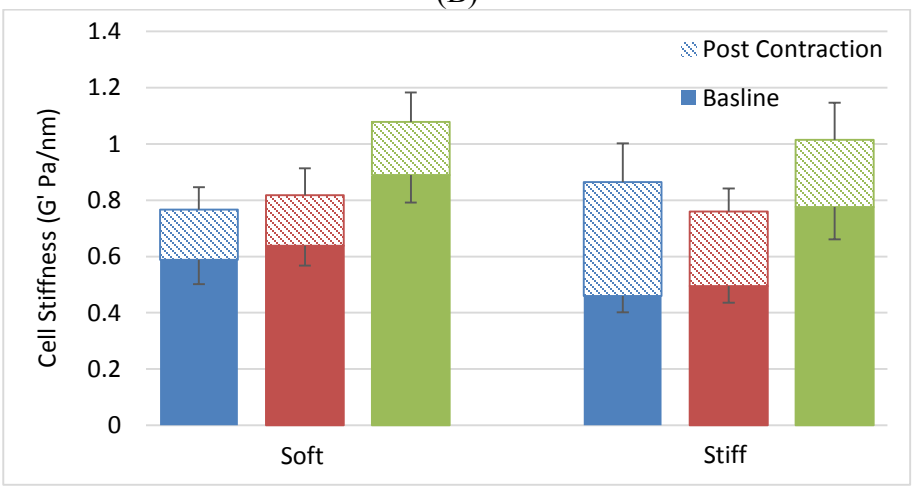

(C)

Figure 4-11 Baseline stiffness and contractility after 7 days of tone modulation on soft and stiff substrates. Cell stiffness (A) appeared to be increased in histamine (10 μM) treated cells soft (600 Pa) and stiff (19 200 Pa) substrates. Cell contractility (B) appeared to be decreased in histamine treated cells. Although change in cell stiffness (contractility) was increased in forskolin treated cells, the absolute stiffness post KCl of histamine treated cells was not significantly different from forskolin or vehicle cells (C). Values are means ± SE, n=21 to 24 from 5 donors. All statistical significance obtained from a two-way ANOVA of substrate stiffness and tone treatment at 7 days with a Bonferroni post-hoc analysis.

4.4 Discussion

The central hypothesis of this aim was that cells with higher tone would demonstrate an augmented contractile phenotype on stiff substrates compared to cells with lower tone or cells on soft substrates. This hypothesis rested on the assumption that a stiff substrate induces a more contractile phenotype in cultured ASM cells, including increased contractility, cell length, and expression of contractile and smooth muscle specific genes. Initially, it appeared that substrate stiffness had little effect on contractile phenotype in vehicle treated cells (Appendix B), contrary to the assumptions made based on previous literature and previous observations in our lab. However, the first principal finding of this chapter was that time is an important factor to consider when studying these cellular responses as the contractile response to substrate stiffness was largely time dependent. Previous literature largely ignores time as a variable and many cell culture studies are carried out on acute time scales, or without controlling for time. Therefore, the experimental design and interpretation became more complex due to the addition of an independent variable that is often not considered. The second principal finding is that ASM cells cultured on stiffer substrates do eventually express many characteristics of the contractile phenotype, including increased baseline stiffness and contractile function, more elongated cells, and increased expression of smMHC mRNA. The final important finding of this aim was that while decreasing cell tone does alter the morphological response to substrate stiffness, it also affects expression of some genes regardless of substrate.

4.4.1 Independent Effects of Substrate Stiffness

In the initial experiments for this aim, I measured cell stiffness under multiple conditions and tested a variety of time points (Appendix B:). It became clear that cellular behaviour was changing over time in culture, which prompted an experimental design that included time as an independent variable, showing that cells generally appear to express a more contractile phenotype over time. Previous studies have shown that ASM cells generally switch to a non-contractile/synthetic phenotype when grown in serum at subconfluence (64), while prolonged serum deprivation allows cells to regain contractile function and increase expression of contractile phenotype marker protein (63, 86) and mRNA (114). In the experiments presented here, cells were grown in very low serum conditions, therefore, the increase of contractile genes, cell length, and contractile function over time is consistent with redevelopment of the contractile phenotype. Interestingly, the phenotypic changes over time were not observed when cells were cultured on soft substrates. While cell shape was sensitive to substrate stiffness at all time points, differences were augmented after 7 days at which point cells on stiff substrates were also more contractile and expressed moderately more smMHC mRNA compared to soft.

Substrate stiffness has been shown to be a potent modulator of cellular processes, however, many of these studies look at much shorter culture times. For example, an increase in cell spreading on stiffer substrates has been shown repeatedly with cells cultured at time points as short as 4 hours (7, 27, 38, 57, 90, 107, 113), while the phenomenon of increased force on stiff substrates has been demonstrated after 24 hours in culture (7, 90, 113). Additionally, increases in SMA protein and mRNA in cells on

stiff substrates have been demonstrated at shorter time periods (70, 82, 107). Thus it is interesting that in the present study, we found that substrate stiffness did not affect cellular responses at earlier time points. However, while a wide range of cellular responses have been studied in a variety of cell types, the study presented here is unique in examining the specific effect on contractile function and phenotype at different time points in ASM cells. Some of these experimental differences may explain the lack of agreement at earlier time points with other studies.

One important distinction between other experiments and the present study was the tool used to measure cellular force. Most of the studies mentioned used traction force microscopy (TFM) and only measured baseline cell force (7, 27, 83, 90, 95, 113), which measures how much force the cell applies to the substrate without any contractile stimulus. In contrast, we have shown differences in the change in cell stiffness after maximal contraction. Stiffness has been shown to be proportional to contractile force measured by TFM (148), and is a reliable indicator of contractile response. Bhana et al. (18) found that cardiomyocytes were more contractile on stiff substrates compared to soft after 5 days in culture using electrical stimulation and measuring cell traction, supporting the finding of this thesis that cells are more contractile on stiff substrates. However, the dynamics of the contractile response have been shown to be more transient within the first 24 hours after subculture compared to a more sustained response at 5 days (7). Thus it is possible that our experimental protocol for OMTC did not measure the differences in the contractile response that may have occurred at earlier time points. As discussed in chapter 1, ASM cells are mechanically plastic (23) and baseline stiffness may not correlate to the maximal contractile ability of the cell. Additionally, it has been theorised

that active and passive force are regulated via divergent pathways (118), suggesting that baseline stiffness and contractility may respond differentially to stimuli. Importantly, it is the contractile force a cell generates in response to a stimulus that is thought to contribute to AHR and airway narrowing.

Potential differences in active and passive force generation highlight the importance of a cell specific response, where much of the analysis of the cellular response to substrate stiffness has been investigated in non-muscle cell types (18, 27, 70, 82, 90, 95, 107). Importantly, these studies measure expression in fibroblasts and use SMA as a marker for differentiation into a muscle cell type. Smooth muscle cells, by definition, express more contractile proteins including SMA, Sm22, and smMHC compared to fibroblasts, and this may cause changes in gene expression to be very small compared to baseline. Studies of both ASM (7) and VSM (113) showed differences in cellular force on stiff substrates compared to soft after only 24 hours. However, while SMA, along with other cytoskeletal proteins, is found to increase in VSM cells after only two days in culture in one study (113), others found no difference in SMA expression with longer culture times (105). While there are few studies that measure contractile phenotype on physiological substrates in ASM cells, a previous study from our laboratory found that contractile protein expression, along with contractile function increased with substrate stiffness after 7 days in culture (152).

It may be important to note that many of the studies mentioned thus far have shown changes in protein instead of mRNA expression presented in this thesis. Interestingly, some have noted that while absolute expression of some proteins did not change, the quality or localisation is affected by substrates stiffness. For example, the nature of SMA

expression is altered in smooth muscle and fibroblasts (38, 107) on different substrate stiffnesses, while calcium binding proteins are colocalised with SMA on soft substrates in smooth muscle cells (113). Therefore, it is possible that differences in contractile function in ASM cells due to substrate stiffness occur post-transcriptionally. However, while the results presented here found no substrate stiffness-dependent transcriptional changes in most genes, differences in smMHC implies that there are some transcriptional effect.

This is unsurprising as other studies overwhelmingly support mechanical regulation of transcriptional pathways. One way this likely occurs is through serum response factor (SRF), a ubiquitous transcription factor that is considered a master regulator of contractile and cytoskeletal genes, including those measured here (93). This transcription factor induces both contractile and proliferative gene programs depending on the activity of cofactors (150), and is known to be regulated by a number of different signaling pathways. Mechanically regulated gene transcription has been shown to involve SRF activation via a signaling pathway sensitive to disturbances in actin polymerisation (70, 146). However, in most studies that describe SRF mediated contractile gene expression, all contractile genes change concomitantly. Thus, the inhibition of smMHC transcription on soft substrates presented here suggests that the phenotypic response to substrate stiffness in ASM cells may occur through alternative mechanisms to those demonstrated in other studies.

Taken together, the results presented here suggest that serum deprivation can induce a contractile phenotype in smooth muscle cells, but only on stiff substrates. Additionally, although some characteristics of the contractile phenotype developed, importantly an increase in contractile function, not all measures changed. This suggests that features of a

contractile phenotype are not always correlated and can become “uncoupled”, similar to the conclusions drawn from Mih *et al.* (94).

4.4.2 Effect of Tone Modulation

While the work discussed up to this point showed that substrate stiffness has a time-dependent effect on contractile phenotype, the central aim of this portion of the thesis was to determine whether tone would alter this response. Studies from our lab and others suggest that the presence of strain is required to observe phenotypic effects of tone modulation (28, 42, 50-52, 55), leading to the hypothesis that a stiff substrate would have a similar effect on cell phenotype as strain did. If this were true, cells on a stiff substrate with high tone would be more contractile. However, here we found that increasing tone with histamine had no effect on almost all measures of contractile phenotype. In contrast, decreasing tone with forskolin altered cell morphology in a time- and substrate-dependent manner. Interestingly, forskolin also affected time-dependent changes in some genes *independently* of substrate stiffness.

There are few studies that have evaluated how tone modulation affects mechanotransduction, but those that do all use fibroblasts at much shorter time points. Results from these studies are consistent in finding that cell relaxation inhibits contractile features on stiff substrates via RhoA signaling but has no, or a reversed effect on soft (70, 82, 94). Indeed, changes in cell area in fibroblasts found by Mih *et al.* are similar to the results presented here where treatment with forskolin had opposing effects on different substrates: inhibiting lengthening on stiff, while allowing cells to spread more on soft (Figure 4-3 and Figure 4-4). The study by Mih *et al.* provided evidence that the decreased spreading on soft was due to cell attachments pulling off the substrate, suggesting that the

substrate does not provide enough resistance to cellular forces under normal circumstances, thus decreasing cell tone allows for cell anchoring and spreading (94). Taken in isolation, this morphological observation might imply that low cell tone plays a protective role in phenotypic changes induced by a stiff substrate, or a fibrotic lung. However, changes in cell shape and size were not reflected in functional changes or gene expression results.

In contrast to morphological changes, forskolin treatment had little effect on contractility (Figure 4-11) or smMHC (Figure 4-7) while inhibiting SMA and Sm22 gene expression at 7 days, regardless of substrate (Figure 4-7). This result is inconsistent with studies in fibroblasts that found lowering cell tone inhibited the increases in traction force, focal adhesion size, stress fiber formation, and expression of SMA mRNA and protein that occurred on stiff substrates (70, 82, 94). However, because we saw no difference in SMA or baseline cell stiffness, which would be analogous to traction forces, on stiff substrates, it is difficult to compare the effects of tone modulation.

As discussed in chapter 1, the cytoskeleton plays an important functional role in mechanotransduction and force generation within the cell, thus it is reasonable to think that changes in the structure, and therefore the shape, of the cell would correlate with contractile function. Additionally, the regulation of contractile genes can occur via pathways dependent on actin polymerisation dynamics (87), again, implying that there may be a functional correlation between cell shape, force, and contractile gene expression. While parallel changes in cell shape and force have been shown repeatedly (5, 47), with some studies even providing evidence that cell shape *determines* force generation (137), more recently, others have demonstrated that cell shape and force are

uncoupled under some conditions and are not necessarily functionally related (27, 66, 90). The data presented here supports the notion that cell shape and cell contractility are not strictly correlated under all conditions.

While the relationship between cell force and shape in non-muscle cells remains vague, the relationship between cell length and cell force in ASM cells has been the subject of a number of studies. It is well known that ASM cells demonstrate mechanical plasticity, referring to the unique ability to reorganise cytoskeletal and/or contractile machinery to adjust force generation to changes in length (106). The molecular mechanisms responsible for mechanical plasticity are still unknown in entirety, but evidence strongly suggests the involvement of both cytoskeletal proteins that may not be smooth muscle specific and the contractile system that is distinct to smooth muscle. Induction of contraction, leading to development of tension, cell stiffening, and cell shortening causes both activation of the contractile machinery by phosphorylation of MLC_{20} and polymerisation of actin (164). Accumulating evidence suggests that although both are necessary for contractile function, they area independent parallel pathways (61). Inhibition of actin polymerisation decreases tension development in response to an agonist without affecting myosin phosphorylation (92), while inhibition of myosin-dependent contractile machinery blocks tension development without affecting the induction of actin polymerisation (8). Thus, it appears that there may be independent systems that likely respond differently to mechanical changes in ASM cells and allow for dynamic, adaptive changes in force generation and cell stiffening. However, these mechanisms are acute, acting on a scale of minutes, and the cumulative effect of chronic perturbations of these systems is largely uninvestigated in ASM. Interestingly, VSM cell

dedifferentiation, which occurs naturally along with loss of tissue tension in organ culture models, can be prevented by inducing actin polymerisation (165), suggesting that disruption of the CSK can influence SM phenotype.

In fibroblasts, some mechanosensitive pathways that regulate contractile and proliferative gene transduction have been characterised. Generally, these studies group all the contractile genes together into a single "contractile program" that is induced or not. The RhoA/ROCK signaling pathway, which regulates SRF activity via actin polymerisation (130), has been implicated in mechanosensing. Fibroblasts cultured on stiff substrates have increased RhoA expression, SRF activity, SMA promoter activity, and ultimately increased SMA protein (70). One would therefore assume that other genes that are part of the contractile program would also be activated, however, here we have shown discordant contractile gene regulation. This is consistent with other ASM specific studies that showed differential changes in smMHC and SMA with changes in serum or the application of relaxants (50, 63).

Interestingly, although forskolin is assumed to cause cellular relaxation by reducing intracellular Ca^{2+} via protein kinase A (PKA), which in turn reduces MLCK activity, this has never been directly demonstrated. More recently PKA activation of RhoA signaling has been implicated (19). In ASM cells, strain has also been shown to cause cellular relaxation through this signaling pathway (128), and in fibroblasts, the application of strain had similar effects on substrate stiffness-dependent morphological differences as relaxants did (107). This suggests that modulation of RhoA signaling would affect actin-cytoskeleton dynamics and affect gene transcription, potentially explaining the effects of forskolin treatment on cell shape demonstrated in this thesis.

However, it is important to keep in mind that in the experiments presented here, the contractile and relaxant agonists were removed before measuring function, shape, and gene expression, unlike other signaling experiments. Therefore, the effects seen here represent the cumulative effect of repeated relaxation and may suggest a role for RhoA signaling and cytoskeletal dynamics. However, my results suggest that substrate stiffness may affect an entirely different pathway that is independent of RhoA and CSK dynamics, potentially affecting contractile machinery directly, as evidenced by the increase in smMHC and contractile function on stiff substrates. In fact, others have shown that stiffness recovery after strain is prevented by inhibiting the RhoA pathway, but not by the MLCK inhibitor ML-7, although, again, this is an acute effect. Taken together, the results presented here imply that activation of independent pathways, perhaps similar to those demonstrated on more acute time scales, can have chronic effects by switching transcription of individual contractile genes on and off. When tone modulation is added to substrate stiffness experiments, it becomes very apparent that the "contractile phenotype" is not a sufficient description of a cellular response as individual measures that define these cells change independently of each other.

4.4.3 Overall Conclusions

Overall, the data presented in this chapter suggest the following conclusions: 1) culture time is an important factor when examining the mechanical response of ASM cells and must be accounted for in future studies, 2) features of the contractile phenotype do not change in a correlated fashion in response to perturbations in cellular mechanics, and 3) low tone and/or soft substrates independently decrease different features that classically define contractile phenotype.

Although the contractile function results presented here were inconclusive when cells were exposed to both soft substrates and chronic relaxation, individually, these variables caused cells to express less contractile mRNA. This may mean that both substrate stiffness and cell tone could be necessary targets in asthma treatment. The results presented here support the idea that that the stiff microenvironment that is thought to occur in the asthmatic airway may encourage increased contractile function by increasing available smMHC. Treatments that decrease cell tone by acting on actin polymerisation pathways may nudge cells towards decreased contractile function by decreasing Sm22 and SMA, but it may be an inefficient treatment as, based on the evidence from this thesis, it would not target the contractile apparatus. It may be that in order to fully reverse AHR, treatments need to target both cytoskeletal stabilisation and the contractile machinery and/or decrease the fibrosis as well as cell relaxation.

4.4.4 Limitations

(1) Variability in OMTC

In OMTC there is inherent variability between beads that is attributed to differences in bead binding (41). Ferrimagnetic beads are coated in RGD protein, which allows them to bind to integrins on the cell surface. Heterogeneity of bead binding has been observed under SEM (40) and the degree of bead binding influences the relationship between torque and displacement. This heterogeneity can be somewhat corrected in contractility measurements by normalising to baseline stiffness. The remaining variability is accepted because a large number of beads can be measured in a single experiment. However, the number of accepted beads in the experiments presented here were much lower than those previously reported (34, 42) and this may have contributed to the small effects in

contractility. It is possible that some aspect of the PA gels, or behaviour of the cells influenced by the PA gel substrate, caused poor bead binding or affected the distribution of bead binding.

The heterogeneity could also be attributed to differences in the cells themselves. Indeed, in previous studies on the effect of serum deprivation on inducing a contractile phenotype, only a distinct subset of cells regained the contractile phenotype (63, 86). Similarly, the prolonged serum deprivation in the experiments presented here may create a more heterogeneous cell population that affects bead binding and/or baseline stiffness measurements.

Additionally, cells treated with histamine for 7 days had a high baseline stiffness, but low contractility. However, the post-KCl stiffness of these cells was still higher than the vehicle or forskolin cells, raising the possibility that a further increase in stiffness could not be measured. Therefore, it is possible that the contractility data is skewed due to lack of sensitivity in measuring very stiff or very soft cells.

(2) Cell-cell interactions

In addition to serum deprivation, cell confluence has been shown to induce a more contractile phenotype (65), demonstrating the importance of cell-cell contacts *in vitro*. Importantly, multiple studies have shown that cell-cell contacts can influence responses to substrate stiffness including shape, CSK organisation, and gene expression (107, 113). In each type of experiment, attempts were made to ensure that cells were at the same confluence in all experimental groups. However, this proved difficult when measuring at specific time points as there is a great deal of inter-donor variability in the rate of cell growth in addition to differences in proliferation rate on soft and stiff substrates (94).

Most importantly, the cell densities required for individual measures of contractile phenotype were different. While OMTC and qRT-PCR required cells to be near confluence, sparsely seeded cells were necessary for shape measurements.

(3) Physiological Relevance of PA Gels

Due to methodological barriers, the stiffness that a cell would actually be exposed to in an asthmatic airway has never been measured. Therefore, the gel stiffnesses selected for these experiments were based on the estimates of the Young's modulus of healthy and fibrotic human lung tissue, which, using AFM, were measured to be approximately 2kPa and greater than 15kPa respectively (22). However, it is important to note that these tissues were not under tensile stress, as would occur in the *in vivo* environment, and therefore may underestimate tissue stiffness.

Assuming that the Young's modulus of the PA gels is physiologically relevant, it is still possible that the cells were responding to something other than stiffness. PA gels are a popular model for substrate stiffness as they are thought to allow for control of stiffness without affecting the surface to which the cell is exposed. This is partially due to the nonfouling surface of polymerised polyacrylamide that prevents any nonspecific cell binding or protein adsorption that may affect cell signaling (49). Therefore, the only substance that the cell can bind to is protein that is chemically linked to the PA gel surface. In this thesis, type I collagen was bound to the surface with sulfo-SANPAH. This commonly used method has been shown to produce uniform collagen coating across the gel that is consistent across stiffnesses (76, 95). The pore size of PA gel has been shown to vary across stiffness and while even the largest pores are thought to be too small to

affect cells (<15nm) (44), others have theorised that this may affect the quality of collagen binding (138).

Finally, there are some characteristics of the airway that are obviously different in this *in vitro* model. First, it is now well known that cells behave very differently in a 2D model, such as the PA gels used here, compared to 3D models. Recent experiments in our laboratory have demonstrated that ASM cells respond differently to the mechanical environment in 3D compared to 2D cultures (154, 162). Furthermore, PA gels were coated with collagen type I in solution. In the physiological environment cells would be exposed to a much more structured ECM that includes other proteins and fibers. In asthma, the composition of the ECM is thought to be altered (9) and studies have found that the contractile function of ASM cells is differently affected by a variety of fibrillary proteins (7). Therefore, the collagen that the cells are exposed to in the model presented here may not simulate a physiologically or pathologically relevant response.

Chapter 5: Conclusion

In this thesis, I attempted to develop and investigate a 2D model that would simulate important aspects of the mechanical microenvironment associated with asthmatic airway remodeling with an aim to measure phenotypic responses of ASM cells. The two aims of this thesis describe the two approaches to developing models that would integrate multiple forms of mechanical stimuli while allowing for independent control. In the first aim, I focused on combining substrate stiffness with chronic oscillatory stretch. In the second aim, I integrated substrate stiffness with modulation of cellular tone.

The structural changes associated with asthmatic airway remodeling are thought to create a stiffer microenvironment for ASM. Based on recent work in our laboratory (152), we have hypothesised that this stiffening may contribute to asthma pathology by inducing a more contractile phenotype in the exposed ASM cells. The specific mechanosensing pathways involved in the substrate stiffness response are largely uncharacterised, yet the response itself is likely altered by other mechanical stimuli. Thus, I hypothesised that the presence of strain or chronic modulation of tone, both of which are factors in asthmatic airways, would alter the phenotypic response to substrate stiffness.

In the first aim, I first attempted to modify a published protocol to combine substrate stiffness and strain in cell culture by binding PA gels to Flexcell silicone membranes. This proved to be more difficult than expected, and the inability to produce Flexwells with fully polymerised soft gels was a barrier in using the model to examine cell phenotype. Troubleshooting of the protocol included various modifications to the original process, development of new methods, and characterisation of critical steps in the

process. Although I was not able to solve the problem in the end, this work has provided useful insight into the protocol.

In the second aim, I successfully developed a model that combines substrate stiffness with chronic tone modulation and measured phenotypic changes in ASM cells. Unexpectedly, initial experiments suggested that culture time plays an important role in the phenotypic response of ASM cells under the experimental conditions. Thus, the experimental design was refined to include various time points after subculture of the cells. Using this adjusted design, I have shown that a stiff substrate can induce a more contractile phenotype in ASM cells via transcriptional regulation, while low cell tone decreases transcriptional induction of genes associated with passive cell stiffness, independent of substrate. These data demonstrate that characteristics associated with contractile ASM cells can be uncoupled under certain conditions, providing evidence that independent mechanosensitive transcriptional pathways may affect ASM phenotype. This suggests that reversal of AHR in the asthmatic airway may require treatments that target both the stiffer environment caused by airway fibrosis and cell tone.

5.1 Statement of Contributions

(1) Demonstrated limitations of the Flexwell model in emulating the range of substrate stiffness thought to correspond to the range of the healthy to asthmatic mechanical airway environment.

(2) Characterised the Flexwell model and provided evidence to help identify problematic portions of the protocol.

(3) Established the importance of long duration exposure times in assessing the phenotypic response of ASM cells to substrate stiffness and tone modulation.

(4) Confirmed that a stiff substrate induced a more contractile phenotype in ASM cells.

(5) Demonstrated uncoupling of classic features associated with the contractile phenotype, including contractile function, cell shape, and transcriptional gene regulation.

(6) Provided evidence for independent transcriptional mechanosensing pathways in ASM cells.

5.2 Future Directions/Suggestions

(1) In this thesis transcriptional mechanosensitive pathways were implicated in contractile gene expression. However, protein quantity and localisation should be assessed alongside gene expression to better understand the cellular response.

(2) ASM cells are functionally plastic, and this thesis focused specifically on the contractile phenotype. However, ASM cells have also been shown to express more proliferative and secretory functionalities, both of which may contribute to asthma. Therefore, it would be useful to measure markers for these phenotypes, as well as proliferative capabilities using 5-Ethynyl-2′-deoxyuridine (EdU) incorporation to probe DNA synthesis.

(3) Although this thesis focused on how one aspect of airway remodeling may influence asthma, inflammation is still a large contributing factor to the disease. Studying how the mechanical response of ASM cells integrates with cytokines and other inflammatory signals, such as TGF-β, would provide further insight into ASM dysfunction in asthma.

(4) Recent studies in our laboratory have found that a stiffer environment enhances contractility of ASM cells in a 3D model (162), similar to the results presented here in a 2D model. Therefore it would be interesting to examine the effect of tone modulation on the contractile response to matrix stiffness in 3D.

(5) While the data presented here provides some interesting clues to the mechanisms responsible for phenotypic changes in response to mechanical stimulation, more targeted studies are needed to fully understand these pathways. This could be accomplished by measuring expression of relevant genes and promoter activity, quantifying/localising proteins upstream of transcriptional regulation (Eg. RhoA, ROCK, SRF etc.), or targeting specific steps in these pathways with pharmacological agents (such as Y27632 to inhibit ROCK, or ML-7 to inhibit MLCK).

(6) This thesis highlights the importance of strain in exploration of asthma pathology, therefore, continuing the work to obtain a reliable model that combines substrate stiffness and strain, and eventually tone modulation, is necessary. The best avenues for this are likely finding alternatives to oxygen plasma to functionalise a silicone surface, use of an alternative to the BioFlex silicone, and investigation of different hydrogels that do not require free radical polymerisation.

References

1. Asthma Fact sheet no. 307. World Health Organisation, 2011.

2. CANSIM Table 105-0501 Asthma, by sex, provinces and territories. Statistics Canada, 2012.

3. Econimic burden of illness in Canada. Public Health Agency of Canada, 1998, p. 52.

4. **Aikawa T, Shimura S, Sasaki H, Ebina M, and Takishima T**. Marked goblet cell hyperplasia with mucus accumulation in the airways of patients who died of severe acute asthma attack. *Chest* 101: 916-921, 1992.

5. **Alford PW, Nesmith AP, Seywerd JN, Grosberg A, and Parker KK**. Vascular smooth muscle contractility depends on cell shape. *Integrative Biology* 3: 1063-1070, 2011.

6. **An SS, Bai TR, Bates JHT, Black JL, Brown RH, Brusasco V, Chitano P, Deng L, Dowell M, Eidelman DH, Fabry B, Fairbank NJ, Ford LE, Fredberg JJ, Gerthoffer WT, Gilbert SH, Gosens R, Gunst SJ, Halayko AJ, Ingram RH, Irvin CG, James AL, Janssen LJ, King GG, Knight DA, Lauzon AM, Lakser OJ, Ludwig MS, Lutchen KR, Maksym GN, Martin JG, Mauad T, McParland BE, Mijailovich SM, Mitchell HW, Mitchell RW, Mitzner W, Murphy TM, Paré PD, Pellegrino R, Sanderson MJ, Schellenberg RR, Seow CY, Silveira PSP, Smith PG, Solway J, Stephens NL, Sterk PJ, Stewart AG, Tang DD, Tepper RS, Tran T, and Wang L**. Airway smooth muscle dynamics: a common pathway of airway obstruction in asthma. *European Respiratory Journal* 29: 834-860, 2007.

7. **An SS, Kim J, Ahn K, Trepat X, Drake KJ, Kumar S, Ling G, Purington C, Rangasamy T, Kensler TW, Mitzner W, Fredberg JJ, and Biswal S**. Cell stiffness, contractile stress and the role of extracellular matrix. *Biochemical and biophysical research communications* 382: 697-703, 2009.

8. **An SS, Laudadio RE, Lai J, Rogers RA, and Fredberg JJ**. Stiffness changes in cultured airway smooth muscle cells. *American journal of physiology Cell physiology* 283: C792-801, 2002.

9. **Araujo BB, Dolhnikoff M, Silva LFF, Elliot J, Lindeman JHN, Ferreira DS, Mulder A, Gomes HAP, Fernezlian SM, James A, and Mauad T**. Extracellular matrix components and regulators in the airway smooth muscle in asthma. *European Respiratory Journal* 32: 61-69, 2008.

10. **Augst AD, Kong HJ, and Mooney DJ**. Alginate hydrogels as biomaterials. *Macromol Biosci* 6: 623-633, 2006.

11. **Bai TR**. Abnormalities in airway smooth muscle in fatal asthma. *Am Rev Respir Dis* 143: 441443, 1991.

12. **Balaban NQ, Schwarz US, Riveline D, Goichberg P, Tzur G, Sabanay I, Mahalu D, Safran S, Bershadsky A, Addadi L, and Geiger B**. Force and focal adhesion assembly: a close relationship studied using elastic micropatterned substrates. *Nature cell biology* 3: 466-472, 2001.

13. **Baldwin L, and Roche WR**. Does remodelling of the airway wall precede asthma? *Paediatric respiratory reviews* 3: 315-320, 2002.

14. **Balestrini JL, Chaudhry S, Sarrazy V, Koehler A, and Hinz B**. The mechanical memory of lung myofibroblasts. *Integrative Biology* 4: 410-421, 2012.

15. **Bara I, Ozier A, Tunon de Lara JM, Marthan R, and Berger P**. Pathophysiology of bronchial smooth muscle remodelling in asthma. *The European respiratory journal* 36: 1174-1184, 2010.

16. **Bearinger JP, Castner DG, Golledge SL, Rezania A, Hubchak S, and Healy KE**. P (AAm-co-EG) interpenetrating polymer networks grafted to oxide surfaces: surface characterization, protein adsorption, and cell detachment studies. *Langmuir* 13: 5175-5183, 1997.

17. **Benayoun L, Druilhe A, Dombret M-C, Aubier M, and Pretolani M**. Airway Structural Alterations Selectively Associated with Severe Asthma. *American journal of respiratory and critical care medicine* 167: 1360-1368, 2003.

18. **Bhana B, Iyer RK, Chen WLK, Zhao R, Sider KL, Likhitpanichkul M, Simmons CA, and Radisic M**. Influence of substrate stiffness on the phenotype of heart cells. *Biotechnology and Bioengineering* 105: 1148-1160, 2010.

19. **Billington CK, Ojo OO, Penn RB, and Ito S**. cAMP regulation of airway smooth muscle function. *Pulmonary pharmacology & therapeutics* 26: 112-120, 2013.

20. **Black JL, and Roth M**. Intrinsic asthma: is it intrinsic to the smooth muscle? *Clinical and experimental allergy : journal of the British Society for Allergy and Clinical Immunology* 39: 962-965, 2009.

21. **Boontheekul T, Hill EE, Kong H-J, and Mooney DJ**. Regulating myoblast phenotype through controlled gel stiffness and degradation. *Tissue Eng* 13: 1431-1442, 2007.

22. **Booth AJ, Hadley R, Cornett AM, Dreffs AA, Matthes SA, Tsui JL, Weiss K, Horowitz JC, Fiore VF, Barker TH, Moore BB, Martinez FJ, Niklason LE, and White ES**. Acellular normal and fibrotic human lung matrices as a culture system for in vitro investigation. *American journal of respiratory and critical care medicine* 186: 866-876, 2012.

23. **Bosse Y, Chin LY, Pare PD, and Seow CY**. Adaptation of airway smooth muscle to basal tone: relevance to airway hyperresponsiveness. *American journal of respiratory cell and molecular biology* 40: 13-18, 2009.

24. **Bosse Y, Chin LY, Pare PD, and Seow CY**. Chronic activation in shortened airway smooth muscle: a synergistic combination underlying airway hyperresponsiveness? *American journal of respiratory cell and molecular biology* 42: 341-348, 2010.

25. **Brown XQ, Ookawa K, and Wong JY**. Evaluation of polydimethylsiloxane scaffolds with physiologically-relevant elastic moduli: interplay of substrate mechanics and surface chemistry effects on vascular smooth muscle cell response. *Biomaterials* 26: 3123-3129, 2005.

26. **Brusasco V, Crimi E, Barisione G, Spanevello A, Rodarte JR, and Pellegrino R**. Airway responsiveness to methacholine: effects of deep inhalations and airway inflammation. *Journal of applied physiology* 87: 567-573, 1999.

27. **Califano JP, and Reinhart-King CA**. Substrate Stiffness and Cell Area Predict Cellular Traction Stresses in Single Cells and Cells in Contact. *Cellular and molecular bioengineering* 3: 68-75, 2010.

28. **Callaerts-Vegh Z, Evans KL, Dudekula N, Cuba D, Knoll BJ, Callaerts PF, Giles H, Shardonofsky FR, and Bond RA**. Effects of acute and chronic administration of beta-adrenoceptor ligands on airway function in a murine model of asthma. *Proceedings of the National Academy of Sciences of the United States of America* 101: 4948-4953, 2004.

29. **Carpenter A, Jones T, Lamprecht M, Clarke C, Kang I, Friman O, Guertin D, Chang J, Lindquist R, Moffat J, Golland P, and Sabatini D**. CellProfiler: image analysis software for identifying and quantifying cell phenotypes. *Genome Biology* 7: R100, 2006.

30. **Chamley-Campbell J, Campbell GR, and Ross R**. The smooth muscle cell in culture. *Physiological reviews* 59: 1-61, 1979.

31. **Chen TJ, Wu CC, Tang MJ, Huang JS, and Su FC**. Complexity of the tensegrity structure for dynamic energy and force distribution of cytoskeleton during cell spreading. *PloS one* 5: e14392, 2010.

32. **Choquet D, Felsenfeld DP, and Sheetz MP**. Extracellular matrix rigidity causes strengthening of integrin-cytoskeleton linkages. *Cell* 88: 39-48, 1997.

33. **Connolly SC, Smith PG, Fairbank NJ, Lall CA, Cole DJ, Mackinnon JD, and Maksym GN**. Chronic oscillatory strain induces MLCK associated rapid recovery from acute stretch in airway smooth muscle cells. *Journal of applied physiology* 111: 955-963, 2011.

34. **Deng L, Fairbank NJ, Fabry B, Smith PG, and Maksym GN**. Localized mechanical stress induces time-dependent actin cytoskeletal remodeling and stiffening in cultured airway smooth muscle cells. *American journal of physiology Cell physiology* 287: C440-448, 2004.

35. **Discher DE, Janmey P, and Wang YL**. Tissue cells feel and respond to the stiffness of their substrate. *Science* 310: 1139-1143, 2005.

36. **Domke J, and Radmacher M**. Measuring the Elastic Properties of Thin Polymer Films with the Atomic Force Microscope. *Langmuir* 14: 3320-3325, 1998.

37. **Emerman JT, and Pitelka DR**. Maintenance and induction of morphological differentiation in dissociated mammary epithelium on floating collagen membranes. *In vitro* 13: 316-328, 1977.

38. **Engler A, Bacakova L, Newman C, Hategan A, Griffin M, and Discher D**. Substrate compliance versus ligand density in cell on gel responses. *Biophysical journal* 86: 617-628, 2004.

39. **Engler AJ, Sen S, Sweeney HL, and Discher DE**. Matrix elasticity directs stem cell lineage specification. *Cell* 126: 677-689, 2006.

40. **Fabry B, Maksym GN, Hubmayr RD, Butler JP, and Fredberg JJ**. Implications of heterogeneous bead behavior on cell mechanical properties measured with magnetic twisting cytometry. *Journal of magnetism and magnetic materials* 194: 120-125, 1999.

41. **Fabry B, Maksym GN, Shore SA, Moore PE, Panettieri RA, Butler JP, and Fredberg JJ**. Signal Transduction in Smooth Muscle: Selected Contribution: Time course and heterogeneity of contractile responses in cultured human airway smooth muscle cells. *Journal of applied physiology* 91: 986-994, 2001.

42. **Fairbank NJ, Connolly SC, Mackinnon JD, Wehry K, Deng L, and Maksym GN**. Airway smooth muscle cell tone amplifies contractile function in the presence of chronic cyclic strain. *American journal of physiology Lung cellular and molecular physiology* 295: L479-488, 2008.

43. **Fisher SA**. Vascular smooth muscle phenotypic diversity and function. *Physiological genomics* 42: 169-187, 2010.

44. **Flanagan LA, Ju Y-E, Marg B, Osterfield M, and Janmey PA**. Neurite branching on deformable substrates. *Neuroreport* 13: 2411, 2002.

45. **Fredberg JJ, Inouye D, Miller B, Nathan M, Jafari S, Raboudi SH, Butler JP, and Shore SA**. Airway smooth muscle, tidal stretches, and dynamically determined contractile states. *American journal of respiratory and critical care medicine* 156: 1752-1759, 1997.

46. **Fritz JL, and Owen MJ**. Hydrophobic recovery of plasma-treated polydimethylsiloxane. *The Journal of Adhesion* 54: 33-45, 1995.

47. **Gadhari N, Charnley M, Marelli M, Brugger J, and Chiquet M**. Cell shape-dependent early responses of fibroblasts to cyclic strain. *Biochimica et Biophysica Acta (BBA)-Molecular Cell Research* 1833: 3415-3425, 2013.

48. **Galbraith CG, Yamada KM, and Sheetz MP**. The relationship between force and focal complex development. *The Journal of cell biology* 159: 695-705, 2002.

49. **Georges PC, and Janmey PA**. Cell type-specific response to growth on soft materials. *Journal of applied physiology* 98: 1547-1553, 2005.

50. **Gosens R, Bos IS, Zaagsma J, and Meurs H**. Protective effects of tiotropium bromide in the progression of airway smooth muscle remodeling. *American journal of respiratory and critical care medicine* 171: 1096-1102, 2005.

51. **Gosens R, Bromhaar MM, Tonkes A, Schaafsma D, Zaagsma J, Nelemans SA, and Meurs H**. Muscarinic M(3) receptor-dependent regulation of airway smooth muscle contractile phenotype. *British journal of pharmacology* 141: 943-950, 2004.

52. **Gosens R, Schaafsma D, Meurs H, Zaagsma J, and Nelemans SA**. Role of Rho-kinase in maintaining airway smooth muscle contractile phenotype. *European journal of pharmacology* 483: 71-78, 2004.

53. **Gosens R, Stelmack GL, Dueck G, McNeill KD, Yamasaki A, Gerthoffer WT, Unruh H, Gounni AS, Zaagsma J, and Halayko AJ**. Role of caveolin-1 in p42/p44 MAP kinase activation and proliferation of human airway smooth muscle. *American Journal of Physiology-Lung Cellular and Molecular Physiology* 291: L523-L534, 2006.

54. **Gosens R, Zaagsma J, Meurs H, and Halayko AJ**. Muscarinic receptor signaling in the pathophysiology of asthma and COPD. *Respiratory research* 7: 73, 2006.

55. **Grainge CL, Lau LC, Ward JA, Dulay V, Lahiff G, Wilson S, Holgate S, Davies DE, and Howarth PH**. Effect of bronchoconstriction on airway remodeling in asthma. *The New England journal of medicine* 364: 2006-2015, 2011.

56. **Gray DS, Tien J, and Chen CS**. Repositioning of cells by mechanotaxis on surfaces with micropatterned Young's modulus. *Journal of Biomedical Materials Research Part A* 66: 605-614, 2003.

57. **Grinnell F, and Ho CH**. The effect of growth factor environment on fibroblast morphological response to substrate stiffness. *Biomaterials* 34: 965-974, 2013.

58. **Gunst SJ**. Contractile force of canine airway smooth muscle during cyclical length changes. *Journal of applied physiology* 55: 759-769, 1983.

59. **Gunst SJ, and Panettieri RA**. *Point:Counterpoint: Alterations in airway smooth muscle phenotype do/do not cause airway hyperresponsiveness in asthma*. 2012, p. 837-839.

60. **Gunst SJ, and Tang DD**. The contractile apparatus and mechanical properties of airway smooth muscle. *The European respiratory journal* 15: 600-616, 2000.

61. **Gunst SJ, and Zhang W**. Actin cytoskeletal dynamics in smooth muscle: a new paradigm for the regulation of smooth muscle contraction. *American journal of physiology Cell physiology* 295: C576-587, 2008.

62. **Hackett TL, and Knight DA**. The role of epithelial injury and repair in the origins of asthma. *Current opinion in allergy and clinical immunology* 7: 63-68, 2007.

63. **Halayko AJ, Camoretti-Mercado B, Forsythe SM, Vieira JE, Mitchell RW, Wylam ME, Hershenson MB, and Solway J**. Divergent differentiation paths in airway

smooth muscle culture: induction of functionally contractile myocytes. *The American journal of physiology* 276: L197-206, 1999.

64. **Halayko AJ, Salari H, Ma X, and Stephens NL**. Markers of airway smooth muscle cell phenotype. *The American journal of physiology* 270: L1040-1051, 1996.

65. **Halayko AJ, and Solway J**. Molecular mechanisms of phenotypic plasticity in smooth muscle cells. *Journal of applied physiology* 90: 358-368, 2001.

66. **Han SJ, Bielawski KS, Ting LH, Rodriguez ML, and Sniadecki NJ**. Decoupling substrate stiffness, spread area, and micropost density: a close spatial relationship between traction forces and focal adhesions. *Biophysical journal* 103: 640-648, 2012.

67. **Hermanson GT**. Chapter 5 - Heterobifunctional Crosslinkers. In: *Bioconjugate Techniques (Second Edition)*. New York: Academic Press, 2008, p. 276-335.

68. **Hillborg H, Ankner JF, Gedde UW, Smith GD, Yasuda HK, and Wikström K**. Crosslinked polydimethylsiloxane exposed to oxygen plasma studied by neutron reflectometry and other surface specific techniques. *Polymer* 41: 6851-6863, 2000.

69. **Hirota JA, Nguyen TT, Schaafsma D, Sharma P, and Tran T**. Airway smooth muscle in asthma: phenotype plasticity and function. *Pulmonary pharmacology & therapeutics* 22: 370-378, 2009.

70. **Huang X, Yang N, Fiore VF, Barker TH, Sun Y, Morris SW, Ding Q, Thannickal VJ, and Zhou Y**. Matrix stiffness-induced myofibroblast differentiation is mediated by intrinsic mechanotransduction. *American journal of respiratory cell and molecular biology* 47: 340-348, 2012.

71. **Huber HL, and Koessler KK**. The pathology of bronchial asthma. *Studies from the Otho SA Sprague Memorial Institute: Collected Reprints* 10: 1, 1922.

72. **Huntsman HD, Ozturk T, Boppart MD, and Kemkemer R**. The effect of substrate stiffness on the apparent stress cells experience during cyclic strain. *The FASEB Journal* 27: 1217.1217, 2013.

73. **Jensen A, Atileh H, Suki B, Ingenito EP, and Lutchen KR**. Selected contribution: airway caliber in healthy and asthmatic subjects: effects of bronchial challenge and deep inspirations. *Journal of applied physiology* 91: 506-515; discussion 504-505, 2001.

74. **Johnson PRA, Roth M, Tamm M, Hughes M, Ge QI, King G, Burgess JK, and Black JL**. Airway Smooth Muscle Cell Proliferation Is Increased in Asthma. *American journal of respiratory and critical care medicine* 164: 474-477, 2001.

75. **Kelley C, Takahashi M, Yu J, and Adelstein R**. An insert of seven amino acids confers functional differences between smooth muscle myosins from the intestines and vasculature. *Journal of Biological Chemistry* 268: 12848-12854, 1993.

76. **Khatiwala CB, Peyton SR, and Putnam AJ**. Intrinsic mechanical properties of the extracellular matrix affect the behavior of pre-osteoblastic MC3T3-E1 cells. *American Journal of Physiology-Cell Physiology* 290: C1640-C1650, 2006.

77. **King GG, Moore BJ, Seow CY, and Pare PD**. Airway narrowing associated with inhibition of deep inspiration during methacholine inhalation in asthmatics. *American journal of respiratory and critical care medicine* 164: 216-218, 2001.

78. **Krishnan R, Park CY, Lin YC, Mead J, Jaspers RT, Trepat X, Lenormand G, Tambe D, Smolensky AV, Knoll AH, Butler JP, and Fredberg JJ**. Reinforcement versus fluidization in cytoskeletal mechanoresponsiveness. *PloS one* 4: e5486, 2009.

79. **Lateef SS, Boateng S, Hartman TJ, Crot CA, Russell B, and Hanley L**. GRGDSP peptide-bound silicone membranes withstand mechanical flexing in vitro and display enhanced fibroblast adhesion. *Biomaterials* 23: 3159-3168, 2002.

80. **Lim TK, Pride NB, and Ingram RH, Jr.** Effects of volume history during spontaneous and acutely induced air-flow obstruction in asthma. *The American review of respiratory disease* 135: 591-596, 1987.

81. **Limouze J, Straight A, Mitchison T, and Sellers J**. Specificity of blebbistatin, an inhibitor of myosin II. *J Muscle Res Cell Motil* 25: 337-341, 2004.

82. **Liu F, Mih JD, Shea BS, Kho AT, Sharif AS, Tager AM, and Tschumperlin DJ**. Feedback amplification of fibrosis through matrix stiffening and COX-2 suppression. *The Journal of cell biology* 190: 693-706, 2010.

83. **Lo CM, Wang HB, Dembo M, and Wang YL**. Cell movement is guided by the rigidity of the substrate. *Biophysical journal* 79: 144-152, 2000.

84. **Ma X, Cheng Z, Kong H, Wang Y, Unruh H, Stephens NL, and Laviolette M**. Changes in biophysical and biochemical properties of single bronchial smooth muscle cells from asthmatic subjects. *American journal of physiology Lung cellular and molecular physiology* 283: L1181-1189, 2002.

85. **Ma X, Cheng Z, Kong H, Wang Y, Unruh H, Stephens NL, and Laviolette M**. *Changes in biophysical and biochemical properties of single bronchial smooth muscle cells from asthmatic subjects*. 2002, p. L1181-L1189.

86. **Ma X, Wang Y, and Stephens NL**. Serum deprivation induces a unique hypercontractile phenotype of cultured smooth muscle cells. *The American journal of physiology* 274: C1206-1214, 1998.

87. **Mack CP, Somlyo AV, Hautmann M, Somlyo AP, and Owens GK**. Smooth Muscle Differentiation Marker Gene Expression Is Regulated by RhoA-mediated Actin Polymerization. *Journal of Biological Chemistry* 276: 341-347, 2001.

88. **Macpherson I, and Montagnier L**. Agar Suspension Culture for the Selective Assay of Cells Transformed by Polyoma Virus. *Virology* 23: 291-294, 1964.

89. **Marinkovic A, Mih J, D., Liu F, and Tschumperlin D, J.** . Transitions In Matrix Stiffness Uncouple Lung Fibroblast Proliferative And Morphological Responses From Cytoskeletal Tension. *American Journal of Respiratory Critical Care* A3562-A3562, 2011.

90. **Marinkovic A, Mih JD, Park JA, Liu F, and Tschumperlin DJ**. Improved throughput traction microscopy reveals pivotal role for matrix stiffness in fibroblast contractility and TGF-beta responsiveness. *American journal of physiology Lung cellular and molecular physiology* 303: L169-180, 2012.

91. **Matthews BD, Overby DR, Mannix R, and Ingber DE**. Cellular adaptation to mechanical stress: role of integrins, Rho, cytoskeletal tension and mechanosensitive ion channels. *Journal of cell science* 119: 508-518, 2006.

92. **Mehta D, and Gunst SJ**. Actin polymerization stimulated by contractile activation regulates force development in canine tracheal smooth muscle. *The Journal of physiology* 519 Pt 3: 829-840, 1999.

93. **Miano JM, Long X, and Fujiwara K**. Serum response factor: master regulator of the actin cytoskeleton and contractile apparatus. *American Journal of Physiology-Cell Physiology* 292: C70-C81, 2007.

94. **Mih JD, Marinkovic A, Liu F, Sharif AS, and Tschumperlin DJ**. Matrix stiffness reverses the effect of actomyosin tension on cell proliferation. *Journal of cell science* 125: 5974-5983, 2012.

95. **Mih JD, Sharif AS, Liu F, Marinkovic A, Symer MM, and Tschumperlin DJ**. A multiwell platform for studying stiffness-dependent cell biology. *PloS one* 6: e19929, 2011.

96. **Morano I, Chai GX, Baltas LG, Lamounier-Zepter V, Lutsch G, Kott M, Haase H, and Bader M**. Smooth-muscle contraction without smooth-muscle myosin. *Nature cell biology* 2: 371-375, 2000.

97. **Murakami T, Kuroda S-i, and Osawa Z**. Dynamics of polymeric solid surfaces treated with oxygen plasma: Effect of aging media after plasma treatment. *Journal of colloid and interface science* 202: 37-44, 1998.

98. **Nemir S, Hayenga HN, and West JL**. PEGDA hydrogels with patterned elasticity: novel tools for the study of cell response to substrate rigidity. *Biotechnology and bioengineering* 105: 636-644, 2010.

99. **Noble PB, Jones RL, Needi ET, Cairncross A, Mitchell HW, James AL, and McFawn PK**. Responsiveness of the human airway in vitro during deep inspiration and tidal oscillation. *Journal of applied physiology* 110: 1510-1518, 2011.

100. **Noble PB, Pascoe CD, Lan B, Ito S, Kistemaker LE, Tatler AL, Pera T, Brook BS, Gosens R, and West AR**. Airway smooth muscle in asthma: Linking contraction and mechanotransduction to disease pathogenesis and remodelling. *Pulmonary pharmacology & therapeutics* 29: 96-107, 2014.

101. **Ozier A, Allard B, Bara I, Girodet PO, Trian T, Marthan R, and Berger P**. The pivotal role of airway smooth muscle in asthma pathophysiology. *Journal of allergy* 2011: 742710, 2011.

102. **Pelham RJ, Jr., and Wang Y**. Cell locomotion and focal adhesions are regulated by substrate flexibility. *Proceedings of the National Academy of Sciences of the United States of America* 94: 13661-13665, 1997.

103. **Pellegrino R, Viegi G, Brusasco V, Crapo RO, Burgos F, Casaburi R, Coates A, van der Grinten CPM, Gustafsson P, Hankinson J, Jensen R, Johnson DC, MacIntyre N, McKay R, Miller MR, Navajas D, Pedersen OF, and Wanger J**. Interpretative strategies for lung function tests. *European Respiratory Journal* 26: 948-968, 2005.

104. **Pepe C, Foley S, Shannon J, Lemiere C, Olivenstein R, Ernst P, Ludwig MS, Martin JG, and Hamid Q**. Differences in airway remodeling between subjects with severe and moderate asthma. *The Journal of allergy and clinical immunology* 116: 544-549, 2005.

105. **Peyton SR, Raub CB, Keschrumrus VP, and Putnam AJ**. The use of poly(ethylene glycol) hydrogels to investigate the impact of ECM chemistry and mechanics on smooth muscle cells. *Biomaterials* 27: 4881-4893, 2006.

106. **Pratusevich VR, Seow CY, and Ford LE**. Plasticity in canine airway smooth muscle. *The Journal of general physiology* 105: 73-94, 1995.

107. **Quinlan AM, and Billiar KL**. Investigating the role of substrate stiffness in the persistence of valvular interstitial cell activation. *Journal of biomedical materials research Part A* 100: 2474-2482, 2012.

108. **Roberts CR, and Burke AK**. Remodelling of the extracellular matrix in asthma: proteoglycan synthesis and degradation. *Canadian respiratory journal : journal of the Canadian Thoracic Society* 5: 48-50, 1998.

109. **Roche W, Williams J, Beasley R, and Holgate S**. SUBEPITHELIAL FIBROSIS IN THE BRONCHI OF ASTHMATICS. *The Lancet* 333: 520-524, 1989.

110. **Roth J, Albrecht V, Nitschke M, Bellmann C, Simon F, Zschoche S, Michel S, Luhmann C, Grundke K, and Voit B**. Surface functionalization of silicone rubber for permanent adhesion improvement. *Langmuir* 24: 12603-12611, 2008.

111. **Rydell-Tormanen K, Risse PA, Kanabar V, Bagchi R, Czubryt MP, and Johnson JR**. Smooth muscle in tissue remodeling and hyper-reactivity: airways and arteries. *Pulmonary pharmacology & therapeutics* 26: 13-23, 2013.

112. **Salerno FG, Pellegrino R, Trocchio G, Spanevello A, Brusasco V, and Crimi E**. Attenuation of induced bronchoconstriction in healthy subjects: effects of breathing depth. *Journal of applied physiology* 98: 817-821, 2005.

113. **Sazonova OV, Lee KL, Isenberg BC, Rich CB, Nugent MA, and Wong JY**. Cell-cell interactions mediate the response of vascular smooth muscle cells to substrate stiffness. *Biophysical journal* 101: 622-630, 2011.

114. **Schaafsma D, McNeill KD, Stelmack GL, Gosens R, Baarsma HA, Dekkers BG, Frohwerk E, Penninks JM, Sharma P, Ens KM, Nelemans SA, Zaagsma J, Halayko AJ, and Meurs H**. Insulin increases the expression of contractile phenotypic markers in airway smooth muscle. *American journal of physiology Cell physiology* 293: C429-439, 2007.

115. **Schwartz MA**. Integrins and extracellular matrix in mechanotransduction. *Cold Spring Harbor perspectives in biology* 2: a005066, 2010.

116. **Schwartz MA, and Ingber DE**. Integrating with integrins. *Molecular biology of the cell* 5: 389-393, 1994.

117. **Scichilone N, Permutt S, and Togias A**. The lack of the bronchoprotective and not the bronchodilatory ability of deep inspiration is associated with airway hyperresponsiveness. *American journal of respiratory and critical care medicine* 163: 413-419, 2001.

118. **Seow CY**. Passive stiffness of airway smooth muscle: the next target for improving airway distensibility and treatment for asthma? *Pulmonary pharmacology & therapeutics* 26: 37-41, 2013.

119. **Sharma V, Dhayal M, Shivaprasad SM, and Jain SC**. Surface characterization of plasma-treated and PEG-grafted PDMS for micro fluidic applications. *Vacuum* 81: 1094-1100, 2007.

120. **Simmons CS, Ribeiro AJS, and Pruitt BL**. Formation of composite polyacrylamide and silicone substrates for independent control of stiffness and strain. *Lab Chip* 13: 646-649, 2013.

121. **Slats AM, Janssen K, van Schadewijk A, van der Plas DT, Schot R, van den Aardweg JG, de Jongste JC, Hiemstra PS, Mauad T, Rabe KF, and Sterk PJ**. Expression of smooth muscle and extracellular matrix proteins in relation to airway function in asthma. *The Journal of allergy and clinical immunology* 121: 1196-1202, 2008.

122. **Smith PG, Deng L, Fredberg JJ, and Maksym GN**. Mechanical strain increases cell stiffness through cytoskeletal filament reorganization. *American journal of physiology Lung cellular and molecular physiology* 285: L456-463, 2003.

123. **Smith PG, Garcia R, and Kogerman L**. Strain reorganizes focal adhesions and cytoskeleton in cultured airway smooth muscle cells. *Experimental cell research* 232: 127-136, 1997.

124. **Smith PG, Janiga KE, and Bruce MC**. Strain increases airway smooth muscle cell proliferation. *American journal of respiratory cell and molecular biology* 10: 85-90, 1994.

125. **Smith PG, Moreno R, and Ikebe M**. Strain increases airway smooth muscle contractile and cytoskeletal proteins in vitro. *The American journal of physiology* 272: L20-27, 1997.

126. **Smith PG, Roy C, Dreger J, and Brozovich F**. Mechanical strain increases velocity and extent of shortening in cultured airway smooth muscle cells. *The American journal of physiology* 277: L343-348, 1999.

127. **Smith PG, Roy C, Fisher S, Huang QQ, and Brozovich F**. Selected contribution: mechanical strain increases force production and calcium sensitivity in cultured airway smooth muscle cells. *Journal of applied physiology* 89: 2092-2098, 2000.

128. **Smith PG, Roy C, Zhang YN, and Chauduri S**. Mechanical Stress Increases RhoA Activation in Airway Smooth Muscle Cells. *American journal of respiratory cell and molecular biology* 28: 436-442, 2003.

129. **Solway J, and Fredberg JJ**. Perhaps airway smooth muscle dysfunction contributes to asthmatic bronchial hyperresponsiveness after all. *American journal of respiratory cell and molecular biology* 17: 144-146, 1997.

130. **Sotiropoulos A, Gineitis D, Copeland J, and Treisman R**. Signal-regulated activation of serum response factor is mediated by changes in actin dynamics. *Cell* 98: 159-169, 1999.

131. **Stamenović D, Suki B, Fabry B, Wang N, Fredberg JJ, and Buy JE**. Rheology of airway smooth muscle cells is associated with cytoskeletal contractile stress. *Journal of applied physiology* 96: 1600-1605, 2004.

132. **Stewart HJ, Guildford AL, Lawrence-Watt DJ, and Santin M**. Substrate-induced phenotypical change of monocytes/macrophages into myofibroblast-like cells: a new insight into the mechanism of in-stent restenosis. *Journal of biomedical materials research Part A* 90: 465-471, 2009.

133. **Thomson RJ, Bramley AM, and Schellenberg RR**. Airway muscle stereology: implications for increased shortening in asthma. *American journal of respiratory and critical care medicine* 154: 749-757, 1996.

134. **Throm Quinlan AM, Sierad LN, Capulli AK, Firstenberg LE, and Billiar KL**. Combining dynamic stretch and tunable stiffness to probe cell mechanobiology in vitro. *PloS one* 6: e23272, 2011.

135. **To T, Cicutto L, Degani N, McLimont S, and Beyene J**. Can a community evidence-based asthma care program improve clinical outcomes?: a longitudinal study. *Med Care* 46: 1257-1266, 2008.

136. **Tokuda EY, Leight JL, and Anseth KS**. Modulation of matrix elasticity with PEG hydrogels to study melanoma drug responsiveness. *Biomaterials* 35: 4310-4318, 2014.

137. **Tolić-Nørrelykke IM, and Wang N**. Traction in smooth muscle cells varies with cell spreading. *Journal of biomechanics* 38: 1405-1412, 2005.

138. **Trappmann B, Gautrot JE, Connelly JT, Strange DGT, Li Y, Oyen ML, Stuart MAC, Boehm H, Li B, and Vogel V**. Extracellular-matrix tethering regulates stem-cell fate. *Nature materials* 11: 642-649, 2012.

139. **Trepat X, Deng L, An SS, Navajas D, Tschumperlin DJ, Gerthoffer WT, Butler JP, and Fredberg JJ**. Universal physical responses to stretch in the living cell. *Nature* 447: 592-595, 2007.

140. **Tse JR, and Engler AJ**. Preparation of hydrogel substrates with tunable mechanical properties. *Current protocols in cell biology* 10.16. 11-10.16. 16, 2010.

141. **Ulrich TA, de Juan Pardo EM, and Kumar S**. The Mechanical Rigidity of the Extracellular Matrix Regulates the Structure, Motility, and Proliferation of Glioma Cells. *Cancer Res* 69: 4167-4174, 2009.

142. **Vogel V, and Sheetz M**. Local force and geometry sensing regulate cell functions. *Nature reviews Molecular cell biology* 7: 265-275, 2006.

143. **von Wichert G, Haimovich B, Feng GS, and Sheetz MP**. Force-dependent integrin-cytoskeleton linkage formation requires downregulation of focal complex dynamics by Shp2. *The EMBO journal* 22: 5023-5035, 2003.

144. **von Wichert G, Jiang G, Kostic A, De Vos K, Sap J, and Sheetz MP**. RPTP-alpha acts as a transducer of mechanical force on alphav/beta3-integrin-cytoskeleton linkages. *The Journal of cell biology* 161: 143-153, 2003.

145. **Walker M**. The Development of a 3D Piezoelectric Active Microtissue Model for Airway Smooth Muscle. 2013.

146. **Wang L, Liu H-W, McNeill KD, Stelmack G, Scott JE, and Halayko AJ**. Mechanical strain inhibits airway smooth muscle gene transcription via protein kinase C signaling. *American journal of respiratory cell and molecular biology* 31: 54-61, 2004.

147. **Wang N, Butler JP, and Ingber DE**. Mechanotransduction across the cell surface and through the cytoskeleton. *Science* 260: 1124-1127, 1993.

148. **Wang N, Tolić-Nørrelykke IM, Chen J, Mijailovich SM, Butler JP, Fredberg JJ, and Stamenović D**. *Cell prestress. I. Stiffness and prestress are closely associated in adherent contractile cells*. 2002, p. C606-C616.

149. **Wang Y, Wang G, Luo X, Qiu J, and Tang C**. Substrate stiffness regulates the proliferation, migration, and differentiation of epidermal cells. *Burns* 38: 414-420, 2012.

150. **Wang Z, Wang D-Z, Hockemeyer D, McAnally J, Nordheim A, and Olson EN**. Myocardin and ternary complex factors compete for SRF to control smooth muscle gene expression. *Nature* 428: 185-189, 2004.

151. **Waters CM, Glucksberg MR, Lautenschlager EP, Lee C-W, Van Matre RM, Warp RJ, Savla U, Healy KE, Moran B, and Castner DG**. A system to impose prescribed homogenous strains on cultured cells. *Journal of applied physiology* 91: 1600-1610, 2001.

152. **West AR, Connolly S, Mih JD, Billiar KL, Tschumperlin D, and Maksym GN**. Increased Extracellular Matrix Stiffness Enhances Airway Smooth Muscle Contractile Phenotype And Contractile Function. In: *C18 NOVEL MECHANISMS DRIVING AIRWAY REMODELING IN ASTHMA*American Thoracic Society, 2011, p. A4052-A4052.

153. **West AR, Syyong HT, Siddiqui S, Pascoe CD, Murphy TM, Maarsingh H, Deng L, Maksym GN, and Bosse Y**. Airway contractility and remodeling: links to asthma symptoms. *Pulmonary pharmacology & therapeutics* 26: 3-12, 2013.

154. **West AR, Zaman N, Cole DJ, Walker MJ, Legant WR, Boudou T, Chen CS, Favreau JT, Gaudette GR, and Cowley EA**. Development and characterization of a 3D multicell microtissue culture model of airway smooth muscle. *American Journal of Physiology-Lung Cellular and Molecular Physiology* 304: L4-L16, 2013.

155. **Whicker S, Armour C, and Black J**. Responsiveness of bronchial smooth muscle from asthmatic patients to relaxant and contractile agonists. *Pulmonary pharmacology* 1: 25-31, 1988.

156. **White J, and Eiser NM**. The role of histamine and its receptors in the pathogenesis of asthma. *British journal of diseases of the chest* 77: 215-226, 1983.

157. **Williams RL, Wilson DJ, and Rhodes NP**. Stability of plasma-treated silicone rubber and its influence on the interfacial aspects of blood compatibility. *Biomaterials* 25: 4659-4673, 2004.

158. **Wilson JW, and Li X**. The measurement of reticular basement membrane and submucosal collagen in the asthmatic airway. *Clinical & Experimental Allergy* 27: 363-371, 1997.

159. **Wright DB, Trian T, Siddiqui S, Pascoe CD, Johnson JR, Dekkers BGJ, Dakshinamurti S, Bagchi R, Burgess JK, Kanabar V, and Ojo OO**. Phenotype modulation of airway smooth muscle in asthma. *Pulmonary pharmacology & therapeutics* 26: 42-49, 2013.

160. **Young RJ, and Lovell PA**. *Introduction to polymers*. CRC press, 2011.

161. **Yuen SL, Ogut O, and Brozovich FV**. Nonmuscle myosin is regulated during smooth muscle contraction. *American journal of physiology Heart and circulatory physiology* 297: H191-199, 2009.

162. **Zaman N**. Influence of loading and matrix stiffness on airway smooth muscle contractile function and phenotype within a 3D microtissue culture model. 2013.

163. **Zhang W, Huang Y, and Gunst SJ**. The small GTPase RhoA regulates the contraction of smooth muscle tissues by catalyzing the assembly of cytoskeletal signaling complexes at membrane adhesion sites. *The Journal of biological chemistry* 287: 33996-34008, 2012.

164. **Zhang W, Wu Y, Du L, Tang DD, and Gunst SJ**. Activation of the Arp2/3 complex by N-WASp is required for actin polymerization and contraction in smooth muscle. *American journal of physiology Cell physiology* 288: C1145-1160, 2005.

165. **Zheng J-P, Ju D, Shen J, Yang M, and Li L**. Disruption of actin cytoskeleton mediates loss of tensile stress induced early phenotypic modulation of vascular smooth muscle cells in organ culture. *Experimental and molecular pathology* 88: 52-57, 2010.

166. **Zuyderduyn S, Sukkar MB, Fust A, Dhaliwal S, and Burgess JK**. Treating asthma means treating airway smooth muscle cells. *The European respiratory journal* 32: 265-274, 2008.

Appendix A: Additional Flexwell Methods

A.1 Bulk PA Polymerisation Experiments

A.1.1 Methods

To measure the effect of initiator concentration on the polymerisation of PA gels, polymerisation time and stiffness were estimated. Polymerisation time was measured by simply noting the time each sample required to reach a non-liquid state (could not be poured out of the beaker), while stiffness was measured using a force transducer (406A, Aurora Scientific, Aurora, ON) mounted on a micromanipulator (MLW-3 three axis water hydraulic, Narishige, Tokyo, Japan). Gels were made to a total volume of 5mls in 25ml glass beakers using PA#4 and PA#2 gels recipes (Table 2-1) as controls or with 2x or 5x the volume of APS or TEMED. Once polymerised, the gels were scooped onto a petri dish and placed underneath the force transducer with a glass microcapillary tube attached to the input tip. Using the micromanipulator, the force transducer was slowly brought down until contact with the gel, which was determined by a change in the force output channel. The movement of the glass tip was captured with a firewire camera (MC-F433C, 1st Vision, Andover, MA) with 40x microscope objective for magnification that was mounted to the other arm of the micromanipulator. A custom LabView program recorded the force and the deflection of the glass tip as it was advanced ~10μm into the gel and returned to the original position. The tracking program used the deflection and force unloading data to estimate the stiffness of the gels (145).

A.1.2 Results

The stiffness measured for the control recipes for PA#2 and PA#4 bulk gels were 392 Pa and 1128 Pa respectively and polymerised in approximately 20 minutes and 5m20s respectively (Figure A-1). Increasing the concentration of either APS or TEMED to 2x and 5x the original amounts apparently decreased the stiffness of the gels, with a higher concentration of TEMED having a slightly more pronounced effect (Figure A-1A). The polymerisation time for PA#4 gels with 2x TEMED and 5x APS were slightly increased by 1m10s and 40s respectively, while 2x APS nearly doubled the polymerisation time (9m11s) (Figure A-1B). When 5x TEMED was added to PA#4 gels, polymerisation time decreased by 1m50s (Figure A-1B). An increase in initiator concentrations in PA#2 gels, caused the gels to become so soft that the probe was unable to detect the gels and stiffness could not be measured.

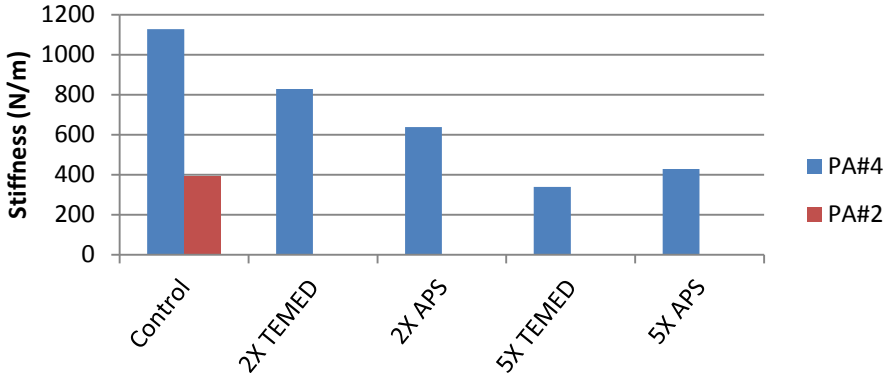

(A)

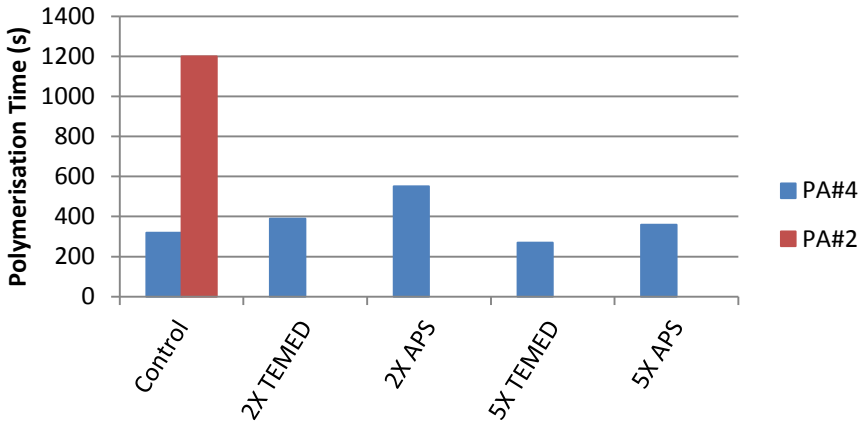

(B)

Figure A-1. Stiffness (A) and polymerisation time (B) of PA#2 and PA#4 gels polymerised in bulk with increased initiator concentrations. The stiffness was determined by the unloading force/deflection curve measured by microindentation.

Although 5x TEMED decreased polymerisation time of the PA#4 gels in bulk, applying this to the Flexwell protocol did not produce fully polymerised gels, and 2x TEMED used in PA#2 gels also did not produce successful gels. Additionally, when the Flexwells were left overnight to increase polymerisation time, the gels were still not fully polymerised.

A.2 Discussion

In these experiments, only PA#2 and PA#4 gels were used, which have the same acrylamide monomer concentration, but PA#4 has approximately twice as much bis-acrylamide. Therefore, it appears that the bis-acrylamide concentration has a much larger effect on polymerisation time than the initiator concentration. If bis-acrylamide concentration has similar effects on polymerisation rate as the monomer concentration, then based on equation 3.1 we would expect that doubling the bis-acrylamide concentration would also double the polymerisation time. However, since bis-acrylamide

actually has two vinyl groups, it may double the effect, potentially explaining why PA#2 gels take 4x as long to polymerise as PA#4 gels. In contrast, polymerisation rate is proportional to the square root of the initiator concentration and would therefore have a much smaller effect compared to bis-acrylamide.

Although the initiator concentration did not appear to affect polymerisation time, increasing initiators drastically reduced gel stiffness. The resulting stiffness of PA gels is difficult to predict as it is a complex measure that is dependent on structural features of the gel well beyond the polymer chain length, and is therefore beyond the scope of this thesis.

A.3 Additional Flexwell Methods

	Coverslip Hydrophobicity																	
1)	Undiluted Surfacil - wipe + RainX	x				x	x		x	x	x		x	x	x	x	x	x
2)	Diluted Surfacil - soak + 24 hr dry + RainX		x									x						
3)	Diluted Surfacil - soak + 2 hr dry			x				x										
4)	Diluted Surfacil - soak + 2hr dry + RainX				x							x						
5)	RainX alone					x												
	PA Polymerisation Solution																	
1)	2x TEMED						x											
2)	5x TEMED							x										
3)	Overnight polymerisation								x									
4)	Vacuum PA solution	x	x	x	x	x	x	x	x			x	x	x	x	x	x	x	x
5)	No vacuum of PA solution									x									
6)	Nitrogen bubbled through PA										x								
	PA Polymerisation Environment																	
1)	Polymerisation under vacuum											x						
2)	Nitrogen "rinse" of coverslips	x	x	x	x	x	x	x	x	x	x	x	x	x	x	x	x	x	x
3)	Increased membrane vacuum time												x						
4)	Plastic chamber + thin tubing	x	x	x	x	x	x	x	x			x	x						
5)	Glass vacuum chamber									x	x			x	x			x	x
6)	Argon gas														x				
7)	Plastic chamber + thicker tubing															x	x		
	PA gel/Silicone Interaction																		
1)	2x hexane wash																	x	
2)	No hexane wash																		x
3)	Longer plasma time																		x

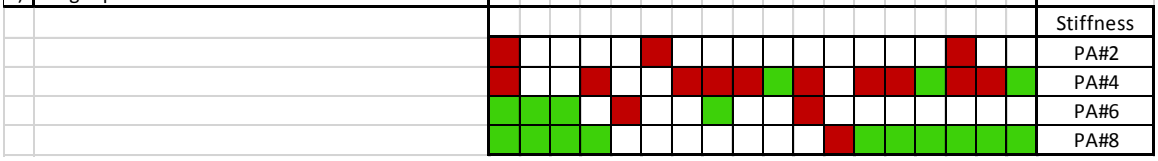

Figure A-2. Modifications made to published Flexwell protocol, numbered for easy comparison with methods below.

A.3.1 Coverslip Hydrophobicity

1) Coverslips were wiped with a Kim wipe soaked in undiluted Surfacil, then wiped dry. Coverslips were then rinsed in hexane, followed by methanol and allowed to air dry for 24 hours before RainX treatment as per #5.
2) Coverslips were soaked for 10 seconds in a 10% Surfacil solution diluted in hexane before being rinsed with hexane and methanol.

Coverslips were allowed to air dry for 24 hours before RainX treatment as per #5.
3) Same as above with a 2 hour air dry time and no RainX treatment.
4) Same as above with a 2 hour dry time and including a RainX treatment.
5) Coverslips were soaked in RainX for 10 minutes and were then carefully dried to remove residue.

A.3.2 PA Polymerisation Solution

1) 14µL of TEMED were added to the PA solution instead of 7.5µL as per Table 2-1. Volume of water was adjusted to obtain a total volume of 5mL.
2) Same as above with 37.5µL TEMED.
3) to 5) are self-explanatory.
6) In place of vacuuming unpolymerised PA gel solutions, nitrogen was bubbles through the solution for 10 minutes by placing a glass pipet connected to a nitrogen tank in the beaker.

A.3.3 PA Polymerisation Environment

1) After top coverslips were placed on unpolymerised solutions on the Flexcell membranes, the vacuum chamber was immediately sealed and placed under vacuum pressure for 30 minutes.
2) The top coverslips were briefly placed under nitrogen flow before being placed on the unpolymerised gel solution on the Flexcell membrane.
3) After TcPM treatment and hexane washes, Flexcell plates were vacuumed for 10 minutes instead of 5 minutes.
4) A plastic vacuum desiccator that was attached to the pump with thin tubing that collapsed slightly was used to dry Flexcell membranes after TcPM treatment.
5) A glass vacuum desiccator that was attached to the pump with the same thin tubing as above was used to dry Flexcell membranes.
6) PA gels were polymerised under a steady flow of argon instead of nitrogen.
7) The plastic vacuum desiccator was attached to the pump with thicker tubing with no collapse and membranes were dried for 5 minutes.

A.3.4 PA Gel-Silicone Interaction

1) Flexcell membranes were rinsed twice with hexane after TcPM treatment.
2) Flexcell membranes were moved directly to the vacuum drying step after TcPM treatment with no rinse.
3) Flexcell membrane was exposed to oxygen plasma for 4 minutes before TcPM treatment.

Appendix B: Additional Contractile Function Experiments

B.1 Methods

B.1.1 Acute Drug Experiments:

Cells were seeded on 18mm glass coverslips in 12 well plates at a density of 360cells/mm^2 and grown for 24 hours in standard media with 10% serum, 1% serum, or in IT media. Beads were added as described in chapter 2.5 before baseline stiffness measurements were taken. After baseline stiffness measurements were taken, a solution containing forskolin, histamine, or Y27632 dissolved in IT media was added for a final concentration of 10μM. Each drug was applied for 3 minutes before the post-drug stiffness measurement was taken.

B.1.2 Chronic Contractility Experiments:

For chronic tone modulation experiments, cells were cultured on soft and stiff substrates (Table 4-1) for 24 hours in standard feeder media containing 10% FBS without drugs to allow cells to adhere to the substrate. The media was then replaced with 1% FBS standard feeder media that contained blebbistatin or vehicle (0.1% DMSO), Y27632 or vehicle (0.1% DMSO), or histamine or control. The media containing drug was refreshed every 24 hours for 3 days. On day 4, 24 hours before OMTC measurements, the media was switched to IT media that contained the appropriate drug. Before beads were added, drug containing media was rinsed out and replaced with standard IT media. Beads were added and baseline stiffness and contractility measurements were performed as described in chapter 2.5.

B.1.3 Short Term Contractility Experiments:

In these experiments, cells were seeded on soft and stiff substrates (Table 4-1) for 24 hours in standard feeder media containing 1% FBS without drugs. Beads were then added and allowed to adhere for 20 minutes before excess beads were rinsed out at which point either control or histamine IT media was added. The cells were incubated for 45 minutes in the treatment media before baseline measurements were taken, followed by the addition of 80mM KCl for 3 minutes to measure contractility.

B.1.4 Spreading Phase Contractility Experiments:

These experiments were conducted with the same treatment and bead addition protocol as the short term contractility experiments as detailed above. However, in spreading phase assays, cells are seeded only 4 hours before beads are added at which point cells have not fully spread on the substrate.

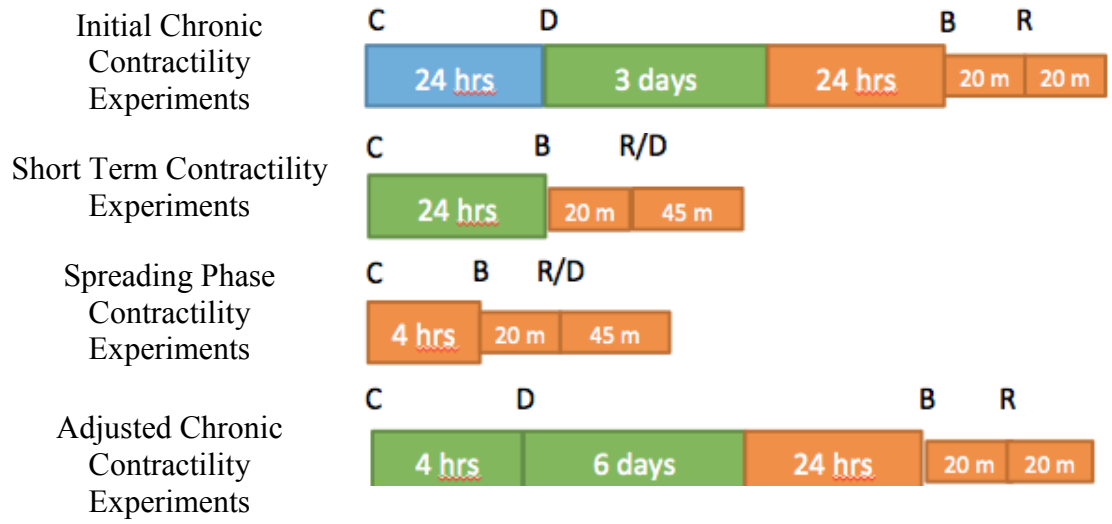

Figure B-1. Chronic and acute tone modulation assay designs. C=cells seeded, D=first drug dose, B=beads added, R=beads rinsed. Colours signify media used: blue=10% feeder, green=1% feeder, orange=IT media. Times are noted for each block.

B.2 Results

Due to the variability observed in OMTC experiments and the time consuming nature of these experiments, I did not complete dose response curves and acute response experiments on all drugs. However, based on does response experiments and previously published literature, I am confident that both Histamine and Forskolin at a concentration of 10μM chronically increase and decrease tone respectively in ASM cell culture (42). Based on chronic experiments it also appears that blebbistatin affects tone chronically at a concentration of 10μM. In contrast, it is unclear whether Y27632 or cantharidin have an effect on ASM cell tone at the tested doses. Therefore, I mainly focus on histamine and forskolin in subsequent OMTC, cell morphology, and gene expression studies.

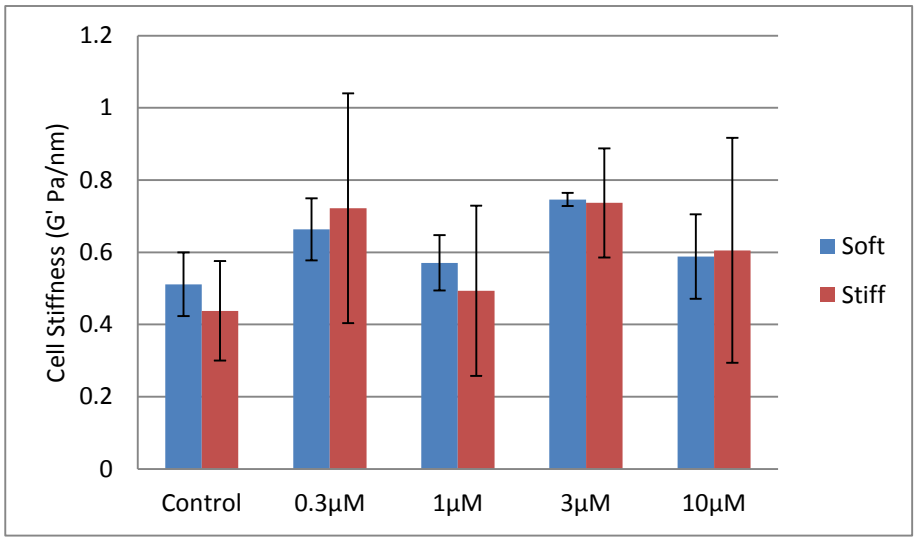

(A)

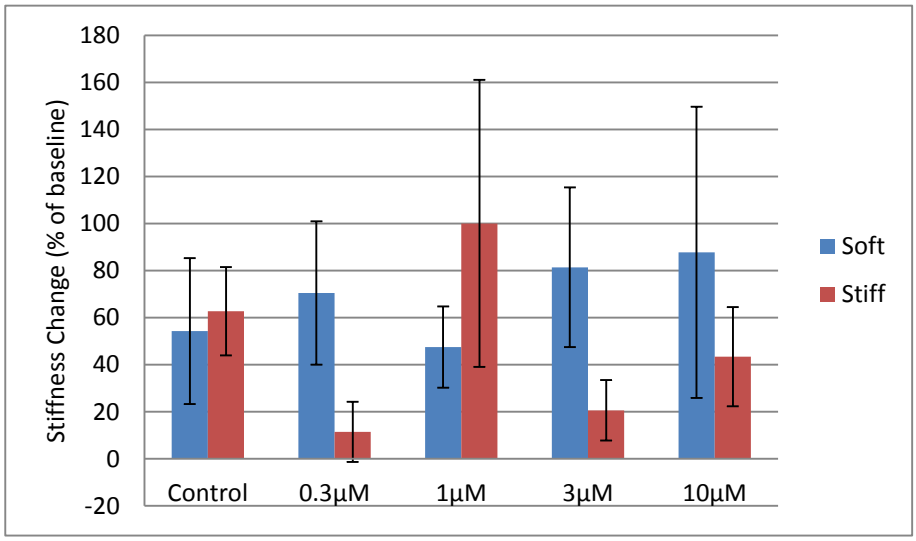

(B)

Figure B-2. Baseline stiffness and contractility for a range of doses of Y27632. Primary ASM cells cultured on soft and stiff substrates for 24 hours in 10% serum feeder media before daily dosing with various drug concentrations. Drug doses were control (0.1% DMSO) or 0.3µM, 1µM, 3Mm, or 10µM in 1% serum feeder for 3 days and in IT media 1 day prior to OMTC. For 0.3µM and 3µM doses n=3-4 from 2 donors. For control, 1µM and 10µM n=6-8 from 3 donors. Values are means ±SE.

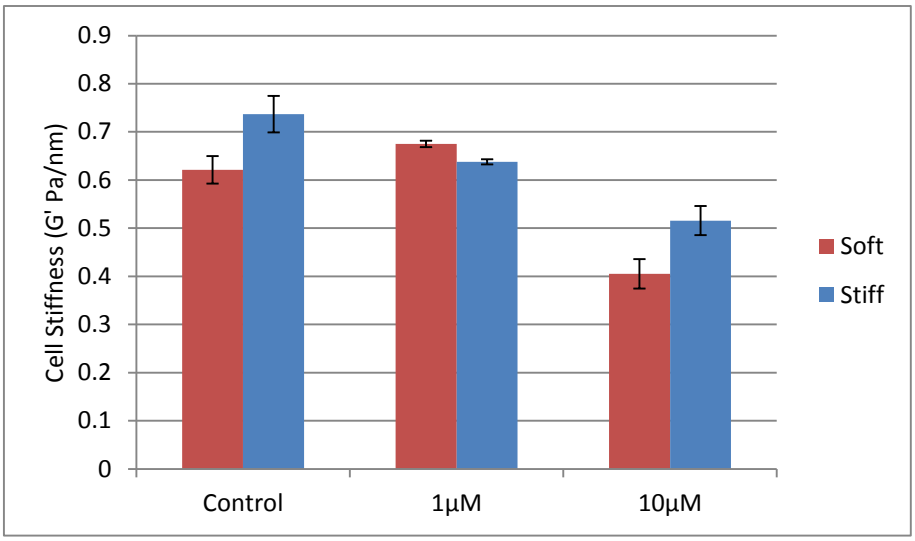

(A)

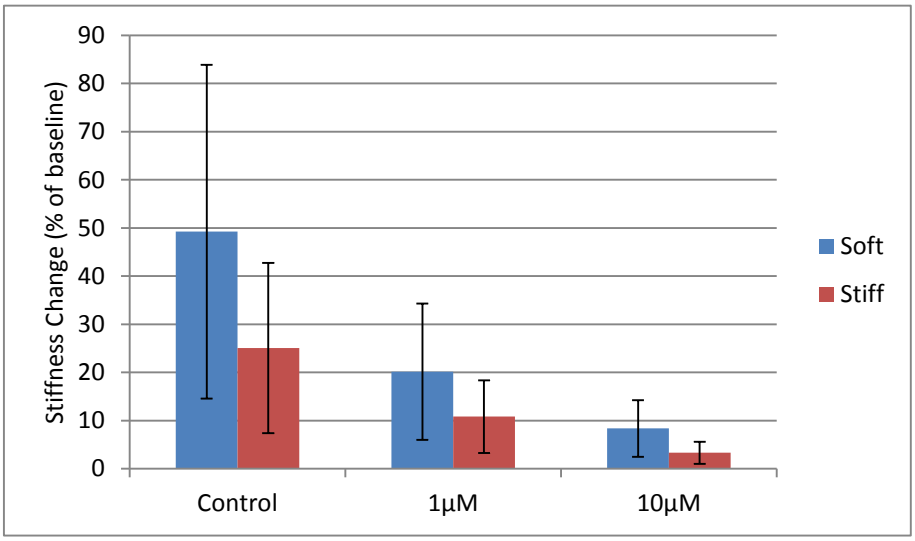

(B)

Figure B-3. Baseline stiffness and contractility for a range of doses of blebbistatin. Primary ASM cells cultured on soft and stiff substrates for 24 hours in 10% serum feeder media before daily dosing with various drug concentrations. Drug doses were control (0.1% DMSO), 1µM, or 10µM blebbistatin in 1% serum feeder for 3 days and in IT media 1 day prior to OMTC. Values are means ±SE calculated from 7 or wells (n=7-8) from 2 donors.

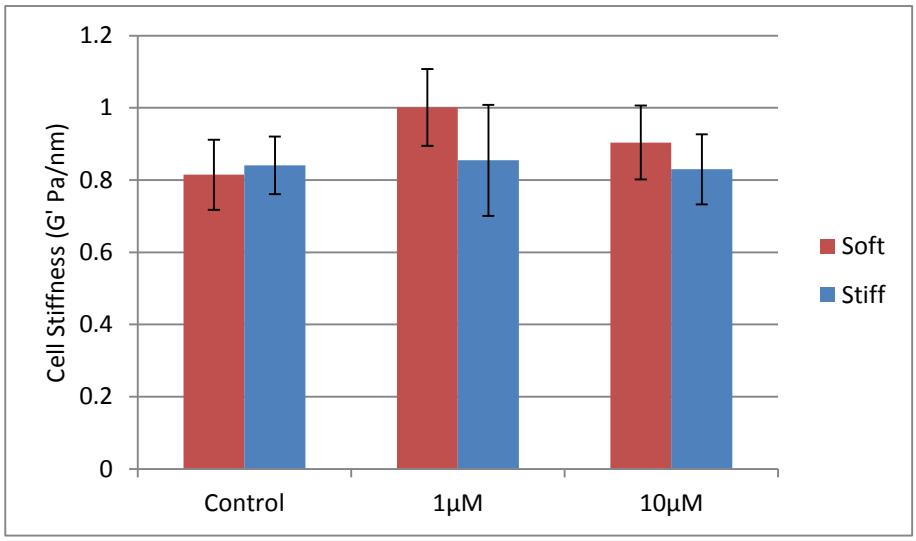

(A)

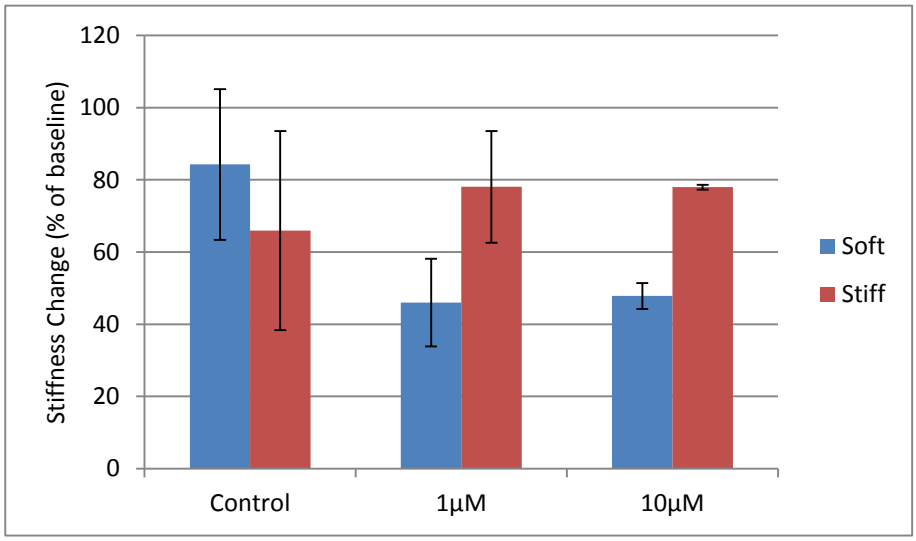

(B)

Figure B-4. Baseline stiffness and contractility for a range of doses of histamine. Primary ASM cells cultured on soft and stiff substrates for 24 hours in 10% serum feeder media before daily dosing with various drug concentrations. Drug doses were control (0.1% DMSO), 1µM, or 10µM histamine in 1% serum feeder for 3 days and in IT media 1 day prior to OMTC. Values are means ±SE calculated from 9 to 12 wells (n=9-12) from 3 donors.

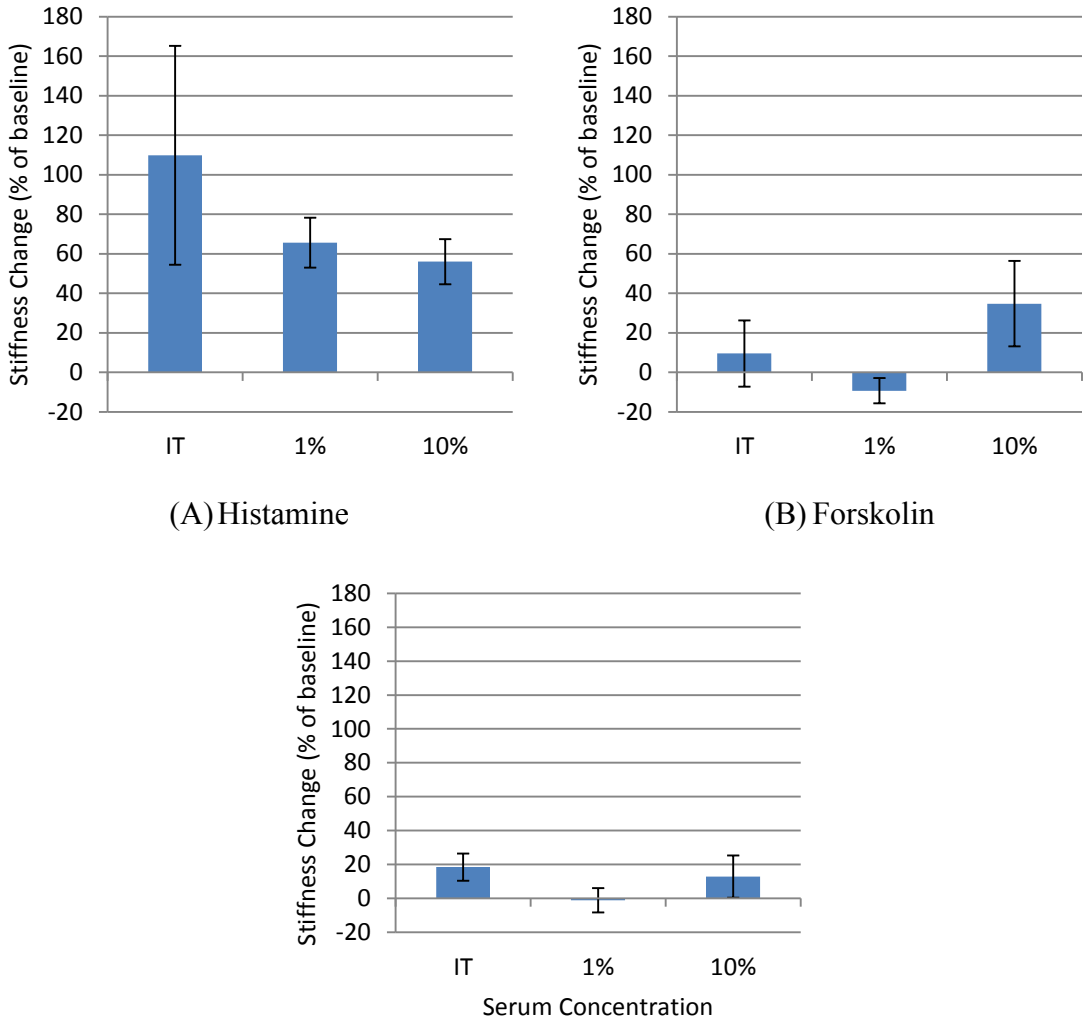

Figure B-5. Acute response to contractile and relaxant agents. Changes in stiffness after 3 minutes of treatment with either histamine (10 μM) (A), forskolin (10 μM) (B), or Y27632 (10 μM) (C) measured by OMTC. Primary ASM cells cultured on collagen coated glass for 24 hours in IT or feeder media containing 1% or 10% serum before testing. Values are means ± SE, n≥6 from 2 donors for histamine and forskolin, and n=4 from one donor for Y27632. There are no significant differences between any media groups in any treatment experiment.

In the first set of experiments I examined the effect of 3 days of treatment on baseline stiffness and contractility using OMTC. Overall, there was a general trend of increasing baseline cell stiffness across treatments (Figure B-6A). Histamine treated cells were significantly stiffer than blebbistatin treated cells ($p<0.05$) on both soft ($G'_{blebbistatin}$=0.43±0.03 Pa/nm and $G'_{histamine}$=0.87±0.06 Pa/nm) and stiff ($G'_{blebbistatin}$=0.52±0.04 Pa/nm and $G'_{histamine}$=0.86±0.12 Pa/nm) substrates. However, 3 day treatment had no significant effects on the contractility of cells (Figure B-6B).

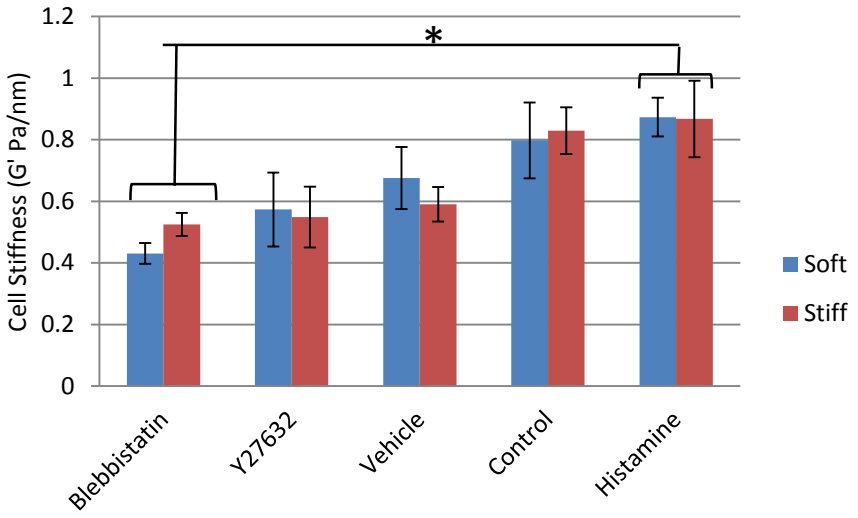

(A)

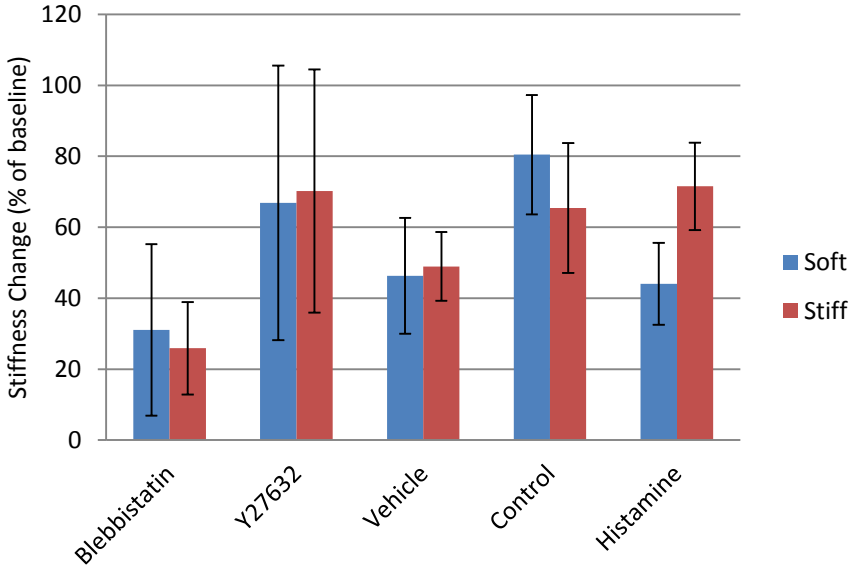

(B)

Figure B-6. Baseline stiffness and contractility after 3 days of tone modulation. Primary ASM cells cultured for 24 hours on soft (1200 Pa) and stiff (19 200 Pa) PA gels for 24 hours before daily treatment with blebbistatin (10 μM), Y27632 (10 μM), histamine (10 μM), control media, or vehicle media (0.1% DMSO). Control and vehicle groups are pooled as they are not significantly different. Baseline stiffness (A) and contractility (B) measured by OMTC. Values are means ±SE, n≥6 from 3 donors, *p<0.05, 2-way ANOVA with Bonferroni post-hoc test.

In ASM cells cultured for only 4 hours, treatment with forskolin for 45 minutes had no significant effects on baseline stiffness or contractility (Figure B-7A and B).

Whereas cells cultured for 4 hours and then treated with histamine for 45 minutes showed reduced contractility (-4.37±9.03% on soft and 5.43±4.80 on stiff), although the treatment effect is only significant on stiff substrates ($p<0.05$) (Figure B-7C and D). This effect on contractility disappeared when cells were cultured for 24 hours before treatment with histamine for 45 minutes (13.15±14.99% on soft and 16.99±6.42% on stiff) and there were no significant effects of drug treatment or substrate stiffness on contractility or baseline stiffness (Figure B-8).

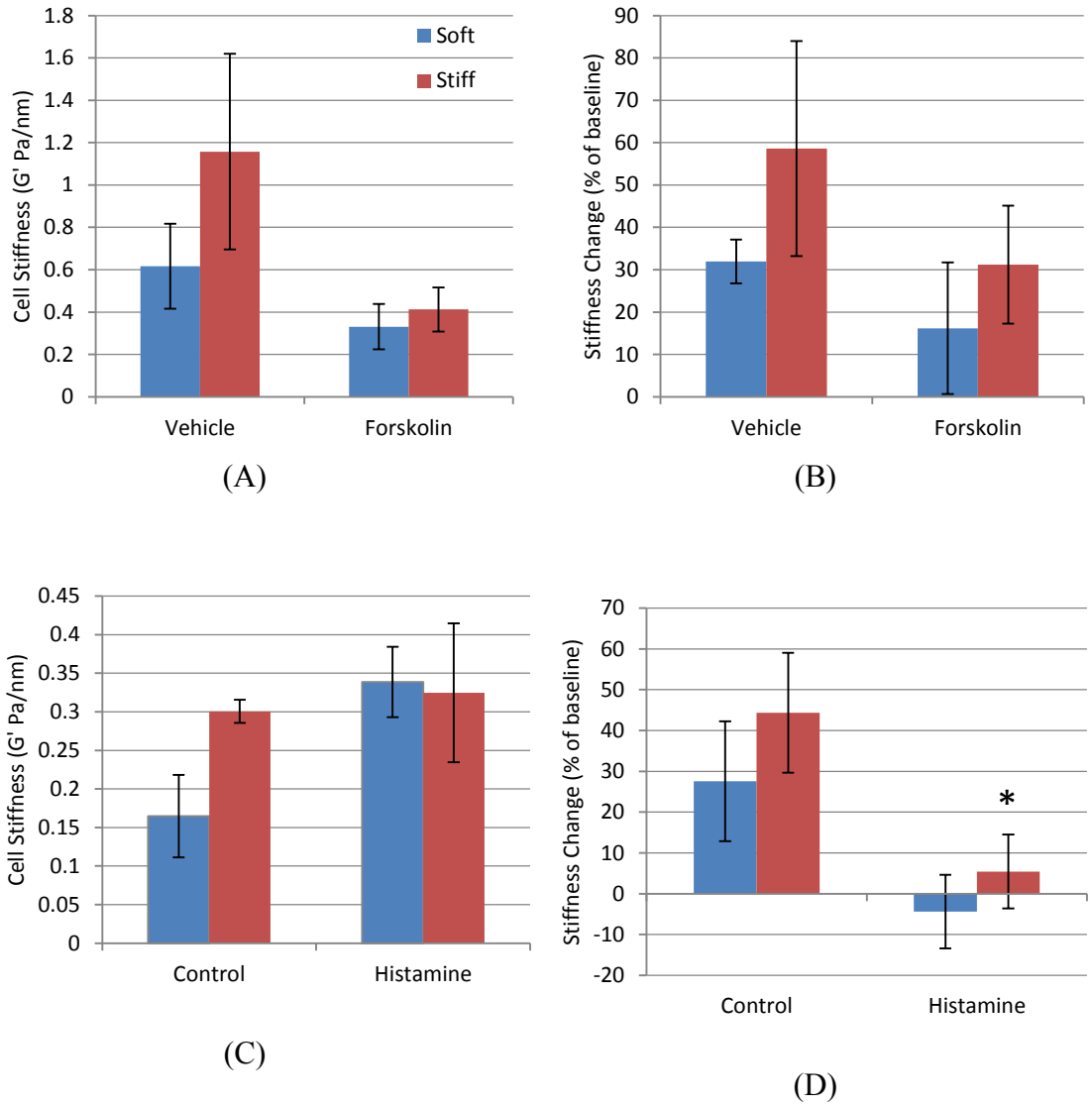

Figure B-7. Baseline stiffness and contractility of 4 hour cultured cells with 45 minute tone modulation. Primary ASM cells cultured for 4 hours on soft (1200 Pa) and stiff (19 200 Pa) PA gels before 45 minute treatment with histamine (10 μM) or control media (A and B), or forskolin (10 μM) or vehicle media (0.1% DMSO) (C or D). Baseline stiffness (A and B) and contractility (C and D) measured by OMTC. Values are means ±SE, n=4 from 2 donors, *$p<0.05$, 2-way ANOVA with Bonferroni post-hoc test.

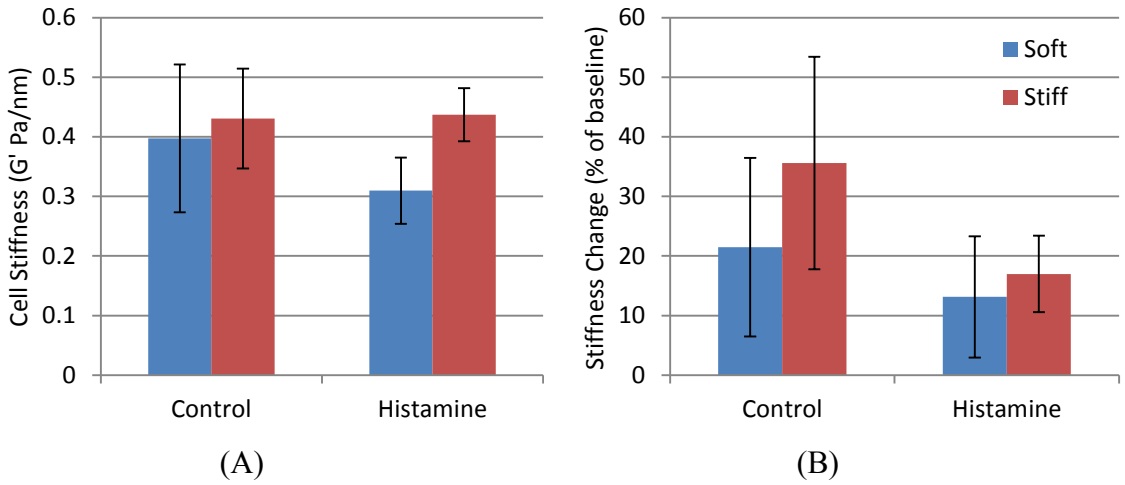

Figure B-8. Baseline stiffness and contractility of 24 hour cultured cells with 45 minute tone increase. Primary ASM cells cultured for 24 hours on soft (1200 Pa) and stiff (19 200 Pa) PA gels before 45 minute treatment with histamine (10 μM) or control media. Baseline stiffness (A) and contractility (B) measured by OMTC. Values are means ±SE, n≥7 from 2 donors, 2-way ANOVA with Bonferroni post-hoc test.

Since time appeared to play a role in the contractile response to tone modulation, I then analysed the OMTC data to examine any differences across time due to treatment or substrate stiffness. On both soft and stiff substrates, baseline tone significantly increased ($p<0.05$) after 4 days in culture (G'_{soft}=0.79±0.12 Pa/nm and G'_{stiff}=0.83±0.08 Pa/nm) compared to 4 hours (G'_{soft}=0.16±0.05 Pa/nm and G'_{stiff}=0.30±0.02 Pa/nm) or 24 hours (G'_{soft}=0.40±0.12 Pa/nm and G'_{stiff}=0.43±0.08 Pa/nm) (Figure B-9A), although contractility was not significantly affected (Figure B-9B). I then analysed whether treatment time affected baseline stiffness or contractility in cells cultured for 24 hours and found that, again, cells become stiffer over time in culture ($p<0.05$), but are unaffected by drug treatment or substrate stiffness (Figure B-10A). Additionally, time does not significantly affect contractility in histamine treated cells on soft or stiff substrates (Figure B-10B).

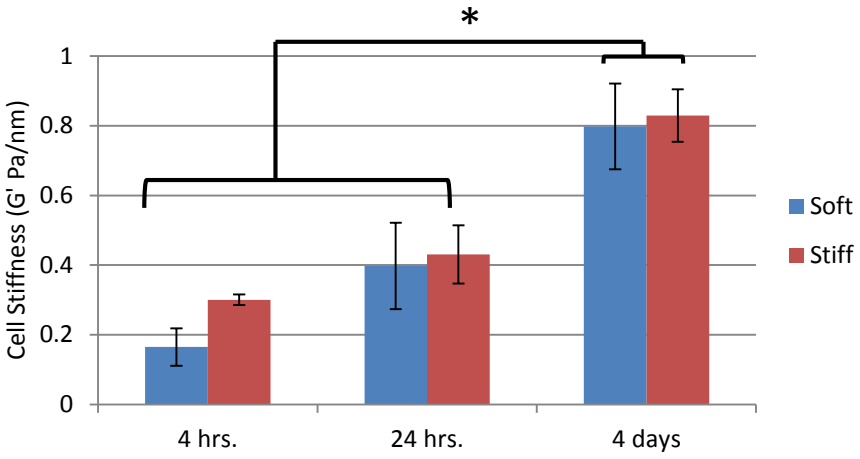

(A)

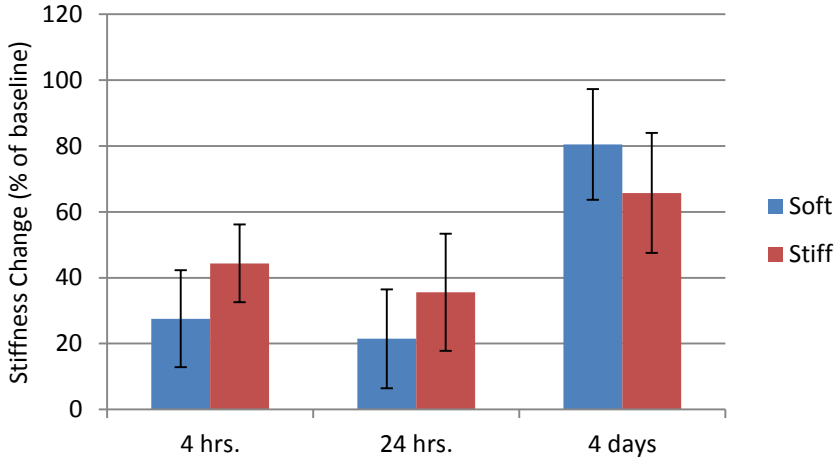

(B)

Figure B-9. Baseline stiffness and contractility over cell growth time. Primary ASM cells cultured for 4 hours, 24 hours, or 4 days on soft (1200 Pa) and stiff (19 200 Pa) PA gels. Baseline stiffness (A) and contractility (B) measured by OMTC. Values are means ±SE, n≥6 from at least 2 donors, *p<0.05, 2-way ANOVA with Bonferroni post-hoc test.

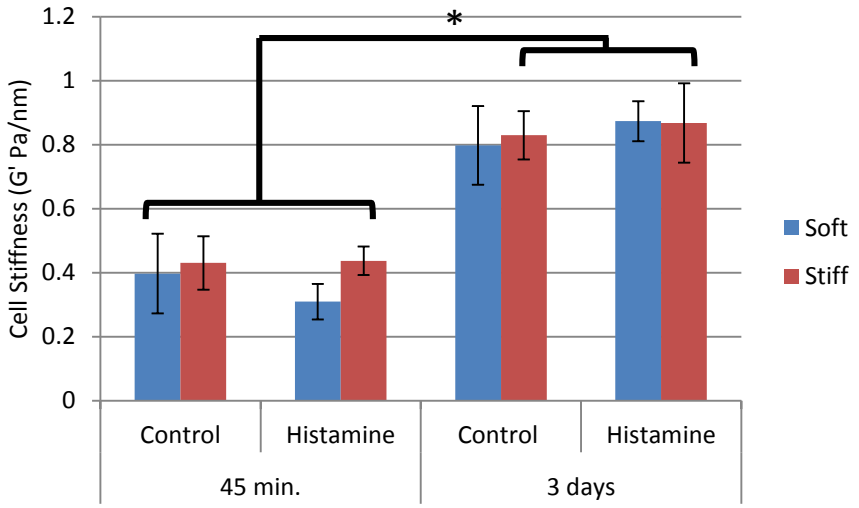

(A)

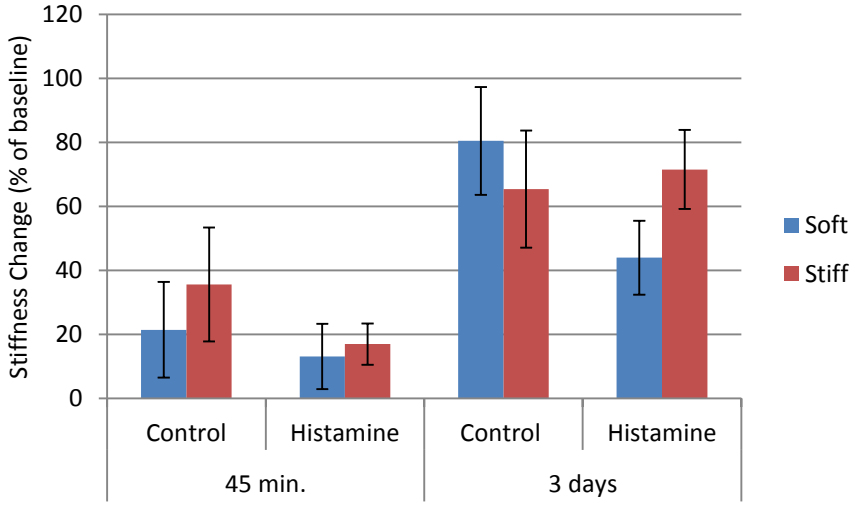

(B)

Figure B-10. Baseline stiffness and contractility after 3 day or 45 minute tone increase. Primary ASM cells cultured for 24 hours on soft (1200 Pa) and stiff (19 200 Pa) PA gels before 3 day or 45 minute treatment with histamine (10 μM) or control media. Baseline stiffness (A) and contractility (B) measured by OMTC. Values are means ±SE, n≥7 from at least 2 donors, *p<0.05, 2-way ANOVA with Bonferroni post-hoc test.

Appendix C: qPCR Reference Gene Selection

The crossing points of three candidate reference genes for each sample of cDNA is displayed below. All three reference genes remained consistent between treatments. Two gene selection software programs were used, Bestkeeper and Normfinder, Candidate reference genes displayed consistency of expression between treatments. Analysis of pooled data using Bestkeeper and Normfinder software demonstrated that YWHAZ was the most stably expressed candidate.

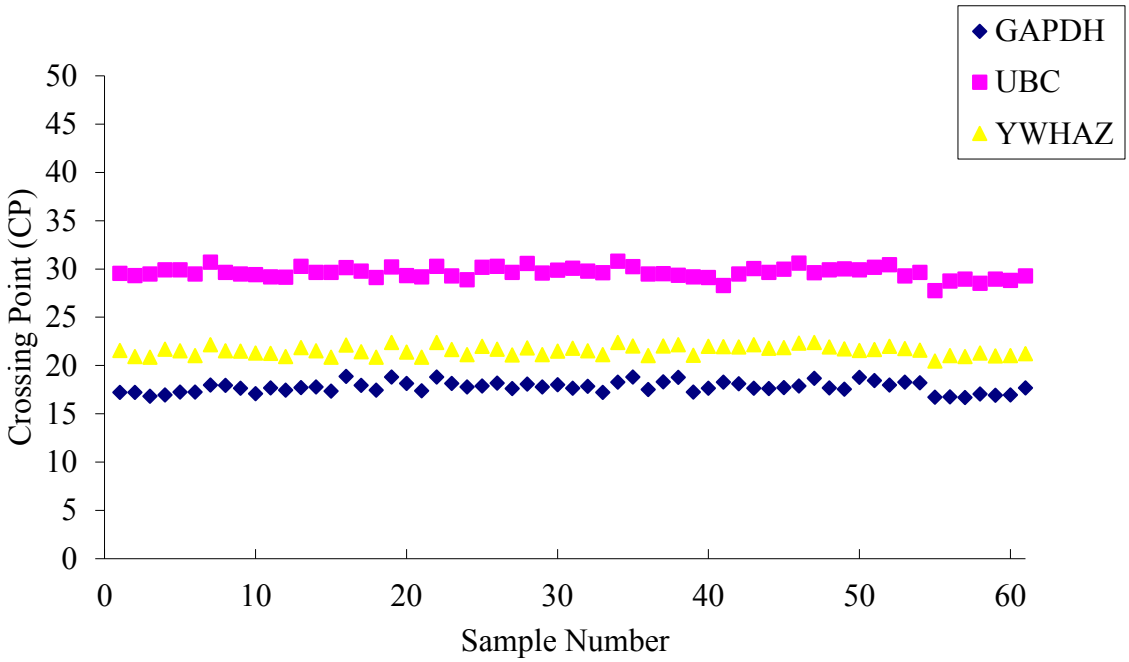

Figure C 1. Stability of candidate reference genes across all samples as generated by Normfinder.

Table C 1. Table of reference gene statistics.

	GAPDH	UBC	YWHAZ
Mean Cp	17.76±0.45	29.62±0.45	21.56±0.40
Bestkeeper Pearson correlation coefficient	0.902	0.777	0.909
Bestkeeper p-value	0.001	0.001	0.001
NormFinder stability value	0.194	0.199	0.134